

University of Alberta

Direct Flotation of Niobium Oxide Minerals from Carbonatite Niobium Ores

by

Xiao Ni

A thesis submitted to the Faculty of Graduate Studies and Research
in partial fulfillment of the requirements for the degree of

Doctor of Philosophy in Materials Engineering

Department of Chemical and Materials Engineering

©Xiao Ni
Spring 2013
Edmonton, Alberta

Permission is hereby granted to the University of Alberta Libraries to reproduce single copies of this thesis and to lend or sell such copies for private, scholarly or scientific research purposes only. Where the thesis is converted to, or otherwise made available in digital form, the University of Alberta will advise potential users of the thesis of these terms.

The author reserves all other publication and other rights in association with the copyright in the thesis and, except as herein before provided, neither the thesis nor any substantial portion thereof may be printed or otherwise reproduced in any material form whatsoever without the author's prior written permission.

Abstract

Currently the recovery of niobium oxide minerals from carbonatite niobium ores relies on the use of non-selective cationic collectors. This leads to complicated process flowsheets involving multiple desliming and multiple reverse flotation stages, and low niobium recovery. In this research, anionic collectors that are capable of strong chemisorption on the niobium minerals were studied with the objective of directly floating the niobium oxide minerals from the carbonatite ores.

In the flotation of both high purity minerals and Niobec ores, it was shown that the combination of hydroxamic acid and sodium metaphosphate was an effective reagent scheme for the direct flotation of niobium oxide from its ores. Batch flotation on the Niobec Mill Feed showed that over 95% of niobium oxide was recovered into a rougher concentrate that was less than 47% of the original feed mass. Preliminary cleaning tests showed that the reagent scheme could also be used to upgrade the rougher concentrate, although the depression of iron oxide minerals required further study.

X-ray photoelectron spectroscopic (XPS) measurement results confirm that OHA (octyl hydroxamic acid) could chemisorb on pyrochlore surface while only physically adsorb on calcite, judging by the chemical shifts of electron binding energies in the elements in both OHA and the mineral surfaces. When hydroxamic acid was adsorbed on calcite surface, the binding energies of the N 1s

electrons, at 400.3 eV, did not shift. However, after adsorption on pyrochlore, the N 1s binding energy peak split into two peaks, one at a binding energy of around 399 eV, representing chemically adsorbed OHA, the other at between 400 and 401 eV. The experimental data suggested a strong chemisorption of the OHA on pyrochlore surface in the form of a vertical head-on orientation of the OHA molecules so that the pyrochlore was strongly hydrophobized even at low OHA concentrations, followed by possibly randomly oriented physisorbed OHA molecules. On the other hand, OHA only physisorbed on calcite forming a horizontally oriented monolayer of OHA. The results explain the observed selectivity of hydroxamic acid in the flotation of niobium oxide minerals from carbonatite niobium ores.

Acknowledgments

During my studies, many people provided their encouragements and supports. I would like to first thank Dr. Qi Liu. Without his insightful guidance and enduring help, this research project would have not completed this smoothly. I have learnt a lot from the invaluable discussions with him. It has been my honor and privilege to be his Ph.D. student.

The financial support from Natural Sciences and Engineering Research Council of Canada (NSERC), COREM and IAMGOLD are also acknowledged. I am also indebted to COREM and IAMGOLD for supplying high purity samples and feed samples. Dr. Liming Huang of COREM must be acknowledged for conducting the assays of my flotation products.

I also would like to thank Dr. Allen Pratt of CANMET and Dr. Jan D. Miller of University of Utah for their suggestions to my studies.

I also owe thanks to Shiraz Merali for conducting XRD analysis, Ph.D. candidate Peng Huang for conducting specific surface area measurement, as well as all the members in ACSES for their assistance with the XPS and ToF-SIMS studies.

To Dr. Mingli Cao and Dr. Kaipeng Wang and all my fellow group members, I would like to thank their academic and technical suggestions and supports.

Finally, I would like to thank my beloved half, my parents and other relatives for their steadfast support during all my years in Canada. With you, anything is possible.

Table of Contents

1.	Introduction.....	1
1.1.	Niobium	1
1.2.	Niobium mineral processing	2
1.3.	The pyrochlore concentrator & issues	3
1.4.	Objectives	10
1.5.	Research Methodologies	11
1.6.	Organization of this thesis	12
2.	Literature review	14
2.1.	Mineral Processing.....	14
2.2.	Froth Flotation	15
2.3.	Electrical double layer (EDL)	18
2.4.	Flotation Reagents	20
2.5.	Collectors	21
2.6.	Adsorption mechanism	24
2.7.	Coordination chemistry.....	25
2.8.	Hydroxamate/hydroxamic acid.....	27
2.9.	Depressant.....	30
2.10.	Salts of phosphoric and polyphosphorus acids	32
2.11.	Reagents tested for Nb-containing minerals	34
3.	Experimental Materials and Methods	36

3.1.	High purity mineral samples	36
3.2.	Niobec ore samples	41
3.3.	Reagents and chemicals	43
3.4.	Synthesis of pure reagents	44
3.4.1.	Octyl hydroxamic acid	44
3.4.2.	Diphosphonic acid	46
3.4.3.	Starch phosphate	47
3.5.	Small-scale flotation	49
3.6.	Batch flotation tests.....	51
3.7.	Adsorption mechanism studies	52
3.7.1.	Infrared spectroscopy (IR)	53
3.7.2.	X-ray photoelectron spectroscopy (XPS)	55
3.7.3.	Adsorption isotherm determination	56
3.7.4.	ToF-SIMS imaging	58
4.	Results and Discussion	60
4.1.	Characterization of pure OHA	60
4.2.	Small-scale flotation	61
4.2.1.	Single mineral flotation using Aero 6493	61
4.2.2.	Mineral mixture flotation using Aero 6493	64
4.2.3.	Single mineral flotation using diphosphonic acid.....	67
4.2.4.	Single mineral flotation using OHA	69

4.3.	Exploratory rougher flotation using Aero 6493	73
4.3.1.	Selectivity ratio	75
4.3.2.	Preparation of Aero 6493	75
4.3.3.	Depressants	78
4.3.4.	Comparison between feed samples	79
4.3.5.	Aero 6493 dosage	82
4.3.6.	NaMP dosage	83
4.3.7.	Pulp pH	86
4.4.	Effort to maximize pyrochlore recovery	86
4.4.1.	NP 22	87
4.4.2.	NP 23-25	89
4.5.	Cleaner flotation.....	93
4.6.	Batch flotation using pure hydroxamic acid	99
4.7.	Effect of neutral oil	103
4.8.	Adsorption mechanism studies	106
4.8.1.	Infrared spectroscopy analysis	106
4.8.2.	X ray photoelectron spectroscopy analysis of OHA treated minerals	112
4.8.3.	X-ray photoelectron spectroscopy analysis of NaHMP treated minerals	119
4.8.4.	The adsorption of hydroxamic acid on mineral surfaces	127
4.8.5.	ToF-SIMS imaging analysis	132
5.	Conclusions and recommendations.....	143

5.1. General Findings	143
5.2. Original contributions	147
5.3. Recommendations for future work	148
References.....	151
Appendix A: Bench-scale flotation tests.....	160
Appendix B. Determination of OHA concentration by UV-Vis spectrophotometry	200
Appendix C. Raw data from XPS measurements	202

List of Tables

Table 1.1 Mineralogical composition of the Niobec ore.	4
Table 3.1 Chemical assays (wt. %) of high purity mineral samples used in small-scale flotation.	37
Table 3.2 Assays of the three plant ore samples (wt. %).	41
Table 4.1 The dosage of Aero 6493 and depressant for exploratory rougher flotation tests.	74
Table 4.2 Batch flotation results of Niobec ore sample using Aero 6493 and NaMP.	81
Table 4.3 Collector dosage and feed samples in batch flotation using pure collector.	100
Table 4.4 Selectivity ratio for different minerals in batch flotation using pure collector.	101
Table 4.5 Batch flotation results of Niobec feed sample using kerosene	104
Table 4.6 Relative atomic ratio on the pure and OHA treated surfaces.	116
Table 4.7 Relative atomic ratio on the pure and NaHMP treated surfaces.	125

List of Figures

Figure 1.1 Process flowsheet of Niobec concentrator (Arrows indicate points of sample collection. for this research. Red arrow: Mill Feed; blue arrow: Carbonate Feed; yellow arrow: Pyrochlore Feed).....	6
Figure 2.1 Froth flotation cell (Webster's online dictionary, 2012).....	16
Figure 2.2 Electrical double layer on the solid particle and potential drop across the double layer (Bulatovic, 2007).	19
Figure 2.3 The surface charges and surface determining ions on hematite (Uwadiale, 1992).	20
Figure 2.4 Molecular structure of hydroxamic acid.....	28
Figure 2.5 Recoveries of different minerals using 10 mg/L alkyl hydroxamic acid (Ren et al., 2004).	30
Figure 2.6 Interaction energy between pyrite and serpentine particles at pH 9 (Lu et al., 2011).	34
Figure 3.1 XRD patterns of (a) pyrochlore (b) calcite (c) quartz.	39
Figure 3.2 Particle size distribution of the three ore samples.	42
Figure 3.3 Molecular structure of salicylhydroxamic acid.	43
Figure 3.4 Apparatus for synthesizing diphosphonic acid.....	47
Figure 3.5 Schematic of the custom-made flotation tube.	50
Figure 3.6 JKTech flotation machine (a) side view (b) top view of 1.5 L flotation cell.	52

Figure 4.1 FTIR spectrum of octyl hydroxamic acid (solid particles in KBr powder).	60
Figure 4.2 Recovery of single minerals under natural pH using Aero 6493 as a collector.....	62
Figure 4.3 Recovery of single minerals with the addition of 45 mg/L Aero 6493 at different pH.	63
Figure 4.4 Flotation recovery of single minerals with the addition of 45 mg/L Aero 6493 at pH 7 and different NaMP concentrations.	64
Figure 4.5 Recovery and grade of pyrochlore with addition of 20 m/L NaHMP at pH 9.....	65
Figure 4.6 Recovery and grade of pyrochlore with addition of 20 m/L NaHMP and 45 mg/L Aero 6493.	66
Figure 4.7 Recovery and grade of pyrochlore with addition of 45 mg/L Aero 6493 and pH 9.....	67
Figure 4.8 Recovery of single minerals using diphosphonic acid as a collector at pH 7.....	68
Figure 4.9 Recovery for single minerals using diphosphonic acid as a collector at pH 4.....	69
Figure 4.10 Recovery of single minerals with the addition of 30 mg/L OHA at natural pH and different oxalic acid concentrations.	70
Figure 4.11 Recovery of single minerals with the addition of 50 mg/L OHA at natural pH and different EDTA concentrations.	71

Figure 4.12 Recovery of single minerals with the addition of 50 mg/L OHA at natural pH and different sodium silicate concentrations.....	72
Figure 4.13 Recovery of single minerals with the addition of 50 mg/L OHA and 100 mg/L sodium silicate at different pH.	73
Figure 4.14 Niobium oxide and carbonate recovery as a function of mass pull for test NP 01 (a) and test NP 02 (b).	77
Figure 4.15 Solid recovery and mass pull of test NP 03.....	78
Figure 4.16 Solid recovery and mass pull of test NP 07.....	79
Figure 4.17 Comparison of solid recovery, niobium oxide recovery and niobium oxide grade on rougher flotation test of three different feed samples.	80
Figure 4.18 Impact of Aero 6493 dosage on the rougher flotation of Mill Feed..	83
Figure 4.19 Impact of sodium metaphosphate dosage on rougher flotation of the Carbonate Float Feed.....	85
Figure 4.20 Flowsheet of test NP 22.....	88
Figure 4.21 Flowsheet of test NP 23.....	90
Figure 4.22 Flowsheet of test NP 25.....	92
Figure 4.23 Comparison of total rougher pyrochlore recovery in tests NP 12, and NP 22 to NP 25.....	93
Figure 4.24 Flowsheet of test NP 27.....	95
Figure 4.25 Recovery (a) grade (b) in the flotation stages of test NP 27.	97
Figure 4.26 Mineral recovery (a) Mineral grade (b) and solid recovery in cleaner stages of NP 28.....	98

Figure 4.27 Particle size distribution of test NP 48 and 49 rougher tail and their feed.	106
Figure 4.28 The infrared spectra of normal octyl hydroxamic acid, sodium hexametaphosphate, metaphosphate treated calcite, hydroxamic acid treated calcite and pure calcite surface.	108
Figure 4.29 Structures of octyl hydroxamic acid and its metal chelates.	109
Figure 4.30 The infrared spectra of normal octyl hydroxamic acid, sodium hexametaphosphate, hexametaphosphate treated pyrochlore, hydroxamic acid treated pyrochlore and pure pyrochlore surface... ..	111
Figure 4.31 XPS spectra of (a) Nb 3d (b) Ca 2p of untreated and OHA treated pyrochlore.	114
Figure 4.32 XPS spectra of Ca 2p of untreated and OHA treated calcite.....	115
Figure 4.33 N 1s spectra of OHA, untreated and treated pyrochlore and calcite by 50 mL 31 mmol/L OHA solution at pH 8.5.....	117
Figure 4.34 XPS spectra of pure and NaHMP treated calcite.....	121
Figure 4.35 XPS spectra of (a) Nb 3d (b) Ca 2p of untreated and NaHMP treated pyrochlore.	123
Figure 4.36 XPS spectra of Ca 2p on pure calcite and NaHMP treated calcite..	124
Figure 4.37 P 2p spectra of NaHMP, untreated and treated pyrochlore.	125
Figure 4.38 XPS spectra of P 2p on pure calcite, pure NaHMP and NaHMP treated calcite.	126

Figure 4.39 Adsorption isotherm of OHA on calcite at pH 8.5 (dashed lines: calculated horizontal orientation and vertical orientation monolayer adsorption density).....	129
Figure 4.40 Adsorption isotherm of OHA on pyrochlore at pH 8.5 (solid lines: averaged adsorption densities at these two plateaus. Dashed line: calculated vertical orientation saturation adsorption density for chemically adsorbed monolayer).	130
Figure 4.41 Adsorption isotherm at low OHA dosage on pyrochlore and calcite at pH 8.5 (dashed lines: calculated horizontal orientation and vertical orientation monolayer adsorption density).	131
Figure 4.42 Proposed self-assembled monolayer of OHA on pyrochlore and horizontal oriented monolayer on calcite at low OHA concentration.	132
Figure 4.43 Positive ion intensity images of $136.2 \times 136.2 \mu\text{m}^2$ size on OHA treated pyrochlore and calcite mixture (weight ratio 1:1) (a) Nb^+ ; (b) Ca^+ ; (c) $\text{C}_8\text{H}_{17}\text{NO}_2^+$	133
Figure 4.44 N 1s spectra of untreated and OHA treated pyrochlore with various concentration.	136
Figure 4.45 Adsorption isotherm of OHA on pyrochlore at pH 8.5 (solid lines: averaged adsorption densities at these two plateaus. Dashed line: calculated vertical orientation saturation adsorption density for chemically adsorbed monolayer. Red vertical lines: equilibrium	

concentration corresponding to a starting concentration of 1 mmol/L
and 2 mmol/L OHA). 138

Figure 4.46 N 1s spectra of untreated and OHA treated calcite with and without
washing. 142

1. Introduction

1.1. Niobium

Niobium (Nb, atomic number 41) is one of the group VB metallic elements in the periodic table along with Vanadium and Tantalum. As one of the refractory metals, niobium exhibits extraordinary resistant to heat, wear, and most of the aggressive organic and inorganic liquids including liquid metal, aqua regia and fused alkali. This corrosion resistance makes niobium an important stabilizer and corrosion inhibitor in steels. Currently about 90% of niobium were consumed as stabilizer and corrosion inhibitor annually (Papp, 2009). The niobium compounds, such as niobium carbide and niobium nitride, can be used as grain refiners to increase the strength, hardness and other mechanical characteristics of steels even at very low concentrations (<0.1 vol.%) (Patel and Khul'ka, 2001). In steel industry, niobium is usually used in the form of ferroniobium (an iron niobium alloy). Due to the increasing need for high performance steel and alloy, the world market demand for niobium has been increasing significantly for the past decade (Belsile, 2009).

The low cross section thermal neutron absorption along with inert chemical properties makes niobium attractive in nuclear industries and a vital element for alloys used in nuclear reactors (Hampel, 1961). The characteristics of temperature stability make niobium-bearing superalloys important for jet and rocket engines

(Hebda, 2001). It is also found to be useful in cryogenic technology, electronics and numismatics (Grill and Gnadenberger, 2006). Because of these unique properties, niobium is expected to have a broader application in the future.

Niobium is not found in pure metallic form in the Earth's crust. It usually exists as oxide minerals (pyrochlore, columbite, fersmite, etc.) which are rare in mass abundance. Currently, Pyrochlore, $(\text{Ca,Na})_2(\text{Nb,Ti})_2\text{O}_6\text{F}$, is the most important commercially exploitable niobium-bearing mineral.

1.2. Niobium mineral processing

Niobium mineral deposits are usually formed in association with carbonatite during the geological evolution. The largest known pyrochlore reserves are in Brazil (Araxa and Catalao) and Australia (Mt Weld), and the latter has not been commercially exploited yet. Currently, Canada has the fourth largest reserves in the world, and it is the third largest producer of niobium.

All the niobium ores contain no more than 1% niobium and have complex mineralogical composition. Currently, commercially operated mines in Brazil and Canada use very similar and complicated flowsheets to concentrate the pyrochlore mineral. The flowsheet includes crushing, grinding, desliming, leaching, gravity separation, flotation, magnetic separation (will be discussed in detail in the next section). They all use cationic collectors (amine) in the pyrochlore flotation stage

(Oliveira et al., 2001; Guimaraes and Weiss, 2001). Some lab scale tests have been done recently on the Mt Weld ores (Aral and Bruckard, 2008). The conclusion is that only one or two processing methods alone (such as flotation, gravity separation or magnetic separation) might not be sufficient for concentrating the pyrochlore. Currently, the niobium mineral industry is facing the problems and shortcomings arising from an ineffective flotation collector and the complicated flowsheet.

1.3. The pyrochlore concentrator & issues

The Saint-Honore pyrochlore deposit in Quebec is mined by IAMGOLD Corporation through its Niobec Mine which is the world third largest ferroniobium producer and the only one in North America; its ferroniobium production was 3,400 tonnes in 2002 (Scales, 2003). The chemical composition of the Niobec ore is very complicated; the majority of the ore is carbonates (65%, mainly dolomite, with some calcite) and silicates (21%, mainly biotite), the rest are sulphides and oxides including ~1% niobium-containing pyrochlore and columbite (the ratio of pyrochlore to columbite is about 10:1) (Table 1.1). The isoelectric point (i.e.p.) of pyrochlore is around 2.6, while that of silicates is ~2. These similar surface charges of the pyrochlore and silicate gangue minerals limit the use of a collector that is only based on electrostatic adsorption (physical adsorption) (Espinosa-Gomez et al., 1987), unless selective depressants are used.

Table 1.1 Mineralogical composition of the Niobec ore.

Mineral	Wt%
Niobium containing minerals	
Pyrochlore & Columbite (10:1)	1.7
Iron gangues	
Iron oxide (Hematite & Magnetite)	2.6
Iron sulfide (Pyrite)	3.0
Phosphate	
Apatite	3.5
Silicate	
Chlorite	2.0
Quartz	4.3
Biotite	11.3
Carbonatite	
Calcite	8.6
Dolomite	55.2

Like the other two large niobium mines in Brazil, the Niobec Concentrator in Quebec currently uses a cationic collector to float pyrochlore and columbite. The collector acts mainly through electrostatic adsorption therefore it also collects other gangue minerals due to their negative surface charges at neutral and alkaline pulp pH. Thus the major gangue minerals must be rejected step by step in various stages prior to niobium mineral flotation, which makes the Niobec flowsheet very complicated (Figure 1.1). Briefly, after comminution, the ore is carried through a desliming stage then followed by reverse carbonate flotation, which produce a slime stream and carbonate concentrate that are discarded. The carbonate flotation tail was deslimed again and the sand fraction sent for magnetic separation to remove the magnetic iron oxide minerals. The magnetic separation tail enters the pyrochlore flotation in which the cationic collector is used to float the niobium oxide minerals at weakly acidic pH. The rougher concentrate is cleaned for 4 times at increasingly lower pH with the final cleaner conducted at pH 2.5. The

final pyrochlore cleaning flotation concentrate was subjected to a two stage reverse flotation using xanthate to remove iron sulfide (pyrite); and between these two reverse sulfide flotation stages, a hydrochloric acid leach is conducted to remove the phosphate gangue (apatite). The final niobium oxide concentrate is dewatered, packed and sent to a converter to produce ferroniobium by aluminothermic reaction.

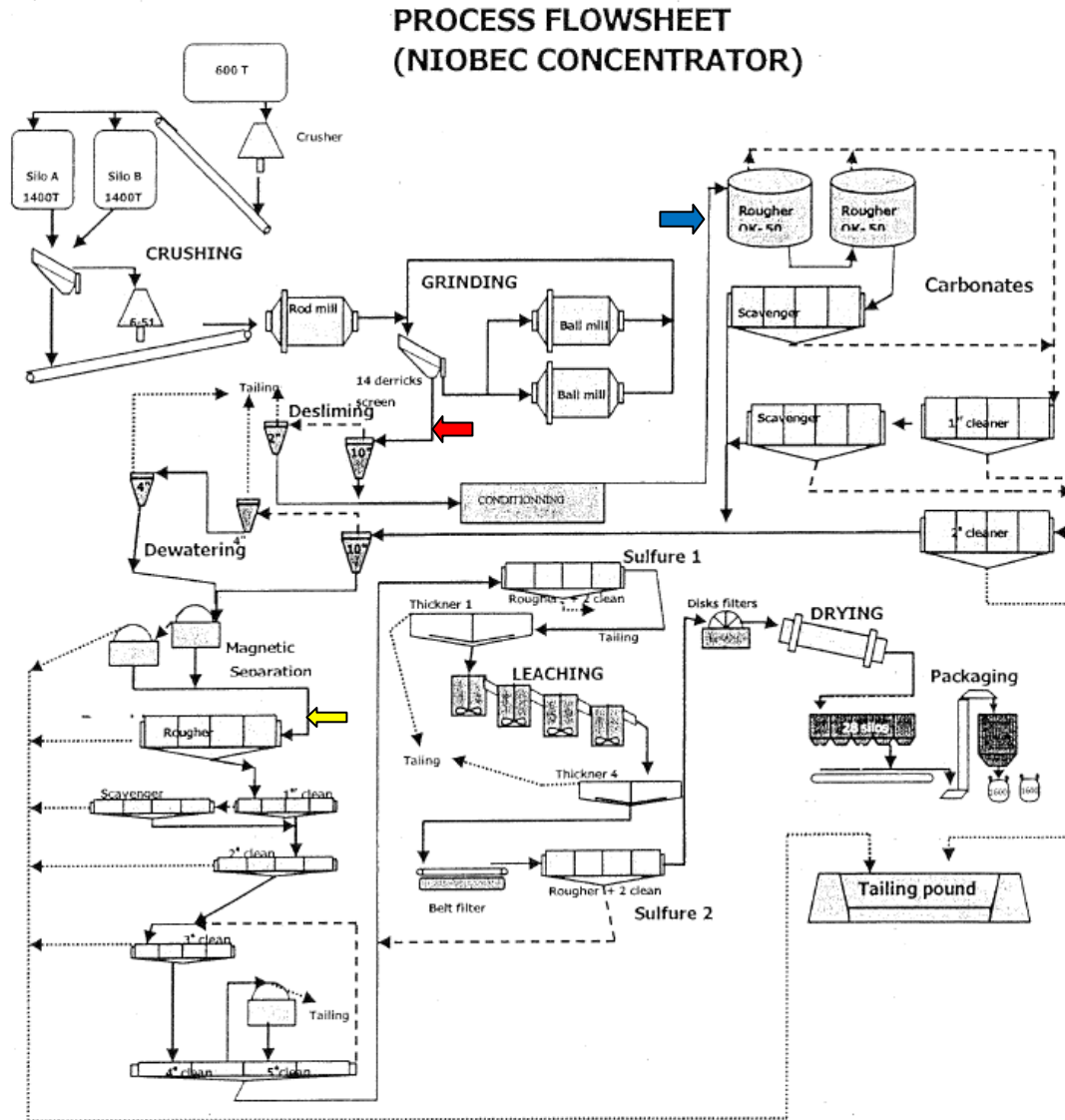


Figure 1.1 Process flowsheet of Niobec concentrator (Arrows indicate points of sample collection. for this research. Red arrow: Mill Feed; blue arrow: Carbonate Feed; yellow arrow: Pyrochlore Feed).

According to IAMGOLD's technical report (2009), the total metallurgical recovery of niobium oxide was 58.9%. The loss of pyrochlore comes from the

shortcomings of the flowsheet, which by our reading of the flowsheet, include the following:

1. Since the cationic collector can also float the gangue minerals, many processing stages including desliming, reverse flotation (of carbonates, pyrite), magnetic separation and leaching are used to reject the gangue minerals before or after pyrochlore flotation. The full recovery of niobium oxide is usually impossible to achieve at each stage in real industry operation; a small amount of pyrochlore loss in each stage is inevitable, which accumulates to significant losses of the pyrochlore mineral.

2. The reverse carbonate flotation is conducted at the very beginning of the flowsheet. This is against one of the important rules-of-thumb in flotation circuit design, i.e., the minor component should be floated to avoid high consumption of reagents and entrainment of the minor components, which are likely to happen when the major components are floated. Since about 65% of the mass in the ore is carbonate, the pyrochlore (less than 1% of the mass) can easily entrain in the carbonate concentrates, which causes loss of the pyrochlore.

3. The double desliming stages discard 15% of pyrochlore in slimes. Clays/slimes (which are usually negatively charged) consume cationic collectors during flotation, so it is necessary to remove them before cationic flotation. However,

pyrochlore is a friable mineral and tends to form slimes during grinding. Desliming is one of the major reasons causing pyrochlore loss.

4. The adjustments of pH are frequently needed during the whole process to enhance the flotation recovery and selectivity. For instance, the current pyrochlore flotation stage need progressively lower pulp pH to reject silicate gangue; however, the subsequent sulfide flotation stage needs to be carried out at a high pH of 10.5. Adjusting slurry pH back and forth increases the complexity of the operation and control of the process, as well as reagent costs.

5. During the cationic flotation of pyrochlore, a very acidic pH of 2.5 is required to reject the silicate gangue minerals. This acidic pulp requires corrosion-resistant equipment and high maintenance costs. Moreover, at such low pH, the carbonates are dissolved consuming large amount of acid. That is one of the reasons that carbonates are removed in a preceding reverse carbonate flotation step.

All the above shortcomings are caused by the lack of an efficient collector for the niobium oxide minerals. The cationic collectors, based on electrostatic adsorption, cannot separate pyrochlore from the gangue minerals. However, a suitable anionic collector based on chemisorption could be the solution to most of the problems encountered in the Niobec ore concentration process. The chemisorbing anionic collector molecules may still adsorb on the negatively charged pyrochlore surface under neutral or slightly alkaline pH because of the formation of the surface

chemical bonds. A suitable anionic collector could drastically simplify the flowsheet, i.e., the slimes may not need to be removed, the reverse carbonate flotation may not be necessary, and the process steps can be reduced while the overall niobium oxide recovery can be significantly increased from the current 58.9%.

1.4. Objectives

From the foregoing description, the objectives of this study are:

(1) As a collaborative research and development project, our major goal is to find a suitable combination of collector and depressant to selectively float the niobium minerals, primarily pyrochlore, from the carbonatite ores of Niobec Mines. A better collector and depressant combination could not only recover the niobium minerals directly from the gangue minerals in fewer steps, it could also be used under natural pulp pH (which is alkaline due to the high concentration of carbonate minerals). The results of this project will be beneficial to the Niobec Mine to build a simpler flowsheet. The results are potentially useful to the other niobium mines over the world as they essentially are using similar flowsheet as the Niobec Mine.

(2) Carry out fundamental studies to understand the action mechanisms of the developed collector(s) and depressant(s). Such a study will benefit the academics in thermodynamics, solution chemistry, surface and colloid science, as well as the mineral processing industry when the new reagent scheme is implemented.

This research will result in a better understanding of the roles of chelating reaction and chemisorption in flotation system and the major reasons for the different hydrophobicity generated after competitive adsorption on niobium

containing minerals and carbonate gangues. The primary drive of this study is to find an alternative reagent combination for pyrochlore ore processing. But the research results may be useful for other oxide minerals such as tantalum, rare earth metals, etc.

1.5. Research Methodologies

Both experimental and analytical studies are carried out to accomplish the aforementioned objectives:

(1) Small-scale flotation: single mineral and mineral mixtures of high purity samples of pyrochlore, calcite, hematite and quartz were tested using various reagents and different reagent concentration and pH; this is a fast and economic screening method of potential candidate reagents.

(2) Batch flotation: the reagents which are proven effective in small-scale flotation will be further tested in batch flotation under various slurry chemistry conditions on Niobec ore samples. Both rougher and cleaner flotation stages are carried out.

(3) Adsorption mechanism studies: The characteristics of adsorbed reagents on the pyrochlore and calcite are investigated by diffuse reflectance Fourier-transform infrared spectroscopy (DRIFTS FTIR), X-ray photoelectron

spectroscopy (XPS) and time of flight secondary ion mass spectroscopy (ToF-SIMS). The adsorption isotherms of flotation reagents on the high purity single minerals are measured by the depletion approach.

1.6. Organization of this thesis

This thesis begins with Chapter One which contains an introduction to the background, objectives and methodologies of the study. This is followed by:

Chapter Two which reviews the literature on the surface and coordination chemistry, flotation reagents with a focus on chelating reagents, as well as reagent design and development during recent decades. Reagents tested for niobium containing minerals are also reviewed in this chapter.

Chapter Three which presents the chemicals and materials used in this work. Mineral samples, reagents and experimental procedures are described.

Chapter Four which presents the flotation test results including both small-scale and batch flotation tests, along with adsorption mechanism studies obtained from adsorption isotherm measurements, diffuse reflectance Fourier-transform infrared spectroscopy (DRIFTS FTIR), X-ray photoelectron spectroscopy (XPS) and time of flight secondary ion mass spectroscopy (ToF-SIMS). The origin of the selectivity of the reagents is also discussed in this chapter.

Chapter Five which contains a summary of the finding, the important conclusions, the contributions and recommendations for future work.

2. Literature review

2.1. Mineral Processing

Mineral processing, also known as ore dressing, mineral dressing, or milling, prepares the ore for extraction of the valuable metal for most of the metallic ores. It usually follows mining. The major objective of mineral processing is to physically separate the value minerals from the gangue minerals (Wills, 1997). This physical upgrading before smelting reduces the bulk of the ore which must be transported and processed in the smelter, lowering energy costs and improve processability. Some of the important mineral processing (physical upgrading) methods include sorting, gravity separation, magnetic separation, and froth flotation, which utilize the differences in physical properties such as appearance, specific gravity, magnetic susceptibility and surface wettability of the minerals.

One challenge of mineral processing is the depletion of high grade ores, and new ore bodies that are found are of relatively lower grades and more complex mineralogy. Moreover, some minerals exist only in low grades in their ores, such as rare earth oxide, uranium, niobium and tantalum. For example, the uranium ore deposit in Trekkopje, Namibia contains only 0.011% U (Chaki et al, 2011), and the niobium ore deposit from where we obtained ore samples contains less than 2% niobium-bearing minerals (Table 1.1).

Anderson et al. (2000) outlined the challenges currently faced by the minerals industry in the mineral processing area:

- 1). Fine particle recovery and separation: Recovery and separation of fine particles by the mineral processing techniques is more difficult and consequently, a significant portion of many value minerals are lost in the fine size fractions generated from fine grinding, which is deemed necessary to treat the increasingly lower grade more complex ores.
- 2). Process design and controls: aiming at improvements in energy and cost savings, this can be assisted by empirical models and simulations.
- 3). Increase separation kinetics.
- 4). Improving energy efficiency and reducing environmental impact.
- 5). Increasing direct conversion and in-situ recovery.

2.2. Froth Flotation

Froth flotation separates different minerals based on their different surface hydrophobicity, which dictates the propensity of the mineral particles to attach to gas bubbles or oil droplets dispersed in ore slurry. Figure 2.1 shows schematically the froth flotation process inside a flotation machine. As can be seen, small

particles with certain degree of hydrophobicity are captured by air bubbles in the slurry, followed by their levitation and collection into a froth layer which ultimately is scrapped away as concentrate, while the hydrophilic particles are left in the pulp and discharged as tailings, leading to the separation of the hydrophobic mineral particles from the hydrophilic mineral particles.

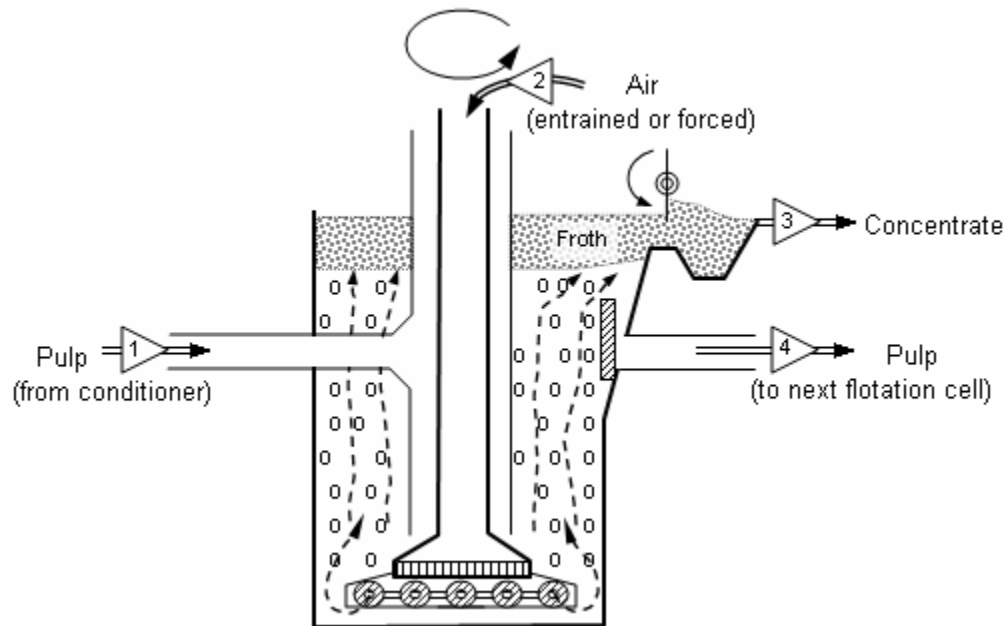


Figure 2.1 Froth flotation cell (Webster's online dictionary, 2012).

Froth flotation is without a doubt the most important method of concentration in mineral processing. By adjusting the pulp chemistry environment with different reagents, it is possible to selectively make one mineral hydrophobic while keeping the rest hydrophilic. It was invented in early twentieth century for treating sulphide minerals initially; nowadays its application has been expanding to include oxides (such as, hematite, cassiterite, malachite, cerussite) and non-metallic ores (such as coal, phosphate, fluorite). The invention of froth flotation

enabled the exploration and utilization of low grade and/or complicated ores which had been considered uneconomic to mine. This is of significant importance for current mining and mineral processing industry due to the gradual depletion of high grade ores.

The application of froth flotation is not limited to the mineral and coal industry. It has also been used in plastic separation (Drelich et al., 1999), plastics recovery from municipal wastes (Shen et al., 2002), removal of ink from recycled paper (Moon and Nagarajan, 1998; van de Ven et al., 2001), waste water treatment (Rubio et al., 2002), oily sewage treatment (Zheng and Zhao, 1993), processing of copper slags (Ozbayoglu and Akgok, 1995), separation of converter matte (Agar et al. 1996), contaminated soil rehabilitation (Mulleneers et al., 1999), separation of mixed ion-exchange resins (Lee et al., 2002), fly-ash beneficiation by removing unburned carbon (Kawatra and Eisele, 1996), and extraction of bitumen from oil sands (Long et al., 2007). These applications for separating materials other than minerals and coal are growing steadily. The fundamental theories and processes of froth flotation are not fully understood, such that froth flotation is still an art rather than science more than a century after its invention.

In froth flotation, air bubbles will attach to mineral particles if they can displace water from mineral surface. Such attachment can only occur on mineral surface which has certain degree of hydrophobicity. And hydrophobicity of the mineral surface can be altered by different flotation reagents.

2.3. Electrical double layer (EDL)

Froth flotation utilizes the differences in the physico-chemical surface properties of particles of various minerals. Basic surface chemistry of mineral particles is utilized in the selective flotation process.

The electrical double layer (EDL) is proposed to describe particle surface charge and it is one of the most important theories in surface chemistry. When mineral surfaces are brought into contact with an aqueous medium, they generally acquire an electric charge unless it is at point of zero charge (PZC: the pH at which the net charge on the surface is zero). Possible charging mechanisms are ionization, ion adsorption, ion dissolution, and isomorphous substitution. The surface charge affects the distribution of nearby ions in the aqueous medium: ions of opposite charge (counter-ions) are attracted towards the surface and ions of like charge (co-ions) are repelled from the surface forming an electrical double layer.

Figure 2.2 shows the potential drop across the double layer into the liquid phase. The layer consists of three parts from solid to the bulk liquid: (1) the potential-determining ions, which may be considered as part of the solid lattice; (2) the counter-ions, held directly to the surface in the plane; (3) the counter ions which form a diffuse atmosphere called the Gouy layer in which the counter-ion population density decreases exponentially as a function of distance from the surface. The potential at the slipping layer is defined as zeta potential; which is

usually used for quantifying the strength of an electrical double layer of a solid particle.

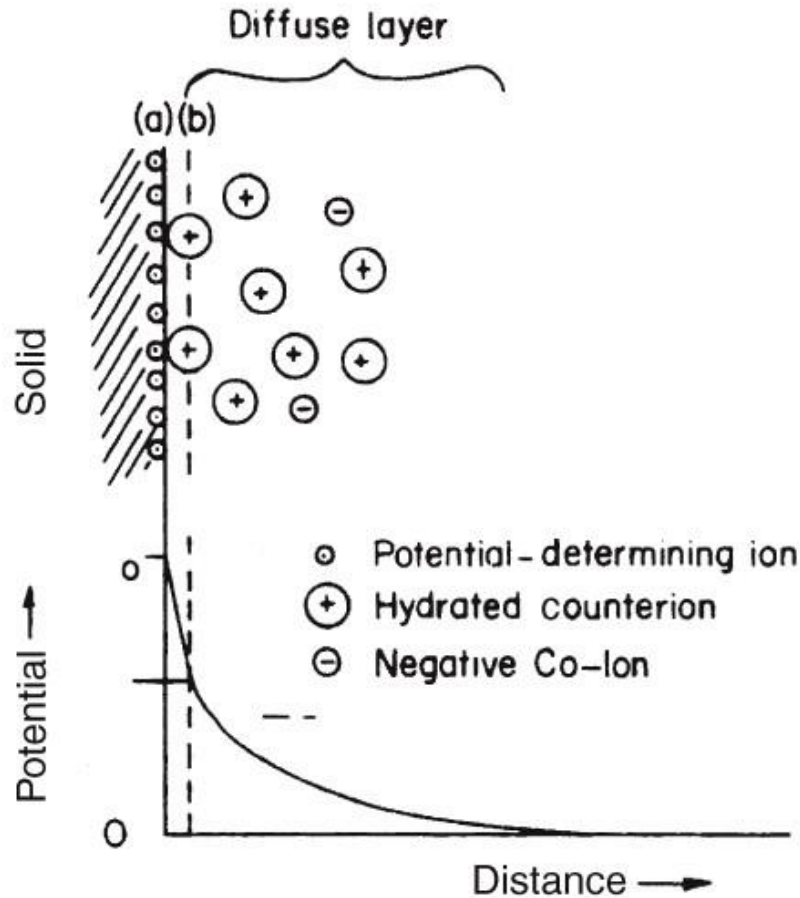


Figure 2.2 Electrical double layer on the solid particle and potential drop across the double layer (Bulatovic, 2007).

The potential determining ions might be the major reason for the formation of the electrical double layer. For many oxides or oxidized minerals, H^+ and OH^- are primarily potential determining ions. For example, the mechanism that hematite acquires surface charge can be illustrated as follows:

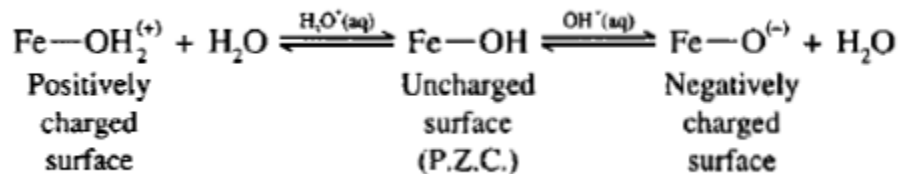


Figure 2.3 The surface charges and surface determining ions on hematite
(Uwadiale, 1992).

Physical adsorption occurs based on the opposite charge of adsorbate and adsorbent. Since H^+/OH^- are important surface determining ions for the majorities of oxide/oxidized minerals, controlling pH would be very important for physisorbing reagents.

2.4. Flotation Reagents

In order to achieve controlled pulp conditions, various chemical compounds can be introduced at different stages of flotation operation. Control of reagent addition is of vital importance in the modern treatment process. Newer and better (more selective) reagents always lead to advances in flotation and drastically improve flotation circuit performances.

By functions of their usage in froth flotation, flotation reagents can be grouped into frothers, regulators, and collectors. While frothers and regulators are described in the following, collectors will be further discussed in the next section.

Frothers are a type of chemical compounds, which can adsorb on water-air interface and decrease the surface tension of water. They increase the strength of water films around bubbles and reduce the bubble size. Most important frothers are neutral molecules, usually they are alcohols. They are functional in both acidic and alkaline pulp. Polyglycol ether was firstly developed as frother in 1950's (Bulatovic, 2007). Its molecular weight and carbon length determines its power and performance. DF250 with formula $\text{CH}_3(\text{OC}_3\text{H}_6)_4\text{OH}$ is able to produce smaller bubbles in flotation (Grau et al., 2005).

Definitions of regulators is arbitrary in current knowledge, they often can be further categorized into three reagent groups: activators, depressants, and pH modifiers. These reagents can enhance the selectivity of flotation by modifying the actions of the collectors on mineral surfaces. Activators and depressants facilitate and prohibit the interactions of collectors with target mineral surfaces, respectively. Both activators and depressants can be either inorganic or organic compounds. The purpose of pH modifier is to regulate the ionic concentration in the pulp by controlling the hydrogen ion concentration. Sodium hydroxide and hydrochloric acid are widely used as pH modifiers which enable pH adjustment between 0 and 14, but typically between pH 4 and 12 in mineral flotation.

2.5. Collectors

Collectors are a group of surfactants that have at least one polar and one non-polar group in their molecular structures.

The basic function of collector is to selectively form a hydrophobic coating on the desired minerals to facilitate their attachment to air bubbles and ultimate recovery into the froth layer. Most collectors are ionizable. Depending on the charges of the ionized groups that are formed, collectors can be categorized into three groups, anionic, cationic and nonionic collectors. Currently, the majority of the commercially used cationic collectors are derived from amine. Anionic collectors can be subdivided into oxyhydryl collectors and sulfhydryl collectors depending on the functional groups. Oxyhydryl collectors are mainly used for oxide ore flotation, and examples of oxyhydryl collectors are fatty acids and sodium dodecyl sulfate (SDS). Sulfhydryl collectors contain thiol functional groups and are mainly used for the flotation of sulfide minerals. Typical examples are xanthate and dithiophosphate. The most commonly used nonionic collectors are hydrocarbon oils such as kerosene and fuel oil, and they are used for the flotation of naturally floatable minerals to enhance the flotation.

The high grade and easy-to-process ores have been gradually depleted, and low-grade, finely disseminated and complex ores have become the major sources of mineral or raw materials (Abouzeid, 2008; Wills, 1997). More selective and specific flotation reagents which are capable of interacting with specific ions on mineral lattice are required to make processing this type of ores possible.

Though many effective reagents have been used throughout the development of mineral processing, there is still the need for novel and more effective reagents for the following reasons:

- a. The enhanced awareness and concern for environment and more strict environmental regulations demand nontoxic and environmentally friendly reagents.
- b. Difficult-to-process ores are becoming more prevalent. These include finely disseminated, polymetallic, and low-grade ores, mixed oxidized-sulfide base metal ores, etc.
- c. The need to improve process and energy efficiency and lower energy consumption.

While in the early years, finding a new collector was mainly based on trial and error, the recent trend is to use more specific strategies to develop a new collector. This approach utilizes the knowledge in coordination chemistry and chemical bonding, which leads to the formation of metal chelates and/or complexes. The initial step usually starts with the evaluation of donor-acceptor interactions between donor atoms (N, S, O or P) in functional groups of the collectors, and acceptor sites (metal atoms in the mineral). Design of new collectors can firstly focus on a basic group such as -C=S^- for sulfide and -C=O^- for oxide minerals,

followed by combining other incorporating donor atoms to build the polar head and finalized by adding a hydrophobic hydrocarbon tail. This approach has been accepted by commercial flotation reagent suppliers to develop a series of flotation collectors (Herrera-Urbina, 2003).

Many chemical compounds have been identified as potential collectors, however, commercial collectors used for most operations have not been changed for several decades. Adaptation of a new flotation reagent in a particular plant operation requires extensive testing.

2.6. Adsorption mechanism

Collectors can adsorb on certain mineral surfaces by its polar or ionized groups while the non-polar groups are oriented to the water phase. This configuration imparts or increases the hydrophobicity of the mineral surface, hence enhances the flotation of the mineral. Adsorption mechanism study is therefore important in flotation collector development. Due to the complexity of the flotation systems, the heterogeneity of the mineral surface, and the presence of various inorganic and organic species in the flotation pulp, a complete understanding of reagent adsorption in a given flotation system is not possible although many cutting edge technologies have been employed in such studies. Nevertheless, some general knowledge has been advanced.

Adsorption at the particle/liquid interfaces can be broadly grouped into two categories, i.e., that which is through physical adsorption, and that which is through chemisorption. Electrostatic interaction plays a significant role in the physical adsorption, and mineral surface condition such as surface charge is very important in physical adsorption. Since pulp pH strongly affects the mineral surface charge as well as the concentrations of ionized collectors, collectors based on physical adsorption usually have a sensitive range of functional slurry pH. On the other hand, in chemisorption, the polar or ionized groups in the collector molecules form chemical bonds with active sites on the mineral surface (usually the metal atoms), thus the collectors can be used in a wider pH range irrespective of mineral surface charge and they often show better selectivity in separating minerals from ores that possess more complex compositions.

In addition, chemisorption is accompanied by physical adsorption (co-adsorption). For Na-oleate on fluorite and barite at an alkaline pH, physical adsorption of non-ionized carboxylic acid could increase the overall hydrophobicity of the adsorbed layer (Peck and Wadsworth, 1965). Unfortunately, there are no current technologies to detect the arrangement of the molecules co-adsorbed on the mineral surfaces.

2.7. Coordination chemistry

Theoretical concepts of coordination chemistry and chemical bonding had led to most new reagents' inventions (Fuerstenau et al., 2000). Coordinate bonds are a special type of covalent bonds where the electrons for sharing are supplied by one atom rather than by the two atoms involved. Coordination compounds consist of a central atom or cation surrounded by electron-rich groups, also known as coordination complexes.

A majority of new developments in collector chemistry involve a functional group that contains two donor atoms capable of bonding a metal acceptor species and of forming a ring structure known as chelate complexes, which are more stable than simple chemical bond. The enhanced stability (chelate effect) is due to a favorable entropic contribution irrespective of the associated enthalpy changes. The large increase in entropy is due to the net increase in the number of unbound molecules released. For metal cations in solution, usually the released nonchelating ligands are water molecules (Crichton, 2012).

Stability constant is usually used to quantify the stability of the chelate complexes. Chelating type collector molecules contain a reactive functional group with atoms such as S, N, O and P in positions which are capable of bonding the same metal atom site through two (bidentate) or more than two different atoms (polydentate) to form a heterocyclic ring including the attached metal atom. For bidentate reagents, they can be grouped into S-S, S-N, N-N, N-O and O-O types depending on the type of atoms which bond to the metal cations.

2.8. Hydroxamate/hydroxamic acid

Recently, chelating collectors have drawn much attention. They have at least two functional groups in their molecular structures which could form coordination bonds with the metal ions on the ore surface. It is usually less pH dependent than the collectors which act through electrostatic interaction and shows better selectivity (Klimpel and Free, 1993; Pradip, 1991; Wang et al., 2006). It is not surprising to see that most of new commercial collectors are chelating reagents.

Hydroxamic acid ($R-CO-NH-OH$) was initially used in analytical chemistry as a chelating agent to conduct chemical analysis. Its molecular structure can be seen as a carboxylic acid molecule with an inserted hydroxylamine group (Figure 2.4). Khalil and Mahmoud (2008) measured the stability constant of varieties of complexes formed between metal cations and hydroxamic acid by titration. They found that calcium and magnesium cations cannot form stable complexes with acetohydroxamic acid (AHA) and benzohydroxamic acid (BHA). Salicylhydroxamic acid (SHA) could form very weak complexes with calcium or magnesium ions, but its stability constant is at least two magnitudes lower than those formed by any transition metal bivalent ions. The order of complexes stability with respect to metal ions is: $Fe(III) > Al(III) > Cr(III) > Cu(II) > Ni(II) > Co(II) > Zn(II)$. It was observed that higher valence metal cations could form stronger complexes. Stability constant with respect to ligand follows this order SHA (salicylhydroxamic acid) $> BHA > AHA$ (Khalil and Fazary, 2004).

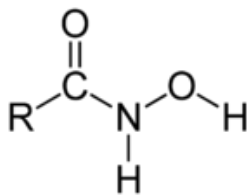


Figure 2.4 Molecular structure of hydroxamic acid.

Hydroxamic acid shows the best collecting power in flotation tests in the neutral and slightly alkaline slurry environment, usually within pH 6-9, and the pH dependence is not as strong as the collectors based only on electrostatic interaction. This pH range fits the majority of the ore slurries without the need for adjustment, which is one of its advantages (Quast, 2000; Sreenivas and Padmanabhan, 2001).

The length and structure of its hydrophobic tail can affect the collecting power of the hydroxamic acid (Natarajan and Nirdosh, 2003). It is suggested that a mixture of hydroxamates with a hydrocarbon tail of 7 to 9 carbon atoms works best (Bulatovic, 2007). The hydroxamic acid with 7 to 9 carbon atoms in the hydrocarbon tail is only slightly soluble in water. To be used as a collector for mineral processing, usually it is prepared as an alcohol solution. Unlike water-soluble collectors whose molecules adsorb on the mineral surface and the hydrocarbon chains increase the surface hydrophobicity, the insoluble alcohol droplets attach and spread on the mineral surface. This alcohol layer increases the hydrophobicity of the surface covered (Wang et al., 2006).

Due to its high selectivity towards metal ions in the alkaline region, hydroxamic acid/hydroxamate was employed as a collector in many oxide ores, like cassiterite, copper oxide ore and rare earth oxide minerals (Marinakis and Kelsall, 1986; Ren et al., 1997; Lee et al., 1998; Quast, 2000; Fuerstenau et al., 2000; Sreenivas and Padmanabhan, 2001). Recently, hydroxamic acid was also studied in the flotation of niobium containing minerals in the laboratory and positive results were reported (Espinosa-Gomez et al., 1987; Zheng et al., 1996; Chen et al., 2005). Studies done by Ren et al. (2004) indicated that the alkyl hydroxamic acid floats fersmite under neutral or mild alkaline pH in the small-scale flotation tests. However, it also floated other gangue minerals which implied that suitable depressants should be employed to separate the niobium mineral from gangue minerals (Figure 2.5). This was also observed in the small-scale flotation tests of niobite conducted by Chen et al. (2005). Currently, from small-scale flotation tests on collector screening, hydroxamic acid seemed to have worked effectively on the niobium containing materials.

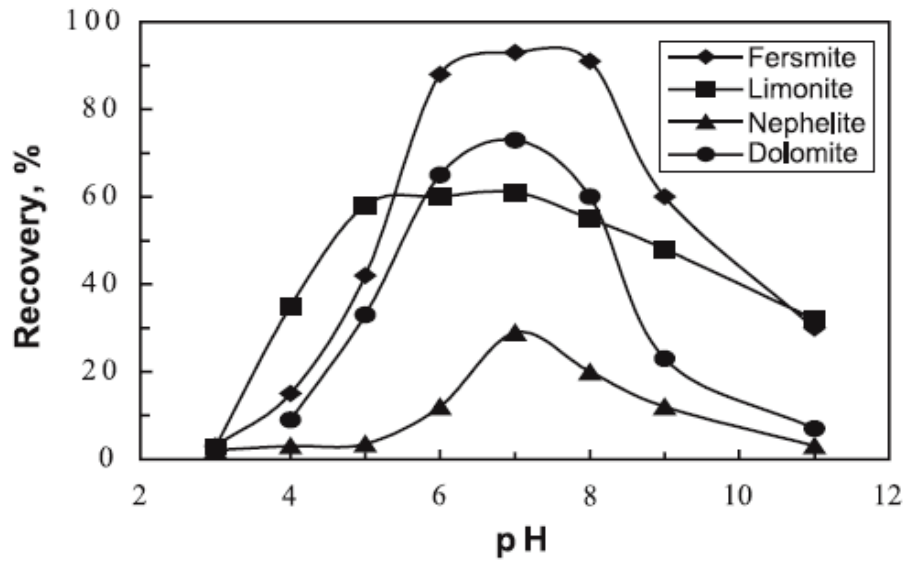


Figure 2.5 Recoveries of different minerals using 10 mg/L alkyl hydroxamic acid (Ren et al., 2004).

Some products based on hydroxamic acid were commercialized. One of them is a collector with a trade name IM50, which is mainly used in Russia. Other collectors containing hydroxamic acids are manufactured by Hoechst (Germany), Cytec (USA) (trade name Aero 6493) (Bulatovic, 2007), and Axis House (Australia) (trade name AM28) (Chowdhury, 2012). Hydroxamic acid is superior to carboxylic acid in terms of selectivity, but its price is higher limiting its usage in high grade oxide ores such as iron ores.

2.9. Depressant

Depressant prevents the attachment of air bubble to mineral surface by changing its hydrophobicity. Unlike collectors which are all organic compounds, depressant

can be inorganic or organic compounds. An important type of organic depressants is polymer such as starch, dextrin, carboxymethyl cellulose, and lignin sulfonates, etc. These polymers can also be modified by grafting functional groups which increase the selectivity of the depressants.

Depressants influence mineral flotation in several different ways, include:

(1) They react with mineral surfaces resulting in a change of the chemical composition which could prevent collector adsorption. For example, sodium cyanide can dissolve copper from the sphalerite surface and prevent the adsorption of xanthate collectors on the sphalerite surface through the copper sites (Buckley et al., 1989).

(2) They can remove collector coating from the mineral surface causing depression of the mineral. For example, sodium sulfide can displace the adsorbed xanthate collectors from galena surfaces (Herrera-Urbina et al., 1999).

(3) They can form a hydrophilic film on the mineral surface. This will make the mineral surface hydrophilic irrespective of the presence of the adsorbed collectors (Hanna and Somsundaran, 1976).

Similar to the history of collector development, most of current commercial depressants have been developed by empirical methods. The strategy for

developing a new depressant is also very similar to that of a new collector. The only difference is that after the polar head is designed, a *hydrophilic* chain containing hydroxyl or carboxyl groups was added in case of depressant. In many cases the polar heads can be hydroxyl groups or carboxyl groups as well (Bulatovic, 2007).

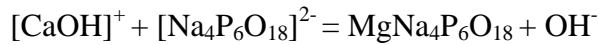
2.10. Salts of phosphoric and polyphosphorus acids

Salts of various phosphoric and polyphosphoric acids are used in flotation process. Sodium metaphosphate and polyphosphate are most important regulators, which are stable in the solution at room temperature. Polyphosphates and metaphosphates are used in flotation for a number of functions such as softening hard water (MacDonald, 1937), depressing iron sulfides during coal flotation (Jiang et al., 1999), and depressing alkaline earth minerals during flotation of nickel-molybdenum ores (Cao et al., 2010), copper-molybdenum ores (Nekhoroshev et al., 1978), beryllium ores (Havens and Nissen, 1964), lead ores (Cap and Machovic, 1962) and tungsten ores (MacDonald, 1937). It is also proven to be an effective depressant for quartz and feldspars in flotation of rare metal and rare earth metal minerals (Shchervakov, 1964).

Sodium metaphosphates have a general formula $\text{Na}_n\text{P}_n\text{O}_{3n}$ or $(\text{NaPO}_3)_n$. The major functional group is the negatively charged $(\text{P}_n\text{O}_{3n})^{n-}$ ion ring which is connected by oxygen bridges. So it is a long-chain inorganic salt, a spiral chain polymer

derived by polymerization from numerous basic structural units, and can be expressed as $(\text{NaPO}_3)_n$, where $n = 20-100$ (Bulatovic, 2007). Sodium metaphosphate (NaMP) was generated from dehydration of sodium orthophosphate along with polyphosphate.

Sodium hexametaphosphate (NaHMP) is a typical metaphosphate with formula $\text{Na}_6(\text{PO}_3)_6$. It was usually used in controlling flotation pulp with slimes or clays. NaHMP has a good capacity of complexation with bivalent metal ions including calcium and magnesium forming $\text{Na}_4\text{MeP}_6\text{O}_{18}$ or $\text{Na}_2\text{Me}_2\text{P}_6\text{O}_{18}$ due to weak acid reaction (Thomson, 1936). Some cations may react with NaHMP or NaMP as follows:



These reactions generate soluble complexes, and surface cations such as Ca^{2+} and Mg^{2+} could be dissolved.

Lu et al. (2011) indicated that NaHMP could depress serpentine (a gangue mineral containing magnesium and prone to sliming) in an alkaline suspension when floating pyrite. The action mechanism is that it lowers the isoelectric point of serpentine by dissolving the calcium from serpentine surface. Thus, the total

interaction energy at pH 9 between serpentine and pyrite became repulsive according to DLVO theory (Figure 2.6).

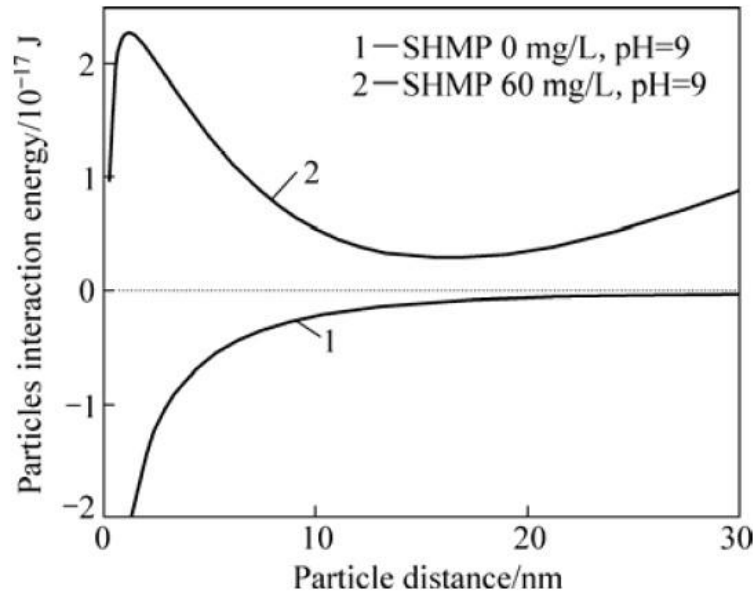


Figure 2.6 Interaction energy between pyrite and serpentine particles at pH 9 (Lu et al., 2011).

2.11. Reagents tested for Nb-containing minerals

Cationic collectors (amines) have been reported widely for the flotation of niobium containing minerals (Burks, 1958; Faucher, 1964; Poliyo and Hirvonen, 1976; Biss, 1982; Rao et al., 1988; Oliverira et al., 2001); it is also used in Niobec concentrator process. However, the attempts of using anionic collectors such as oleic acid were also made in the past (Shapovalov et al., 1958; Abeidu, 1974). Other two particular types of anionic collectors, hydroxamate and phosphonate were investigated in lab scale as collectors for niobium containing minerals but

have not been used in industrial operations (Espinosa-Gomez et al., 1987; Zheng et al., 1996; Chen et al., 2001).

Oxalic acid has been proven to be a selective gangue depressant during pyrochlore flotation using cationic collector (Bulatovic, 2010). Sodium hexametaphosphate (as in the commercial product Calgon) and sodium pyrophosphate were also investigated as a potential depressant. The addition of 50 g/t Calgon can depress the gangue minerals while doubling the niobium grade in the concentrates (Pavlor, 1976).

3. Experimental Materials and Methods

3.1. High purity mineral samples

High purity sample of pyrochlore (57.1% Nb_2O_5) in a powder form (-75+38 μm) was obtained from COREM. The sample was isolated from the Niobec ore by repeated gravity and magnetic concentration. Calcite (58.34% CaO) and quartz (99.07% SiO_2) samples were purchased from Ward's Scientific Establishment, Ontario. Hematite sample was obtained from the spiral concentrate stream of Wabush Mine, Newfoundland and Labrador. The calcite and quartz samples were first separately crushed by a hammer, ground in a mechanized agate mortar and pestle grinder and screened to collect the -75+38 μm for small-scale flotation tests, and the -25 μm for adsorption mechanism studies. The hematite samples were ground in the agate mortar and pestle grinder directly to collect the corresponding fractions since they were received as powder form. The pyrochlore was used in small-scale flotation without further size reduction and it was ground to collect the -25 μm for adsorption mechanism studies. The chemical assays of the mineral samples are shown in Table 3.1. Since Nb_2O_5 content in pure pyrochlore is 66.55%, this sample contains approximately 86% pyrochlore.

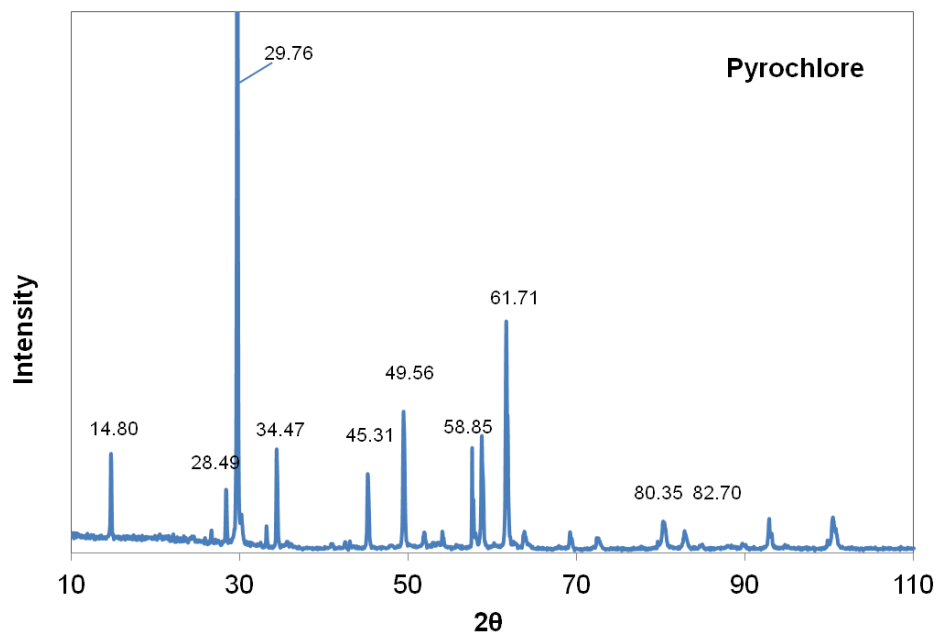
Table 3.1 Chemical assays (wt. %) of high purity mineral samples used in small-scale flotation.

Sample name	Pyrochlore ¹	Calcite ²	Quartz ²	Hematite ²
SiO ₂	2.83	0.02	99.07	2.63
Al ₂ O ₃	0.33	0.02	0.20	0.12
Fe ₂ O ₃	10.10	0.01	0.03	93.38
MgO	0.14	0.22	0.02	<0.01
CaO	11.90	58.34	0.03	0.04
Na ₂ O	4.50	0.03	0.02	<0.01
K ₂ O	0.25	<0.01	<0.01	0.01
TiO ₂	4.10	<0.01	<0.01	0.02
MnO	0.40	0.02	<0.01	2.71
P ₂ O ₅	0.11	<0.01	<0.01	0.02
Nb ₂ O ₅	57.10	--	--	--
ZrO ₂	1.18	--	--	--
Ta ₂ O ₅	0.31	--	--	--
BaO	0.39	<0.01	<0.01	0.04
Y ₂ O ₃	0.08	--	--	--
SrO	0.98	--	--	--
ThO ₂	1.32	--	--	--
Ce ₂ O ₃	0.63	--	--	--
La ₂ O ₃	0.16	--	--	--
Nd ₂ O ₃	0.25	--	--	--
LOI	1.68	43.7	0.45	0.96

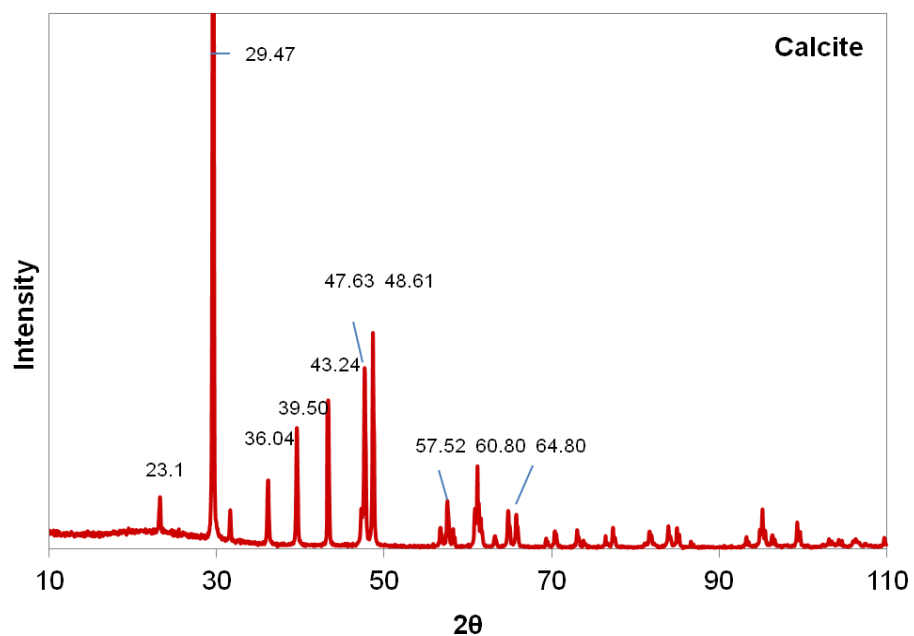
Assay done by: ¹ COREM, Quebec City, Quebec. ² Inspectorate America

Analytical Division, Richmond, British Columbia.

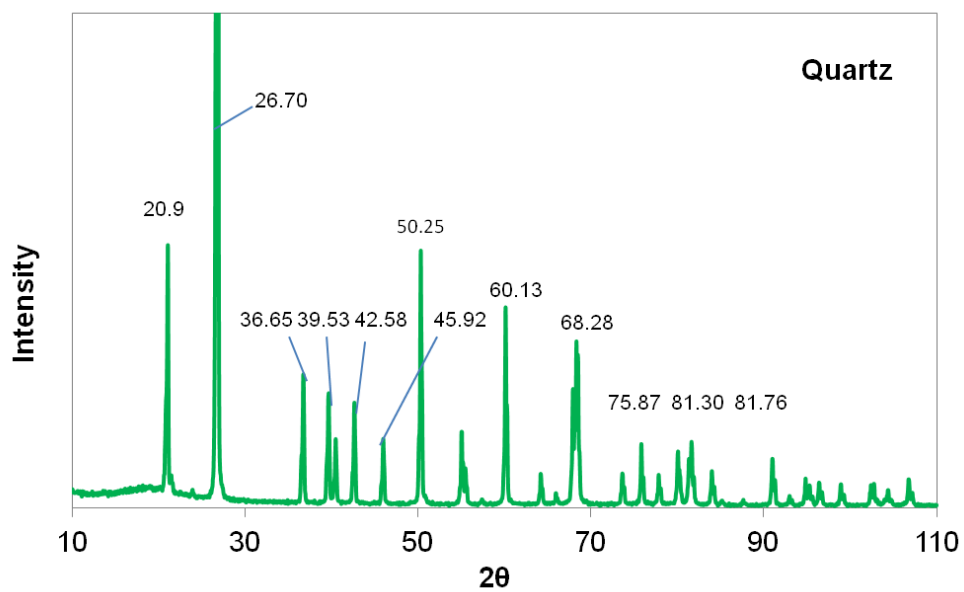
The XRD patterns of pyrochlore, calcite and quartz are shown in Figure 3.1. The XRD patterns were obtained on a Rigaku rotating anode XRD system with copper anode as the X-ray source and curved graphite as a monochromator, operating at 40 kV and 110 mA and under continuous mode (2 degrees per min). Matching peaks were all labeled on the spectrum. Most of the peaks match the pure standard crystal which indicated that the purity of the mineral samples is relatively high.



(a)



(b)



(c)

Figure 3.1 XRD patterns of (a) pyrochlore (b) calcite (c) quartz.

The high purity mineral pyrochlore and calcite were employed in adsorption mechanism studies to represent the niobium containing value mineral and the carbonatite gangue. Dolomite is the major carbonate gangue mineral in the Niobec ore, however some studies have proved that dolomite responds to anionic collector similarly with calcite (Hirva and Tikka, 2002; Liu and Liu, 2004). So we chose the most common carbonatite mineral, calcite, in our small-scale and adsorption mechanism studies. The specific surface areas of the -25 μm pyrochlore and calcite samples were determined by Quantachrome Autosorb 1MP (Quantachrome Instruments USA) using nitrogen as adsorbate based on the BET theory, and the results are 0.88 and 1.27 m^2/g , respectively. For FTIR and XPS measurements the -25 μm fraction was further ground to approximately 2 μm .

3.2. Niobec ore samples

Three ore samples were taken from three different points of the process flowsheet in Niobec Mines (Figure 1.1), which were labeled as Mill Feed, Carbonate Float Feed, and Pyrochlore Float Feed. All three samples were collected in wet slurry form. After decanting the process water, the samples were air-dried under room temperature, split into 500-gram batches and stored in sealed plastic bags for batch flotation tests. The assays and particle size distribution of these three samples are listed in Table 3.2 and Figure 3.2. It is not clear why the Carbonate Feed had a slightly lower Nb_2O_5 contents than the Mill Feed. This could be due to random fluctuations in plant sampling and chemical analysis, or it may also be possible that the slimes contain more Nb_2O_5 .

Table 3.2 Assays of the three plant ore samples (wt. %).

	Mill Feed	Carbonate Feed	Pyrochlore Feed
Nb_2O_5	0.70	0.67	0.86
Fe_2O_3	9.44	8.34	8.33
CaO	28.90	29.20	27.10
MgO	11.90	12.00	11.80
SiO_2	7.18	7.56	11.50
Al_2O_3	1.96	2.01	3.02
K_2O	1.04	1.13	1.79
MnO	0.71	0.72	0.69
Na_2O	0.24	0.24	0.30
P_2O_5	4.29	4.11	2.95
TiO_2	0.23	0.22	0.27
ZrO_2	0.11	0.096	0.12
Ta_2O_5	< 0.01	< 0.01	< 0.01
LOI	30.2	32.2	30.7

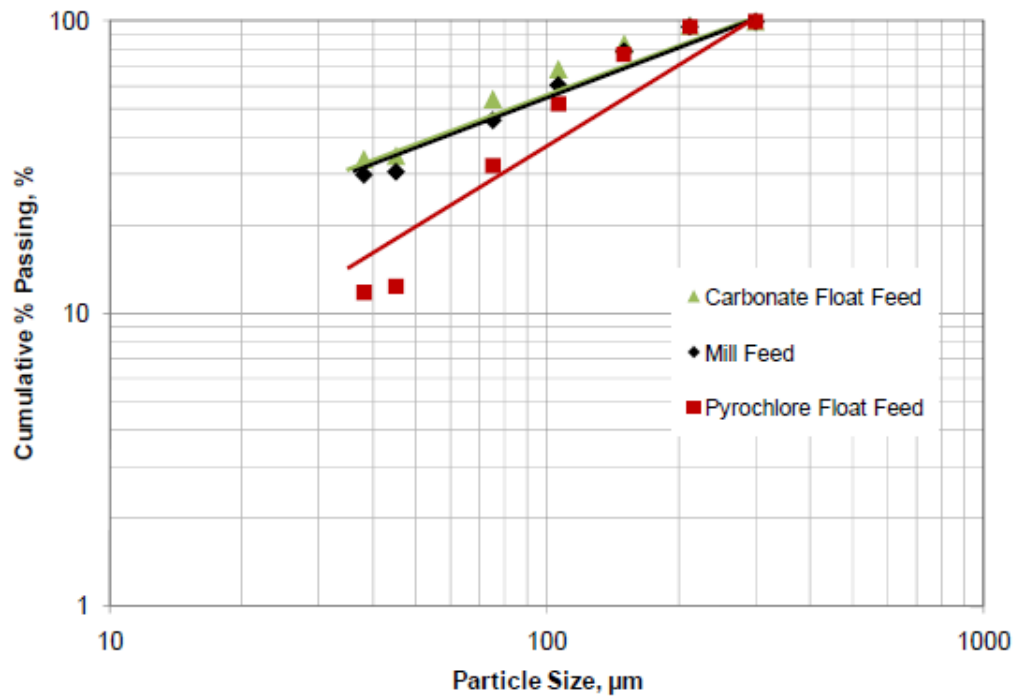


Figure 3.2 Particle size distribution of the three ore samples.

In order to study the effect of iron oxide gangue mineral content on the flotation, a feed sample was obtained by manually removing the magnetite from the Pyrochlore Float Feed using a hand magnet (purchased from Fisher). Magnetic separation is often used to separate the iron-containing minerals from other non-magnetic minerals. Magnetite can be removed by low-intensity magnetic separators for its ferromagnetism (Wills, 1997). For the magnetic separation, a 500 g pyrochlore flotation feed was spread on a smooth surface, and then the magnetic concentrate was collected by manually moving the hand magnet on the sample surface. The magnetic concentrate was found to weigh about 5 g and assayed 86.10% Fe_2O_3 , 3.02% CaO , 2.23% SiO_2 and 0.23% Nb_2O_5 .

Approximately 11% of the iron oxide gangue could be removed from the initial Pyrochlore Float Feed through this magnetic separation step with niobium oxide loss at 0.3%.

3.3. Reagents and chemicals

Commercial hydroxamic acid collector was acquired from Cytec (Cytec Aero 6493). High purity octyl hydroxamic acid (OHA) and diphosphonic acid were both synthesized in our lab (Section 3.4.1) from the chemicals purchased from Sigma-Aldrich. A high purity salicylhydroxamic acid (SHA) was purchased from Sigma-Aldrich. The hydrocarbon chain of salicylhydroxamic acid (Figure 3.3) is a phenol group which has greater polarity than the straight saturated aliphatic carbon chain in octyl hydroxamic acid. Thus it has better solubility and quicker dissolution rate than OHA in water. SHA was used to study the influence of hydrocarbon tail on the flotation of pyrochlore.

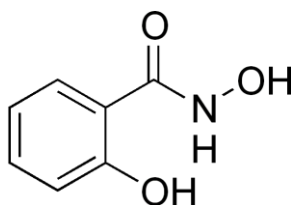


Figure 3.3 Molecular structure of salicylhydroxamic acid.

Sodium metaphosphate (NaMP, molecular formula: $(\text{NaPO}_3)_x \text{Na}_2\text{O}$ where $x \approx 13$), sodium hexametaphosphate $(\text{NaPO}_3)_6$, sodium silicate (modulus 1.0), oxalic acid, EDTA, tannic acid, catechol, sodium hydroxide and hydrochloric acid were all purchased from Fisher Scientific. Dowfroth 250 (DF250), obtained from Charles & Tennant (Canada) Co. Ltd., was used as a frother in some batch flotation tests. Potato starch was purchased from Sigma Aldrich. Distilled water was used in all tests.

3.4. Synthesis of pure reagents

3.4.1. Octyl hydroxamic acid

Normal octyl hydroxamic acid (OHA) was synthesized through the following steps that were adopted from Dutta and Ghosh (1967) with modifications:

1. Mix a solution of hydroxylamine hydrochloride ($\text{NH}_2\text{OH HCl}$, 0.2 mol, 14 g) in methanol (100 mL) with a solution of KOH (0.3 mol, 17 g) in methanol (50 mL) at 0°C (ice water bath) with stirring. Keep the mixture at 0°C (15 min) and precipitated KCl is filtered.

2. To the filtrate is added methyl octanoate ($\text{CH}_3(\text{CH}_2)_6\text{COOCH}_3$, 0.1 mol, 16 g).

The mixture is kept at room temperature for 24 h.

3. Concentrate the mixture with by evaporation with a fan.
4. The concentrated mixture is cooled in an ice water bath. The hydroxamic acid is precipitated by dilute HCl.
5. The precipitated hydroxamic acid is filtered, washed with ice cold water, and recrystallized twice from 0.5 mol/L hot acetic acid.

3.4.2. Diphosphonic acid

1-hydroxyalkylidene-1,1-diphosphonic acid was synthesized through the following steps that were adopted from Largman and Sifniades (1983) with modifications:

1. Add 1.5 mol of octanoic (caprylic) acid and 1.5 mol of distilled water to a reactor.
2. Add 1 mol of phosphorous trichloride through a funnel to the reactor over approximately 45 min while keeping the temperature between 30-40°C.
3. Keep the reactor at 40 °C for one hour after all phosphorous trichloride is added; then raise the temperature to 80°C and maintain for one hour, then raise temperature to 120°C and maintain for four hours.
4. Remove the heating pad and allow the reactor to cool overnight.
5. Remove hydrochloric acid by vacuum distillation at 100°C for one hour.
6. Stop vacuum distillation and add distilled water amounting to 10 wt. % of reaction mixture over approximately 10 min at 100°C.

7. Allow the mixture to hydrolyze for one hour between 50-80°C.
8. Vacuum distill the liquid for one hour at 100°C.
9. Stop heating and distillation, and collect the cooled product.

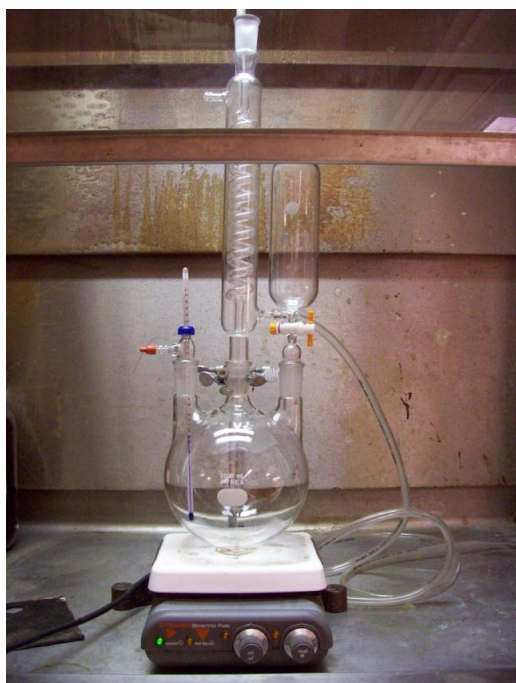


Figure 3.4 Apparatus for synthesizing diphosphonic acid.

3.4.3. Starch phosphate

Phosphate group had been shown to possess selective depressing function towards carbonate minerals (MacDonald, 1937). Starch was also reported as an effective depressant for carbonate (Irannajad et al., 2009) and iron gangues (Nanthakumar

et al., 2009). Therefore, it seemed reasonable to speculate that starch phosphate may be a better depressant than either metaphosphate or starch.

Acidic phosphorylation method is used as it generates mono starch phosphate with higher degrees of substitution. The molar ratio of phosphate/starch (AGU, anhydroglucose unit) is set to 0.5:1. It was synthesized through the following steps that were adopted from Passauer et al. (2010) with modifications:

1. Dissolve 3.7 g (0.031 mol) of NaH_2PO_4 in distilled water and make a 20 mL solution. Adjust the pH of solution to 6 with NaOH.
2. Add 10 g (0.062 mol) of starch in the salt solution and stir for 20 min to get consistent thick slurry.
3. Transfer the slurry into a coated baking pan; keep the pan in an oven for 12 hours under 50 °C until the slurry is dry.
4. Bake the dried mixture at 150 °C for 3 h.
5. Cool the mixture down to room temperature. Wash the unreacted NaH_2PO_4 away with ethanol/water (50/50) under 60 °C on a Buchner funnel.
6. Air-dry the sample for 24 h.

The final product is a yellowish powder and easily soluble in cold water giving a clear yellowish solution. The yield of this reaction is around 75%. Further characterization of the modified starch has not been carried out.

3.5. Small-scale flotation

Small-scale flotation is a fast and economic method to test a prospective combination of collector/depressant, and to select a proper pH range which the reagents can exhibit best performance. As discussed in the literature review, alkyl hydroxamic acid and some other chelating anionic collector could be effective collector(s) for niobium oxide; sodium metaphosphate could be effective depressant for the gangue minerals such as carbonates. Small-scale flotation tests were carried out to screen these reagents under various reagent concentrations and pH.

A custom-made glass flotation tube, shown in Figure 3.5, was used in the small-scale flotation tests. The base of the tube is a sintered glass frit with 1.6 μm pores, above which a magnetic stirring bar is placed to agitate the flotation pulp. The narrow throat connecting to the collection bulb ensures minimum mechanical entrainment.

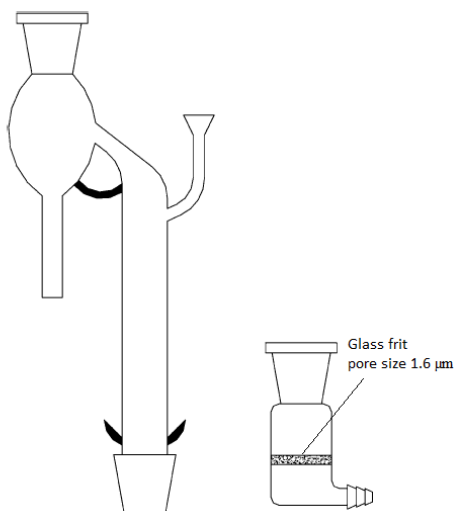


Figure 3.5 Schematic of the custom-made flotation tube.

In small-scale flotation, Aero 6493, high purity OHA and phosphonic acid were used as collectors. Sodium hexametaphosphate was used as a depressant. High purity single mineral samples including pyrochlore, calcite, quartz and hematite were tested in the small-scale flotation tests. In a typical test, 1.5 g -75+38 μm sample were mixed with 150 mL distilled water in a 250-mL beaker and agitated for 2 min under natural pH, followed by 1 min of conditioning after adjusting the pulp pH by sodium hydroxide or hydrochloric acid if desired. A designed dosage of collector was added with 1 min conditioning. This was repeated after the addition of a depressant (when used). Then the conditioned pulp was transferred to the flotation tube and floated with nitrogen gas at a flow rate of 10 mL/min for 1.5 min. For mineral mixture flotation tests, the procedure was the same except that 1 g of each desired mineral sample was used to prepare the mineral mixtures that were floated in the flotation tube. The grade and recovery was determined by

hydrochloric acid leaching, since calcite is soluble in hydrochloric acid but pyrochlore is not.

3.6. Batch flotation tests

Generally, batch scale flotation is a more reliable and trustworthy method than the small-scale flotation in a glass flotation tube. The batch flotation tests were carried out using a state-of-the-art bottom-drive open-top flotation machine purchased from JKTech, Australia (Figure 3.6). A 1.5 L flotation cell was used for all batch flotation tests. Compressed air was used for all flotation tests. Agitation speed was fixed at 1,200 rpm for most of the tests except those mentioned otherwise. Batch flotation was carried out on the ore samples taken from Niobec Mine concentration plant to test the reagents identified from small-scale flotation tests. The procedures and metallurgical balances of all batch flotation tests can be found in Appendix A.

In a typical test, approximately 750 mL distilled water was added to the 1.5 L cell. Then 500 grams of ore feed sample was slowly added to the cell followed by 2 min of conditioning. The natural pH was recorded but not adjusted. Collector at a desired dosage was added with 3 min conditioning. Then the desired dosage of depressant was added with 2 min conditioning. Throughout the batch flotation tests, froth depths were fixed at around 1 cm, and for the 1.5 L cell that was used, this required a constant air flow rate of 7 L/min and continuous addition of small

quantities of distilled water. Froth was scraped and collected in a pan for later assay. After the flotation, the final pulp pH was recorded.

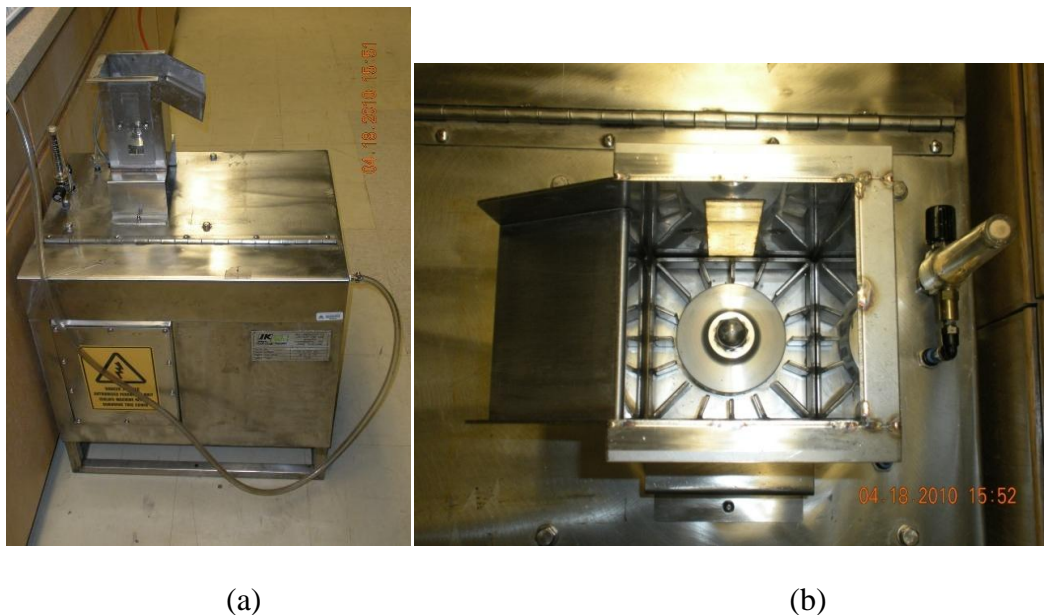


Figure 3.6 JKTech flotation machine (a) side view (b) top view of 1.5 L flotation cell.

3.7. Adsorption mechanism studies

Adsorption mechanism studies were carried out to investigate the interaction between the reagent molecules and mineral surface. This knowledge could help us better use the reagent in the industry operations. Collectors that are based on chemisorption could form new compounds on the mineral surface, which could be detected by some surface characterization methods. In this project, FTIR, XPS, adsorption isotherm and ToF-SIMS were employed to study the reagent's adsorption mechanism. FTIR and XPS were mainly used to study the

characteristics of reagent's interaction with the mineral surface. Adsorption isotherm and ToF-SIMS were employed to study the adsorption isotherm and configurations of the reagents on the pure single minerals and their mixtures. Based on these results, we were able to decipher the adsorption behaviors of the reagents on the different mineral surfaces and the resulting flotation behaviors.

3.7.1. Infrared spectroscopy (IR)

Infrared spectroscopy is one of the commonly used and mature techniques normally for *qualitatively* identifying and studying chemicals based on the absorption of characteristic infrared wavelength by chemical bonds. In mineral processing, it can be particularly useful to study adsorption by comparing the distinct differences of absorption spectra between pristine and collector treated minerals. If the collector molecules adsorbed on the surface, the absorption peaks of collector molecules will be shown on the spectrum of the treated mineral particles. Since new chemical bonds were created after collector molecules react with the mineral surface during chemisorption, new peaks or peak shifts can be observed on the absorption spectrum of collector treated mineral particles. Since it is a relatively inexpensive method, many researchers tend to use it first in the adsorption study. Studies of collector adsorption on niobium containing minerals using IR were published (Zheng et al., 1996; Ren et al., 2004; Chen et al., 2005).

In this study, IR will be used by comparing differences on the absorption spectra of hydroxamic acid, the pristine mineral surface and treated mineral surface.

Infrared absorption spectra of pure and reagent treated mineral particles were measured using a Nicolet 8700 FT-IR spectrophotometer in a Smart collector. KBr disc with 0.5 wt% of desired mineral particles were scanned within the wavenumber range of 400-4,000 cm^{-1} . Pure KBr disc was used as a reference.

The samples tested in FT-IR investigations were pyrochlore or calcite particles with or without reagent treatment. The preparation procedure of collector treated mineral sample is as follows: (1) 50 mL 0.5 wt% (31 mmol/L) hydroxamic acid was prepared in a 100 mL beaker at pH 8.5 (the natural pH of flotation pulp in batch flotation). (2) 1.5 g of the high purity mineral sample was added into the beaker and the mixture was agitated for 1 h under room temperature. (3) The pulp was filtered and decanted. (4) Then the particles were washed by 50 mL deionized water at pH 8.5 for five times. (5) Finally, these particles were dried and kept in a desiccator until analysis. For depressant treated mineral, the samples were prepared in the same procedure but the mineral sample was added into 50 mL 5 wt% (82 mmol/L) sodium hexametaphosphate solution.

3.7.2. X-ray photoelectron spectroscopy (XPS)

X-ray photoelectron spectroscopy (XPS) provides a *qualitative* and *quantitative* method to study the solid surface, usually used together with IR. XPS spectra are obtained by irradiating a material with a beam of X-rays while simultaneously measuring the kinetic energy and number of electrons that escape from the top several nm of the material (Adamson and Gast, 1997; Watts and Wolstenholme, 2003). XPS is a more specific method to study the surface chemistry than IR, and it has the unique ability to identify different chemical states.

In this project, XPS was used to analyze the mineral surfaces both by comparing the electron binding energy peak location and peak intensity, from which the relative atomic concentration of different elements could be determined on the pyrochlore surface. Combined with the IR results, we can get a better understanding of hydroxamic acid adsorption on the pyrochlore as well as other mineral surfaces.

The X-ray photoelectron spectroscopy (XPS) characterization of samples was carried out on a Kratos Axis 165 spectrometer with monochromatised Al $K\alpha_{1,2}$ radiation as an excitation source ($h\nu = 1486.6$ eV). The analysis area was about $400\ \mu\text{m} \times 700\ \mu\text{m}$. Survey scans were conducted using an electron analyzer with a pass energy of 160 eV and a step size of 0.35 eV, and then high resolution scans were carried out within specific binding energy ranges at a constant pass energy

of 20 eV and a step size of 0.1 eV. All measurements were carried out at pressures below 10^{-8} Pa. All the spectra obtained were calibrated using C 1s at 284.8 eV. Sample powders were loaded into the sample holder by creating a surface as smooth as possible by unaided eyes.

The integral areas of selective peaks on the full survey scan of minerals were divided by relative sensitivity factors (RSFs) and normalized, from which relative atomic concentrations was obtained. If de-convolution of spectrum was needed, it was carried out by commercial software CasaXPS (version 2.3). It allows us to optimize the peak positions, intensities and widths by minimizing the sum of squared differences between the experimental data and the synthesized spectrum generated by sum of the component peaks.

The OHA or NaHMP treated mineral samples were prepared following the same procedures for samples used in FTIR. Besides high concentration (31 mmol/L) OHA as in FTIR test, low concentration OHA solutions (2 mmol/L and 1 mmol/L) were also used to treat the pyrochlore surface. Solid OHA and sodium hexametaphosphate crystals were tested directly in the XPS spectrometer.

3.7.3. Adsorption isotherm determination

Adsorption isotherm describes the equilibrium of the adsorption of reagent molecules on mineral surface at constant temperature. Only the adsorption isotherms of OHA on pure minerals were measured in this project.

Adsorption densities of the OHA on the pyrochlore and calcite minerals were measured at pH 8.5 and room temperature (20 °C). One gram of the -25 µm mineral (pyrochlore or calcite) was added to a conical flask, then 150 mL solution with different OHA concentrations was added. Control blank was run using 150 mL 5 mmol/L OHA but no mineral was added. Natarajan et al. (2010) have shown that usually 30 min is sufficient for adsorption/desorption of hydroxamic acid to attain equilibrium on mineral surfaces. We used a 4 h equilibration time to ensure that the adsorption has reached equilibrium. The control blank test indicated that the OHA solution concentration did not detectably change after 4 h shaking at pH 8.5, verifying that the concentration difference after adsorption is not caused by decomposition.

The flask was stoppered and agitated in a Jeio Tech SI 600 shaking incubator for 4 h at 180 rpm and room temperature. The flask was then removed and allowed to stand still for 2 h, and the upper portion of the solution was filtered using a 0.2 µm pore size syringe filter for colorimetric measurement of the OHA concentration. The colorimetric measurements were carried out on a Jenway 6405 UV/Vis spectrophotometer. The concentration of OHA was determined by the absorbance of its Fe³⁺ chelates at 520 nm (See Appendix B). Although

hydroxamic acid absorbs UV light, direct UV light scanning was found inaccurate. On the other hand, the OHA-ferric chelate shows strong absorbance at visible light region (520 nm) and fits well with Beer-Lambert law (Majumdar, 1972; Yale, 1993). The adsorbed octyl hydroxamic acid was determined by the difference of the initial and equilibrium OHA concentration. It was verified that calcium ions were not able to form colored chelates or precipitates with hydroxamic acid even at a very high calcium concentration (20 mmol/L), so that this method is still valid for semi-soluble carbonate minerals such as calcite. A standard calibration curve was obtained with $R^2 > 0.99$ within the OHA concentration range of 0.3 mmol/L to 2.4 mmol/L. Dilution was used before absorbance measurement if the solution's concentration was higher than the aforementioned calibration concentration range.

3.7.4. ToF-SIMS imaging

ToF-SIMS (time-of-flight secondary ion mass spectrometry) is a mass spectrometry of ionised particles which are emitted when a surface is bombarded by energetic primary particles (Vickerman and Briggs, 2001). It is very sensitive technique for analysing organic chemicals and cations on the substrates. In mineral processing, it is one of few techniques that could give direct illustration of the reagent's adsorption density difference on mineral mixture, which could be the proof of its selectivity for a specific mineral (Khmeleva et al., 2006; Parolis et al., 2007). ToF-SIMS was used to indicate the OHA adsorption density on the pyrochlore/calcite mixture.

In this study, secondary ion mass images were obtained from a ToF-SIMS IV instrument (ION-TOF GmbH). Bi^+ ions were used as an analytical source operated at 25 kV and a pulsed target current of approximately 1.0 pA. Low-energy electrons were used to compensate for surface charging caused by primary ion beam on the insulating surfaces. The mass spectra were calibrated by positive ion peaks of H^+ , CH_3^+ and Na^+ . $136.2 \times 136.2 \text{ }\mu\text{m}^2$ size images obtained by mapping specific ion intensity were collected in a burst alignment mode with 128×128 pixels per image. Total primary ion beam dose for analysed area was kept below 1×10^{12} ions per cm^2 , ensuring static conditions. Data analysis was carried out using IonImage (version 4.1) software.

Samples tested in ToF-SIMS were prepared as follows: 3 g of mineral mixture (pyrochlore:calcite at 1:1) was agitated in 50 mL of 0.5 mmol/L OHA solution for 5 minutes at pH 8.5, then it was filtered and rinsed by five aliquots of 50 mL deionized water at pH 8.5 and dried in a vacuum desiccator. A pellet for analysis was made using 1 g of dried mineral mixtures in a mechanical press.

4. Results and Discussion

4.1. Characterization of pure OHA

The final product of OHA is white feather like crystal. The yield was ~75%. The pure crystal can be dissolved in water but the solubility is smaller than 1g/100g water. The synthesized phosphonic acid and starch phosphate was not further purified so only OHA was characterized by Fourier transform infrared spectroscopy (FTIR). The FTIR spectrum of the OHA is shown in Figure 4.1.

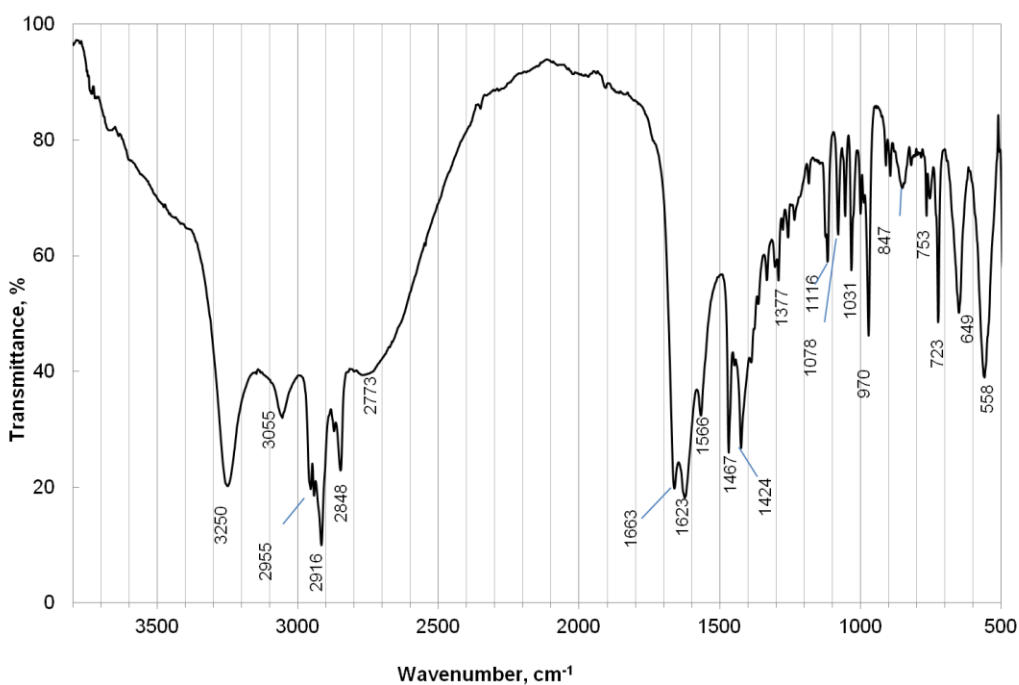


Figure 4.1 FTIR spectrum of octyl hydroxamic acid (solid particles in KBr powder).

All the peaks on the FTIR spectrum match those on the spectrum of alkyl hydroxamic acid reported by Cytec (Higgins et al., 2006). The sharp peak at 3250 cm^{-1} represents the N-H stretching band. The broad peak at around 3000 cm^{-1} is hydrogen bonded O-H groups. Peaks within $2955\text{--}2848\text{ cm}^{-1}$ are due to the C-H bonds. Carbonyl group was detected in the double bond region at 1663 and 1623 cm^{-1} . The peaks at 1566 cm^{-1} and 1467 cm^{-1} represent C-N-H group bending and stretching.

4.2. Small-scale flotation

4.2.1. Single mineral flotation using Aero 6493

The selectivity of Aero 6493 was examined in small-scale flotation tests on pyrochlore, calcite and quartz. Figure 4.2 shows the flotation recovery of pyrochlore, calcite and quartz single minerals as a function of the concentration of Aero 6493. As can be seen, Aero 6493 floated both pyrochlore and calcite under natural pH. Quartz flotation recovery was much lower.

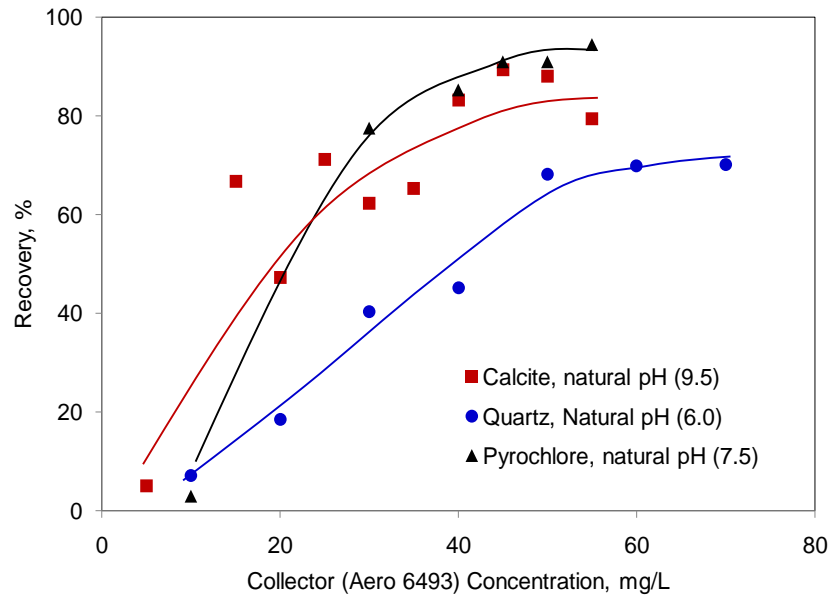


Figure 4.2 Recovery of single minerals under natural pH using Aero 6493 as a collector.

Figure 4.3 shows the recovery with the addition of 45 mg/L of Aero 6493 as a collector at different pH. As can be seen, Aero 6493 worked better at pH 8-9 for pyrochlore while it showed similar floatability within the pH range 5-12 for calcite.

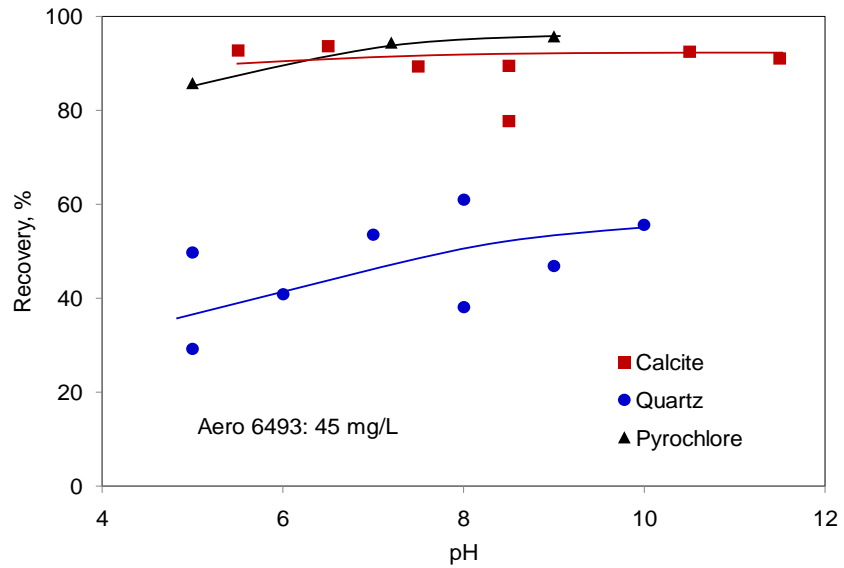


Figure 4.3 Recovery of single minerals with the addition of 45 mg/L Aero 6493 at different pH.

The addition of sodium metaphosphate (NaMP) following Aero 6493 significantly depressed the flotation of calcite. On the contrary, it slightly promoted the pyrochlore flotation, as can be seen from Figure 4.4.

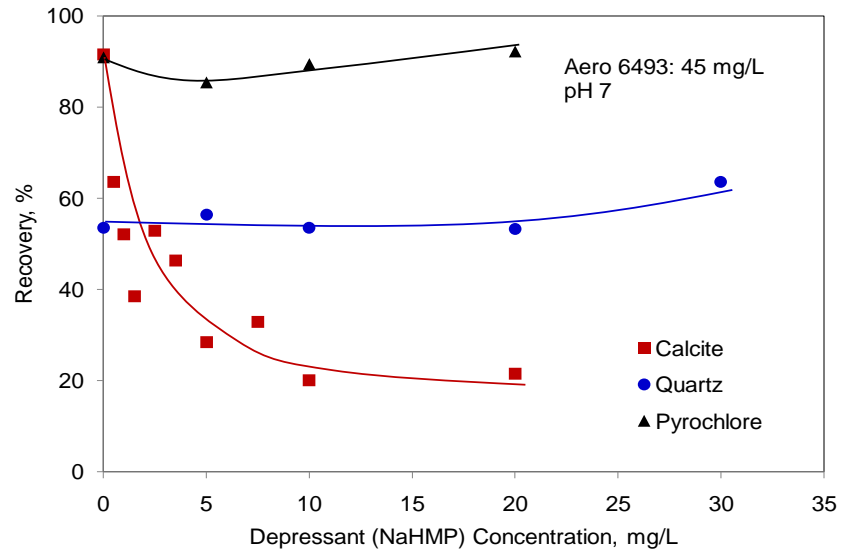


Figure 4.4 Flotation recovery of single minerals with the addition of 45 mg/L Aero 6493 at pH 7 and different NaMP concentrations.

4.2.2. Mineral mixture flotation using Aero 6493

Figure 4.5 shows pyrochlore recovery and concentrate grade in mineral mixture (pyrochlore:calcite 1:1) flotation tests as a function of Aero 6493 concentration. As can be seen, pyrochlore recovery increases as the concentration of Aero 6493 increases, however, maximum grade was reached at 30 mg/L of collector concentration.

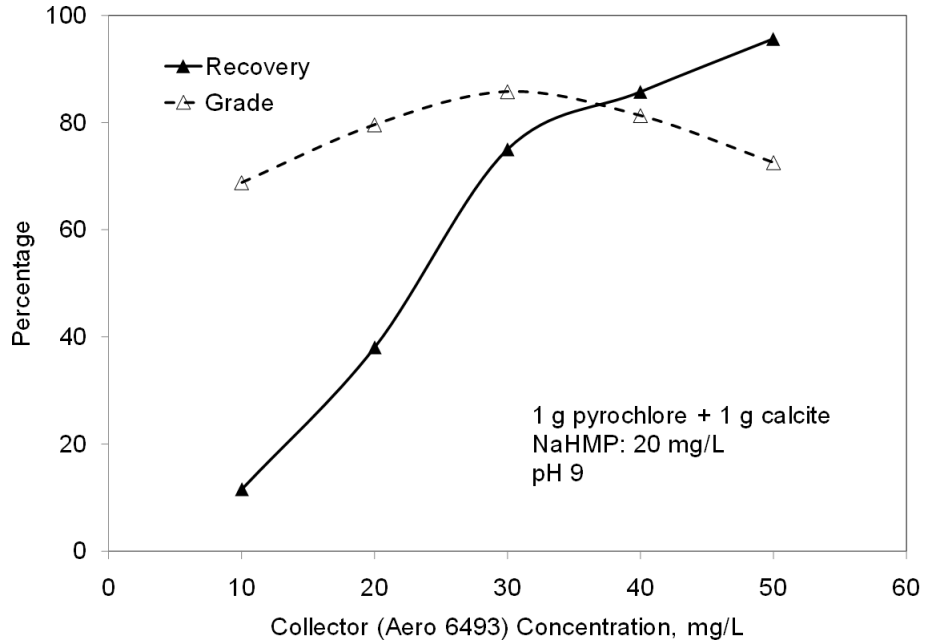


Figure 4.5 Recovery and grade of pyrochlore with addition of 20 m/L NaHMP at pH 9.

Figure 4.6 shows pyrochlore recovery and concentrate grade in mineral mixture (pyrochlore:calcite 1:1) flotation tests as a function of pulp pH. At 45 mg/L Aero 6493 and 20 mg/L NaHMP, the pyrochlore recovery increases slightly as pH increases. However, pyrochlore grade reached maximum around 9.

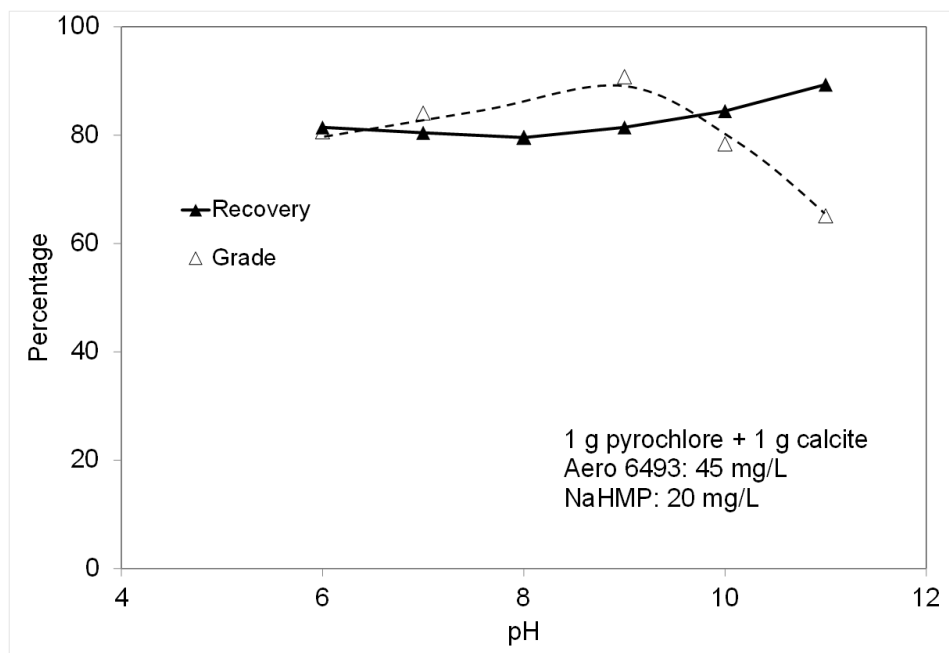


Figure 4.6 Recovery and grade of pyrochlore with addition of 20 m/L NaHMP and 45 mg/L Aero 6493.

Figure 4.7 shows pyrochlore recovery and concentrate grade in mineral mixture (pyrochlore:calcite 1:1) flotation tests as a function of sodium hexametaphosphate concentration. At 45 mg/L Aero 6493 and pH 9, the addition of NaHMP could slightly promote the pyrochlore recovery. However, it also slightly depressed the pyrochlore grade, i.e., it assisted with the flotation of other gangue minerals as well.

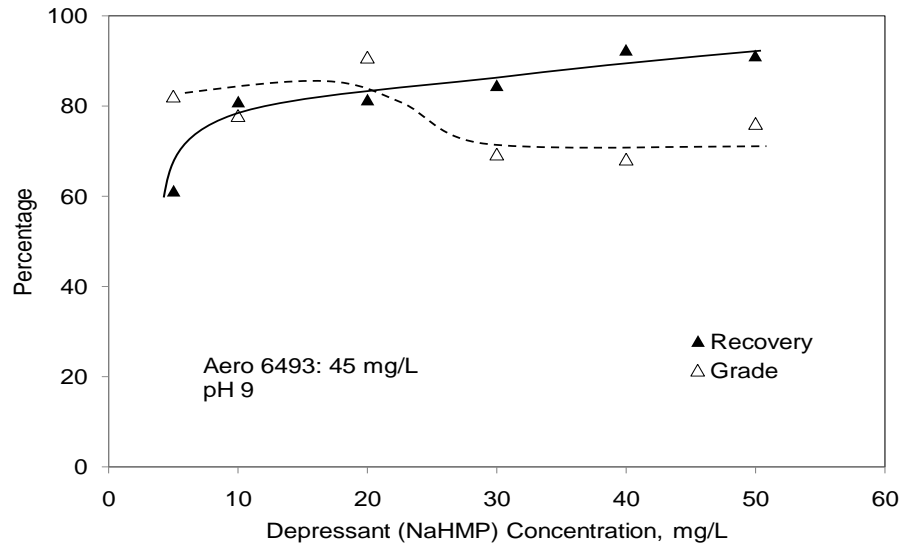


Figure 4.7 Recovery and grade of pyrochlore with addition of 45 mg/L Aero 6493 and pH 9.

It can be concluded from the mineral mixtures flotation tests results that, at 45 mg/L Aero 6493, 20 mg/L NaHMP, and pH 9, the separation between pyrochlore and calcite can be achieved.

4.2.3. Single mineral flotation using diphosphonic acid

Only single mineral flotation tests were carried out using the synthesized diphosphonic acid. Figure 4.8 shows the flotation recovery of pyrochlore, calcite, quartz and other gangue minerals as a function of the concentration of diphosphonic acid concentration at pH 7. As can be seen, pyrochlore could not be floated by the diphosphonic acid at the natural pH of 7 while calcite floated well.

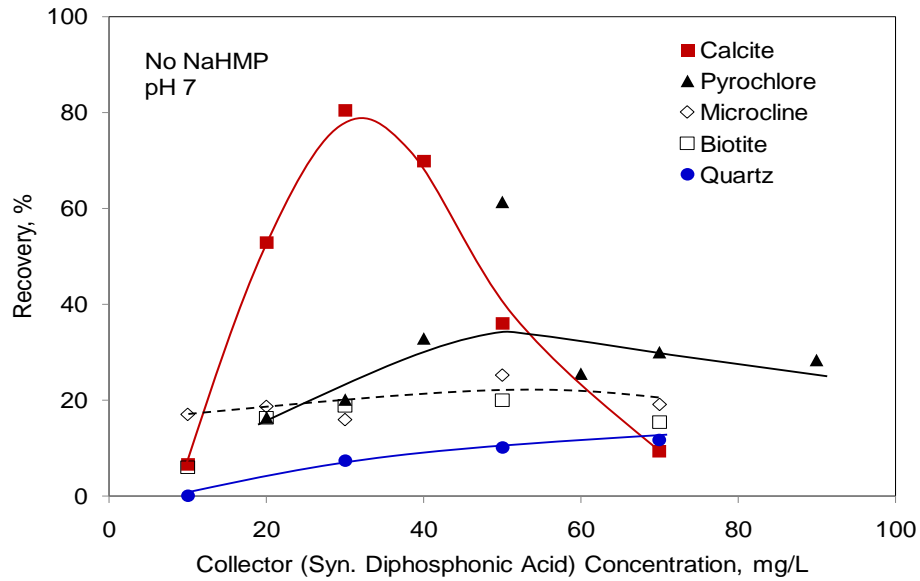


Figure 4.8 Recovery of single minerals using diphosphonic acid as a collector at pH 7.

Figure 4.9 shows the flotation recovery of pyrochlore and quartz as a function of the concentration of diphosphonic acid at pH 4. It seemed that a separation window exists at this pH. However, we were not able to conduct the same test on carbonates because it was not possible to maintain pH at 4 in the presence of the carbonate minerals. Since the natural pH of the ore pulp is around 8.5, the diphosphonic acid collector was considered unsuitable.

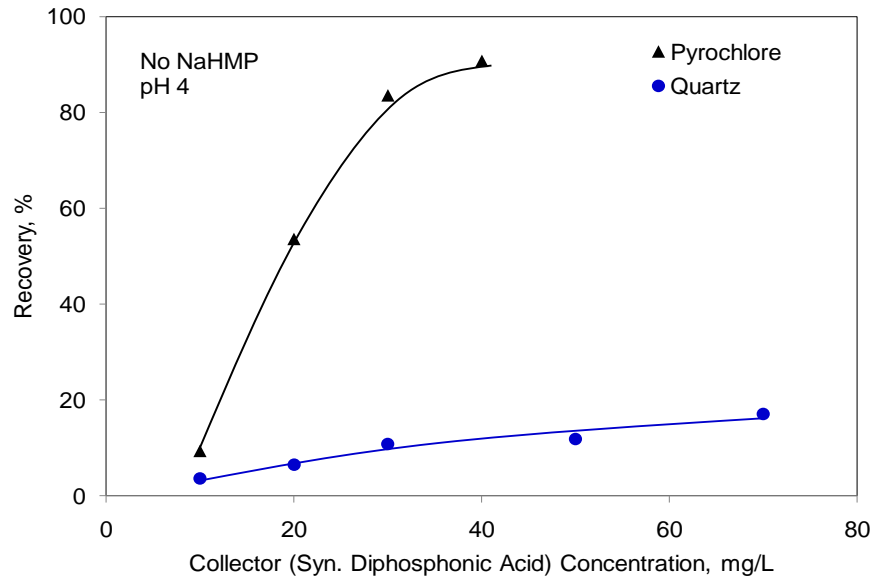


Figure 4.9 Recovery for single minerals using diphosphonic acid as a collector at pH 4.

4.2.4. Single mineral flotation using OHA

A series of single mineral flotation tests were carried out to look for an effective depressant for the iron oxide. Several depressants (oxalic acid, EDTA, tannic acid, catechol and sodium silicate) were screened.

Figure 4.10 shows the recovery of hematite and pyrochlore using 30 mg/L OHA at different oxalic acid concentrations. As can be seen, the oxalic acid depressed hematite above a dosage of 20 mg/L, but it also depressed the pyrochlore, and the separation window is not obvious, thus it is not an effective depressant for iron oxide during pyrochlore flotation.

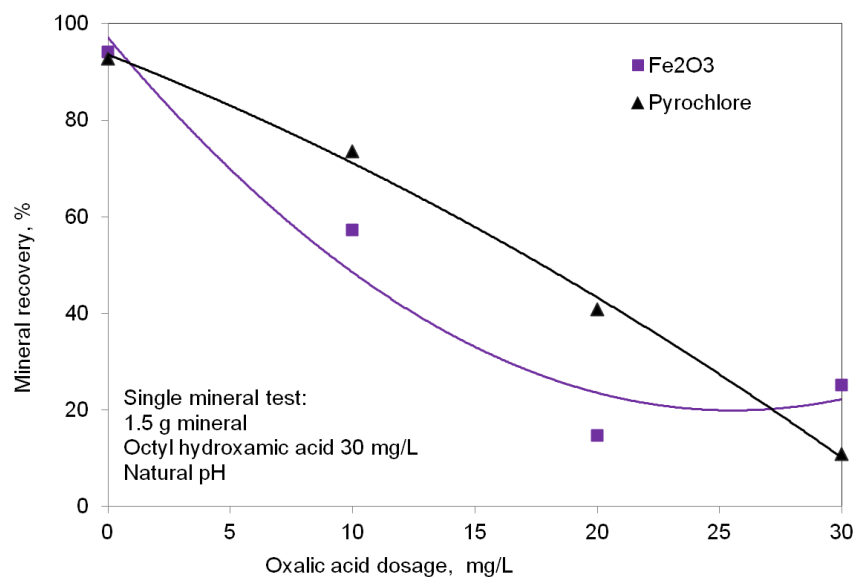


Figure 4.10 Recovery of single minerals with the addition of 30 mg/L OHA at natural pH and different oxalic acid concentrations.

Figure 4.11 shows the recovery of hematite and pyrochlore using 50 mg/L OHA at different EDTA concentrations. Unlike oxalic acid, EDTA did not depress hematite but it depressed the pyrochlore slightly. The separation window is not obvious, thus it is not an effective depressant for iron oxide during pyrochlore flotation, either.

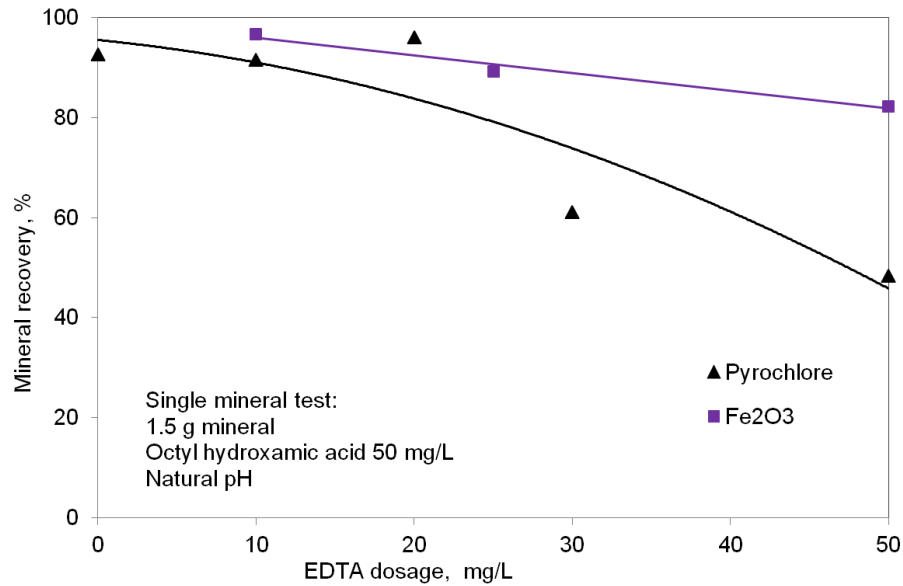


Figure 4.11 Recovery of single minerals with the addition of 50 mg/L OHA at natural pH and different EDTA concentrations.

Figure 4.12 shows the recovery of hematite and pyrochlore using 50 mg/L OHA at different concentrations of sodium silicate. A separation window exists at high sodium silicate concentration, where iron oxide was depressed while pyrochlore flotation was hardly affected.

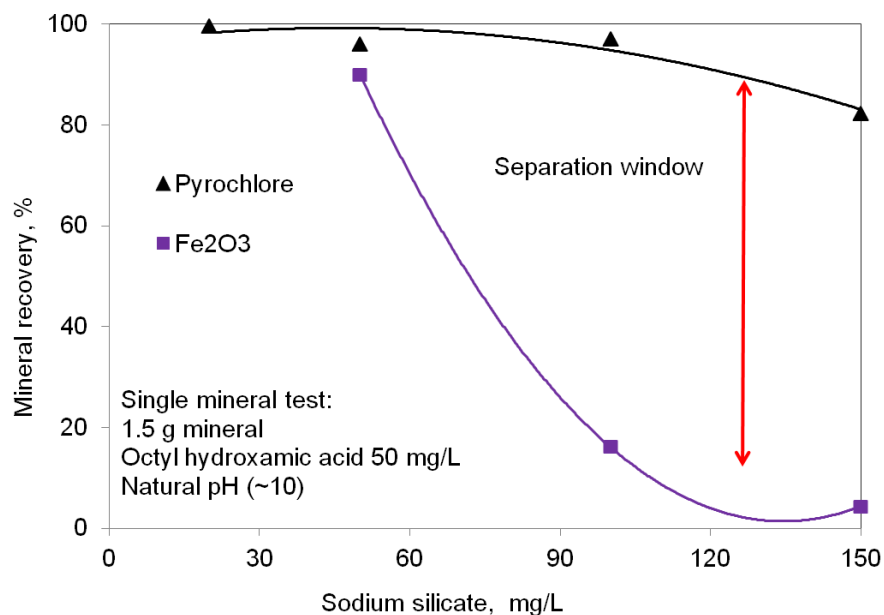


Figure 4.12 Recovery of single minerals with the addition of 50 mg/L OHA at natural pH and different sodium silicate concentrations.

Figure 4.12 indicated that sodium silicate could be the potential depressant for iron oxide in pyrochlore flotation. Thus, one more set of test was carried out to find the optimum pH for sodium silicate. Figure 4.13 shows the recovery of hematite and pyrochlore using 50 mg/L OHA and 100 mg/L sodium silicate at different pH. A separation window exists at alkaline pulp condition. Sodium silicate could depress hematite above pH 9 while pyrochlore was not affected.

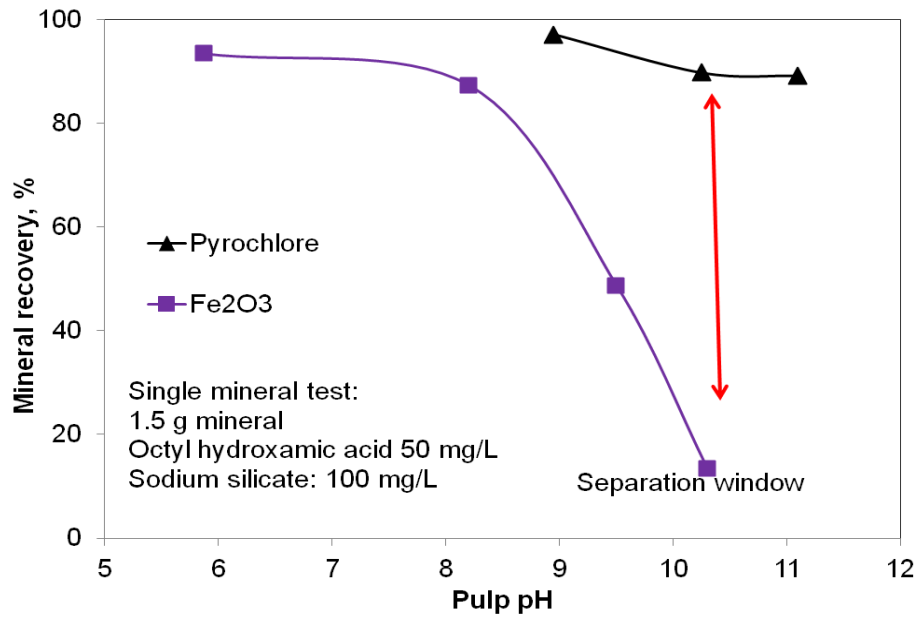


Figure 4.13 Recovery of single minerals with the addition of 50 mg/L OHA and 100 mg/L sodium silicate at different pH.

4.3. Exploratory rougher flotation using Aero 6493

Initially, a series of exploratory rougher flotation tests were carried out. The three different types of Niobec ore samples were floated under various conditions such as collector dosage, depressant type and dosage, agitation speed, all of which are illustrated in Table 4.1. Flotation froth was scraped for a total of 5 min, divided into the 1st rougher concentrate (2 min) and the 2nd rougher concentrate (3 min).

Table 4.1 The dosage of Aero 6493 and depressant for exploratory rougher flotation tests.

Test	Ore type	A 6493, g/t	NaMP, g/t	Starch, g/t	Kerosene, g/t	Stirring speed, rpm
NP 01	Carbonate Feed	500				1,200
NP 02	Carbonate Feed	500 ¹				1,200
NP 03	Carbonate Feed	500	250			1,200
NP 04	Carbonate Feed	500 ¹	250			1,200
NP 05	Carbonate Feed	500	500			1,200
NP 06	Carbonate Feed	1,000	500			1,200
NP 07	Carbonate Feed	500		250 ²		1,200
NP 08	Carbonate Feed	1,000		250 ²		1,200
NP 09	Carbonate Feed	500	250			1,200
NP 10	Mill Feed	500	500			1,200
NP 11	Pyrochlore Feed	500	500			1,200
NP 12	Mill Feed	1,000	500			1,200
NP 13	Mill Feed	1,500	500			1,200
NP 14	Carbonate Feed	500	250	150		1,200
NP 15	Carbonate Feed	500	250	500		1,200
NP 16	Mill Feed	1,000	500		250	1,200
NP 17	Mill Feed	1,000	500		250	1,750
NP 18	Mill Feed	1,000	500		2,000	1,200
NP 19	Mill Feed	1,000	500		5,000	1,200
NP 20	Mill Feed	1,000	500		2,000	1,750
NP 21	Mill Feed	1,000	500		5,000	1,750

¹collector was emulsified with 100 ml distilled water in a kitchen blender

²starch phosphate synthesized from potato starch

4.3.1. Selectivity ratio

From the results of the small-scale flotation tests on pure minerals and mineral mixtures, it seemed that Aero 6493 and NaMP was a suitable combination of collector/depressant for the Niobec ore. The reagent combination was verified in the batch flotation tests using real ore samples.

The flotation response of a particular mineral in the batch flotation was characterized by a parameter called “selectivity ratio”, (S_M). It was defined as the ratio of the recovery of that mineral to the total recovery of the solid mass floated to the concentrate: $S_M = \frac{\text{Mineral recovery}}{\text{Solid recovery}}$

It is obvious that the higher the selectivity ratio, the higher recovery can be obtained for that mineral with respect to solid recovery (mass pull). Thus, this ratio can be used to indicate the selectivity between different minerals. For the same mineral between different tests, higher selectivity ratio also means higher grade in the concentrate.

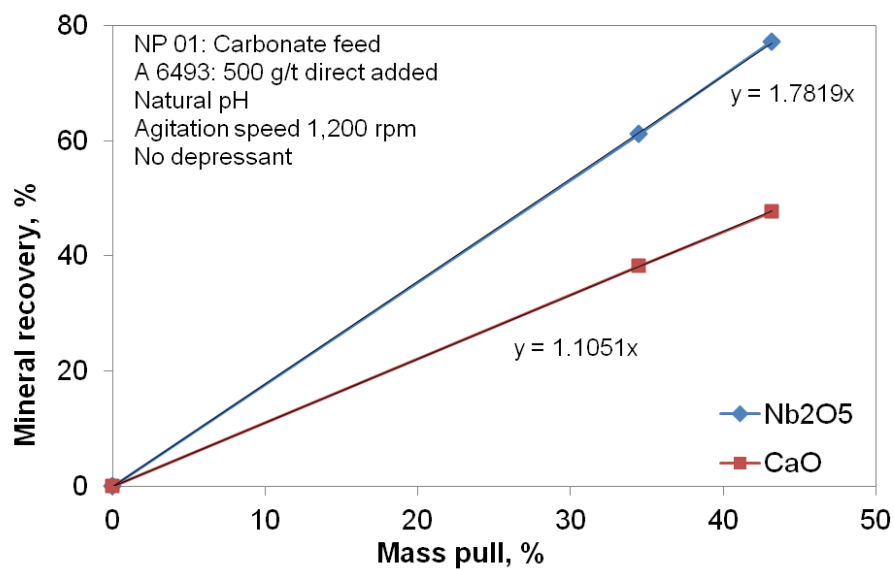
4.3.2. Preparation of Aero 6493

Since Aero 6493 contains insoluble chemicals (long chain alcohols as indicated by Cytec), the method of addition of the Aero 6493 to the flotation cell was studied: the Aero 6493 was either directly added to the pulp, or emulsified with

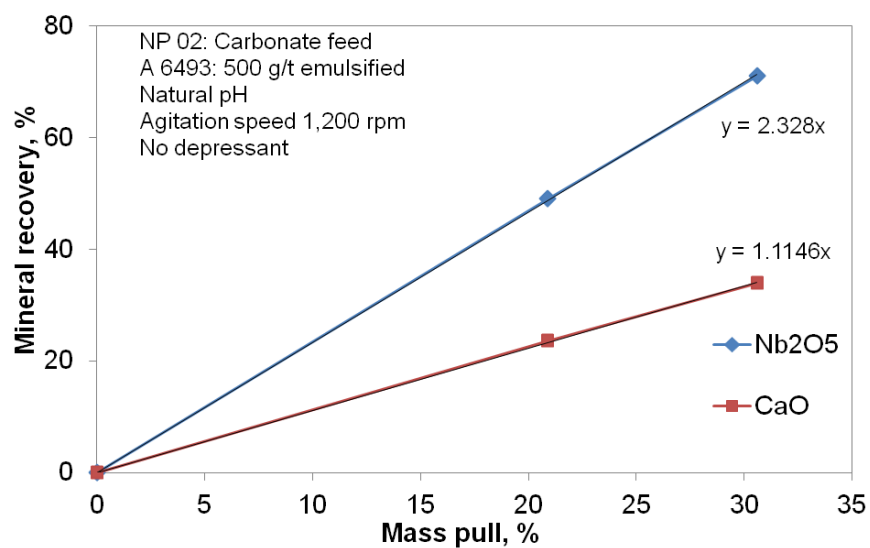
100 mL of distilled water in a kitchen blender for 1 min, then the emulsion was added to the pulp.

Tests NP 01 and NP 02 examined the impact of collector addition method on the flotation behavior. The major ingredients in Aero 6493 is alkyl hydroxamic acid and long chain alcohol. Aero 6493 cannot be totally dissolved in water, leaving some oily droplets on the water/air interface (NP 01). Therefore, the Aero 6493 was emulsified using a kitchen blender, and the emulsified collector solution was added into the pulp (NP 02). This was compared with direct addition of the Aero 6493 collector (NP 01). The results indicate that the direct addition of Aero 6493 (NP 01) led to higher niobium oxide recovery in two rougher stages. However, the direct addition of the Aero 6493 also floated more solid mass into the rougher concentrate, i.e., it was not as selective as emulsified Aero 6493. At a fixed mass pull to the rougher concentrate, emulsified Aero 6493 gave higher pyrochlore recovery (NP 02).

The selectivity ratio of pyrochlore (shown in Figure 4.14), S_{Nb} , of test NP 02 (2.3), is higher than that of NP 01 (1.8). Emulsification seemed to be a better way to prepare the collector. However, it needs more tests to confirm. Since the grade of concentrates is not the major concern in the rougher flotation and the emphasis at this stage is recovery, the subsequent flotation tests were conducted without emulsifying the Aero 6493.



(a)



(b)

Figure 4.14 Niobium oxide and carbonate recovery as a function of mass pull for test NP 01 (a) and test NP 02 (b).

4.3.3. Depressants

NP 03 proves that sodium metaphosphate (NaMP) is a very selective depressant for carbonates (Figure 4.15). The recovery of carbonate is depressed significantly by roughly 40% compared with NP 01 (Table 4.2), while niobium oxide recovery was only decreased by slightly over 10%. The S_{Nb} therefore increased to 6.2 (over three times higher than that of NP 01).

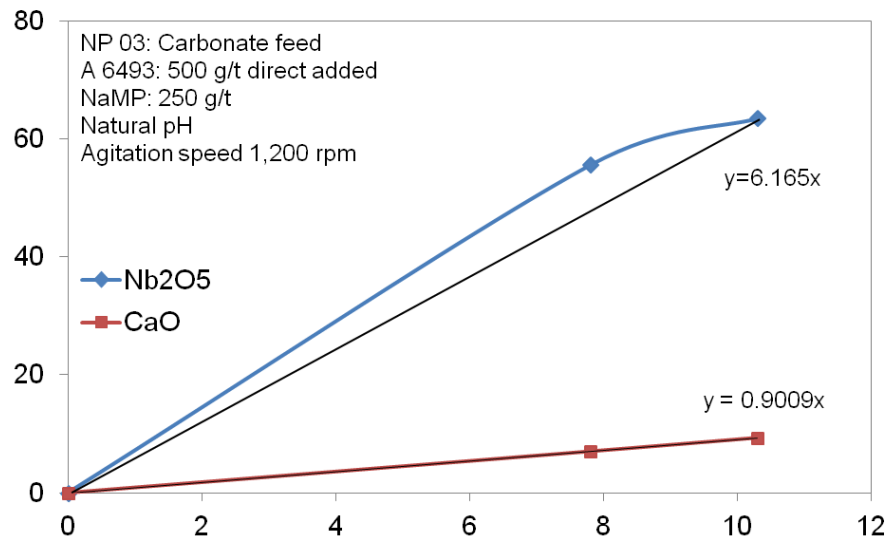


Figure 4.15 Solid recovery and mass pull of test NP 03.

Besides sodium metaphosphate, modified starch was also tested in the batch-scale flotation tests as a potential depressant. Starch has the ability to depress carbonate gangue (Somasundaran et al., 1969; Parsonage et al., 1984; Irannajad et al., 2009; Mohammadkhani et al., 2011). Modified starch with grafted phosphate groups was studied in NP 07 and 08. The combination of sodium metaphosphate and

unmodified potato starch was studied in NP 14 and 15. Compared with NP 03 discussed in the previous paragraph, it seems that the modified starch was more selective than sodium metaphosphate. However, it is not very conclusive at this point; more tests need to be carried out in the future. Since characterization of starch phosphate is not systematically carried out, for most of the subsequent tests, sodium metaphosphate was used as a depressant.

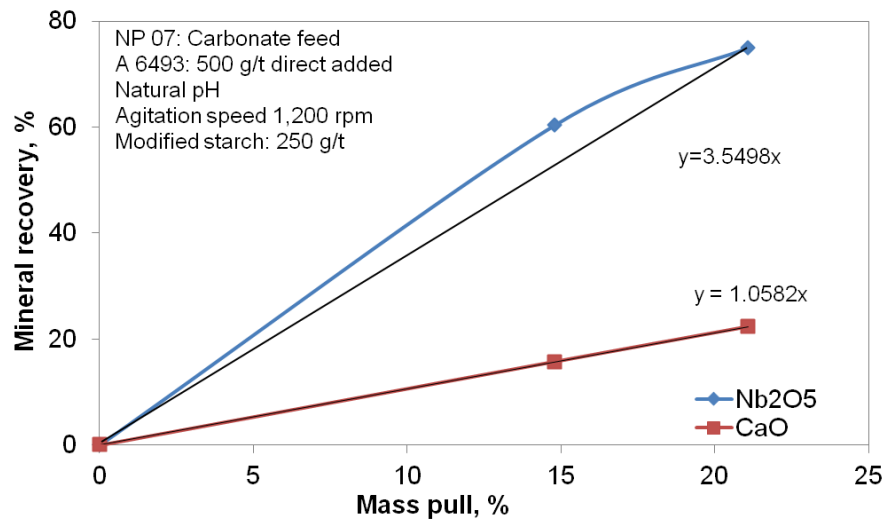


Figure 4.16 Solid recovery and mass pull of test NP 07.

4.3.4. Comparison between feed samples

Table 4.2 lists the results of all the exploratory tests which already mentioned earlier in Table 4.1. Based on the obtained information, we can systematically compare the effect of feed sample's mineralogy, collector dosage and depressant dosage on the flotation behavior.

As can be seen from Figure 4.17, under the same rougher flotation conditions, the highest niobium oxide recovery was achieved with Pyrochlore Float Feed along with the highest niobium oxide grade in the rougher concentrate. On the contrary, the Mill Feed sample had the lowest niobium oxide recovery and grade in the rougher concentrate. After 5 min of flotation, over 80% of pyrochlore could be recovered from the Pyrochlore Float Feed while only less than 40% from the Mill Feed. This is understandable as the Pyrochlore Float Feed had gone through pre-concentration which removed most of the slimes, carbonates and Fe minerals. The Mill Feed, on the other hand, had not gone through the pre-concentration.

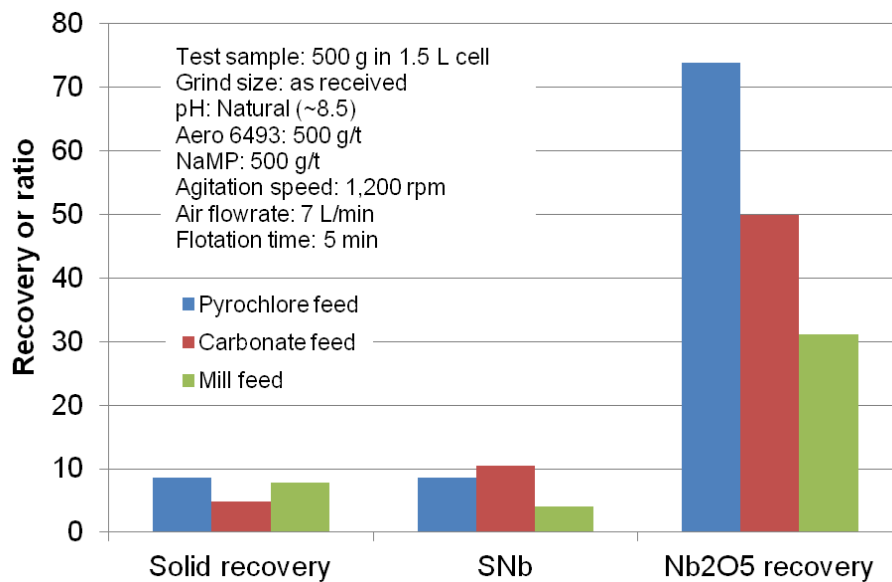


Figure 4.17 Comparison of solid recovery, niobium oxide recovery and niobium oxide grade on rougher flotation test of three different feed samples.

Table 4.2 Batch flotation results of Niobec ore sample using Aero 6493 and NaMP.

Test #	Assay (%)			Distribution (%)			Sep. Eff. [#] (%)		S _{Nb}
	Nb ₂ O ₅	CaO	SiO ₂	Nb ₂ O ₅	CaO	SiO ₂	vs. CaO	vs. SiO ₂	
NP01	1.25	32.86	2.97	77.2	47.6	17.0	29.6	60.2	1.78
NP02	1.55	32.93	2.34	71.0	33.9	9.5	37.1	61.5	2.32
NP03	4.11	26.90	4.88	63.5	9.3	6.7	54.2	56.8	6.17
NP04	2.30	27.30	5.33	15.5	4.2	3.3	11.3	12.2	3.16
NP05	6.99	23.92	3.50	50.0	3.8	2.2	46.2	47.8	10.42
NP06	2.82	33.60	2.45	62.6	16.5	4.7	46.1	57.9	4.26
NP07	2.34	31.2	2.56	74.9	22.3	6.9	52.6	68	3.55
NP08	1.16	33.3	3.08	83.9	53.3	19.3	30.6	64.6	1.77
NP09	4.96	26.9	4.50	50.2	6.0	4.0	44.2	46.2	7.61
NP10	2.70	21.7	5.57	31.1	6.8	6.1	24.3	25	3.99
NP11	7.52	21.5	10.34	73.9	6.8	8.0	67.1	65.9	8.59
NP12	2.69	27.7	4.27	74.1	18.1	11.5	56.0	62.6	3.9
NP13	1.99	30.2	4.40	71.3	25.9	15.4	46.1	55.9	2.83
NP14	3.12	30.2	4.45	46.3	9.7	5.6	36.6	40.7	4.87
NP15	2.34	30.6	5.69	48.4	13.4	9.8	35.0	38.6	3.75
NP16	2.78	25.4	5.90	49.7	10.6	10.0	39.0	39.7	4.07
NP17	0.59	22.5	7.19	5.1	4.7	6.2	0.4	-1.1	0.82
NP18	3.21	26.8	4.39	65.1	12.9	8.7	52.2	56.4	4.62
NP19	1.89	26.7	5.97	43.8	14.5	13.4	29.3	30.4	2.75
NP20	0.75	23.9	7.23	6.9	5.2	6.5	1.7	0.4	1.06
NP21	0.81	26.2	7.25	18.0	14.3	16.3	3.7	1.7	1.13
Feed	0.67	29.20	7.56	100.0	100.0	100.0	0.0	0.0	1.0

* Aero 6493 were emulsified before adding

[#] Separation Efficiency was calculated by (Nb₂O₅ Recovery – CaO Recovery), or (Nb₂O₅ Recovery – SiO₂ Recovery)

4.3.5. Aero 6493 dosage

The niobium oxide recovery in the initial tests on the Mill Feed (test NP 10 in Table 4.1) is far from satisfying. Tests NP 12 and NP 13 were conducted with increasing Aero 6493 dosage on the Mill Feed while the depressant (NaMP) dosage was kept at 500 g/t. As can be seen from Figure 4.18, when the Aero 6493 dosage was increased from 500 g/t to 1,000 g/t, the recovery of niobium oxide almost doubled. But the solid recovery also doubled simultaneously. It indicated that 500 g/t is not enough for pyrochlore recovery. When the Aero 6493 dosage was increased to 1,500 g/t, pyrochlore recovery did not increase any further, while carbonate recovery steadily increased. These observations proved that value grain liberation from the gangue minerals is probably the limiting factor for further improvement in pyrochlore recovery. During the rougher flotation, it was indeed observed that the initial rougher concentrate was made up of very fine particles, which probably contained most of the liberated pyrochlore particles.

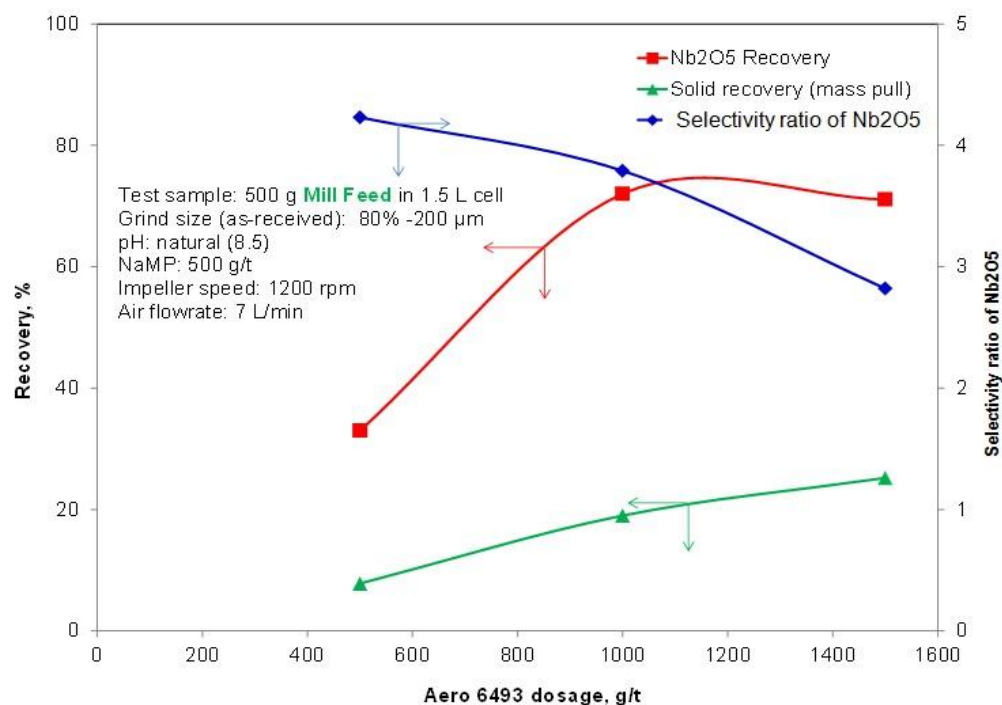


Figure 4.18 Impact of Aero 6493 dosage on the rougher flotation of Mill Feed.

4.3.6. NaMP dosage

The rougher flotation results showed that Aero 6493 was able to float carbonate minerals as well. This observation was consistent with the results in small-scale flotation. However, the carbonate recovery was much lower than that of niobium oxide indicating some degree of natural selectivity of hydroxamic acid between pyrochlore and carbonate minerals.

In order to further depress the carbonate gangue, sodium metaphosphate (NaMP) was used and proved as a selective depressant. The effect of sodium metaphosphate dosage on the flotation of carbonate float feed can be seen in

Figure 4.19. This figure presents the results of tests NP 01, 03 and 05, in which 500 g/t Aero 6493 was used with increasing dosages of NaMP up to 500 g/t. As can be seen, the increasing depressant dosage lowered the solid recovery and carbonate recovery at a faster rate than niobium oxide recovery. From 0 to 500 g/t NaMP, the niobium oxide recovery dropped 25 percentage points from 77% to 52%, while solid recovery decreased 38 percentage points from 43% to 5%, and calcium oxide recovery dropped 44 percentage points from 48% to 4%, which clearly indicated the strong selective depressive function of NaMP towards carbonate. The silicate recovery was also slightly lowered. A dosage of 250 g/t NaMP seemed appropriate. At this dosage, the carbonate was significantly depressed while the niobium oxide recovery was not affected significantly.

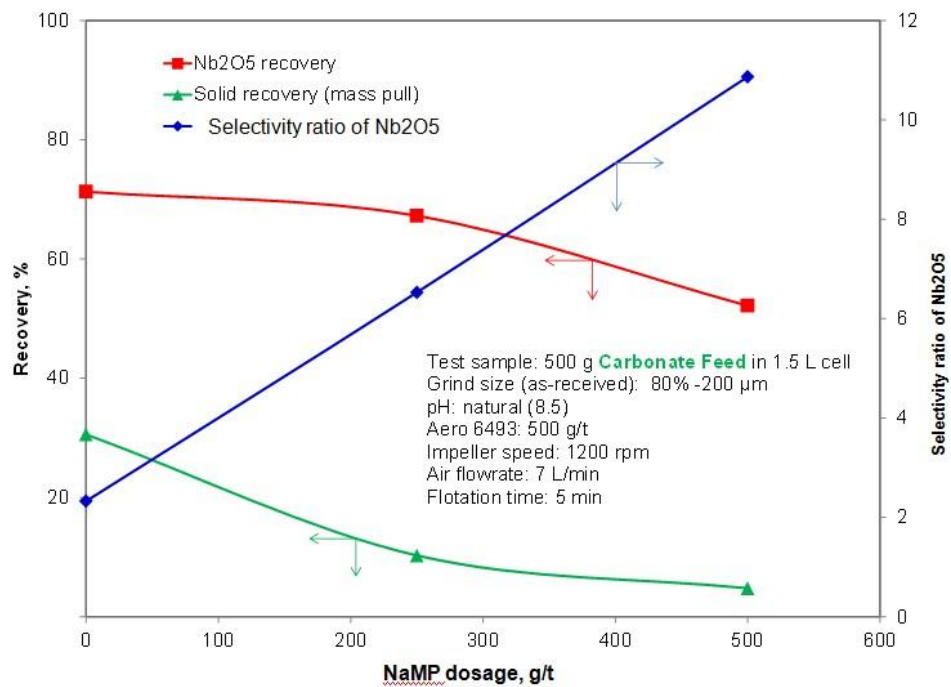


Figure 4.19 Impact of sodium metaphosphate dosage on rougher flotation of the Carbonate Float Feed.

4.3.7. Pulp pH

All the batch flotation tests were conducted at the natural pH; no pH adjustment was carried out for any of the tests. For all batch flotation tests, either using Aero 6493 or OHA as a collector, the pH values before adding reagents (initial) and after flotation (final) were all within the range of 8-9.5. The final pH after flotation using SHA was around 8. Slightly alkaline pH might come from semi-soluble carbonate gangue minerals. Throughout the flotation process, the pulp pH matches to the optimum value for Aero 6493 obtained from small-scale flotation results (i.e., pH 9). This is an advantage of hydroxamic acid over the current cationic collector used. Less pH adjustment could decrease the salinity of the pulp and the need for fresh water, and prevent corrosion.

4.4. Effort to maximize pyrochlore recovery

The reagent combination Aero 6493/NaMP was shown to be effective for Niobec ore in exploratory tests. However in all of the tests conducted, the pyrochlore recovery in rougher stages was lower than 90%. For instance in NP 12 (1,000 g/t Aero 6493, 500 g/t NaMP), the total pyrochlore recovery was about 72% at a rougher concentrate weight yield of 19%. Low recovery in rougher stages would lead to significant loss in overall recovery after several cleaner stages were added. Thus the effort to maximize the recovery in rougher stages was made. After the exploratory rougher tests, four tests NP 22-25 were carried out on the Mill Feed sample.

4.4.1. NP 22

In the previous exploratory tests, the total flotation time was set to 5 min and reagent addition and conditioning was done in the beginning. However, this might not be sufficient for pyrochlore recovery. To verify this, NP 22 was carried out with five stages of rougher, with reagent addition in each stage. The total dosage of Aero 6493 and NaMP was 1,750 and 750 g/t, respectively, and the total flotation time was 23 min. The flowsheet of test NP 22 is shown in Figure 4.20. With progressive addition of reagents and extended flotation time, the total recovery reached 85%. To further increase pyrochlore recovery without recovering the carbonate and silicate gangue, a regrinding stage was used in the rougher flotation. The regrinding was done either on the Mill Feed, or on the rougher tail after 2 stages of rougher flotation. This will be discussed in the following section.

500 g Niobec Mill feed sample (80% -200 μm)
in 1.5 L cell , 1,200 rpm, natural pH (8.4)

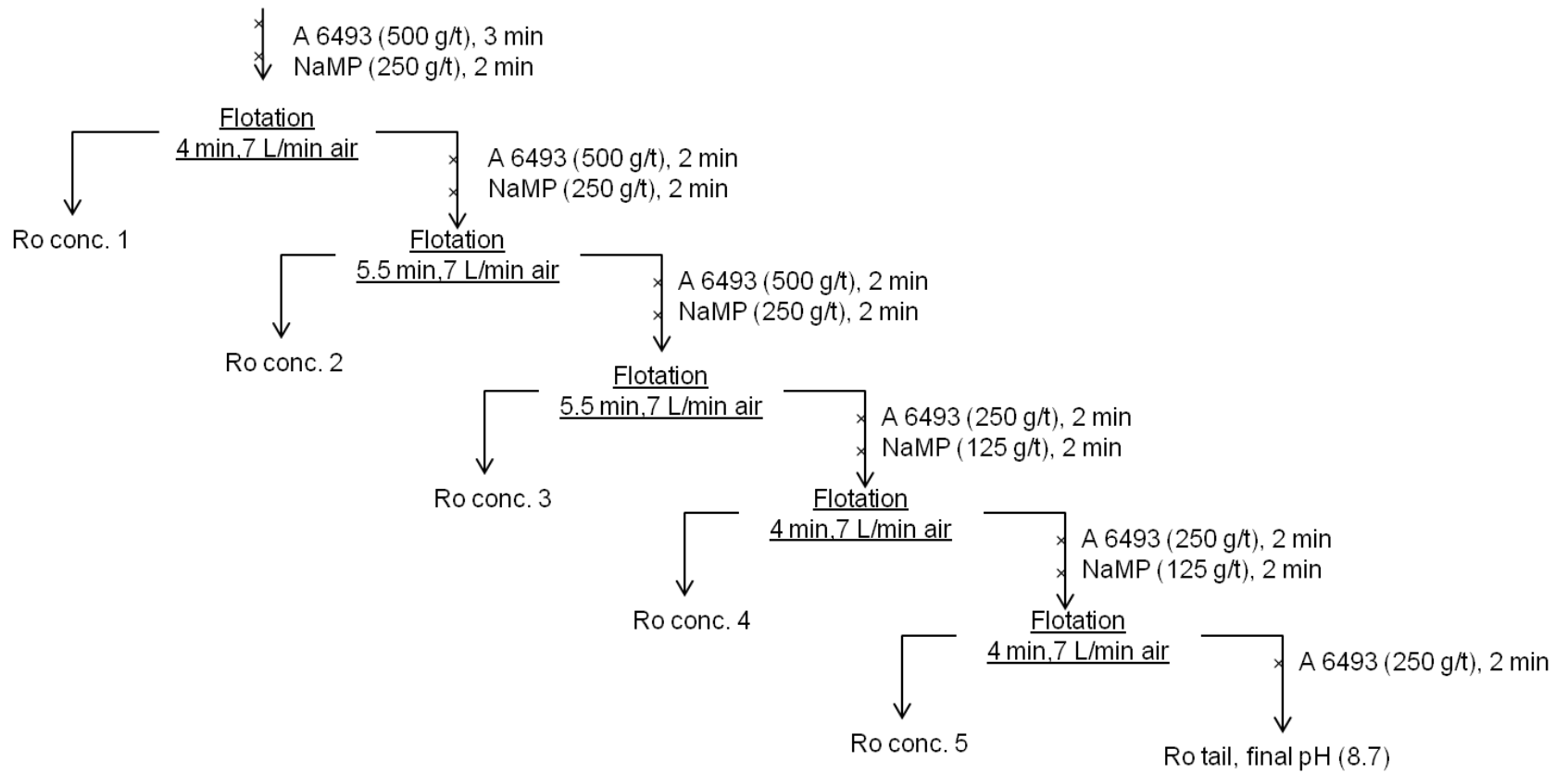


Figure 4.20 Flowsheet of test NP 22.

4.4.2. NP 23-25

In test NP 23, the Mill Feed sample was screened into -106 μm and +106 μm size fractions. The +106 μm size fraction was dry ground in an 8" ball mill for 8 min using about 11 kg of -1"+1/2" mild steel balls and then combined with the -106 μm and floated (Figure 4.21). The total recovery of NP 23 is 71.5%, lower than 74.1% of NP 12, indicating that the further grinding the feed could not increase the pyrochlore recovery.

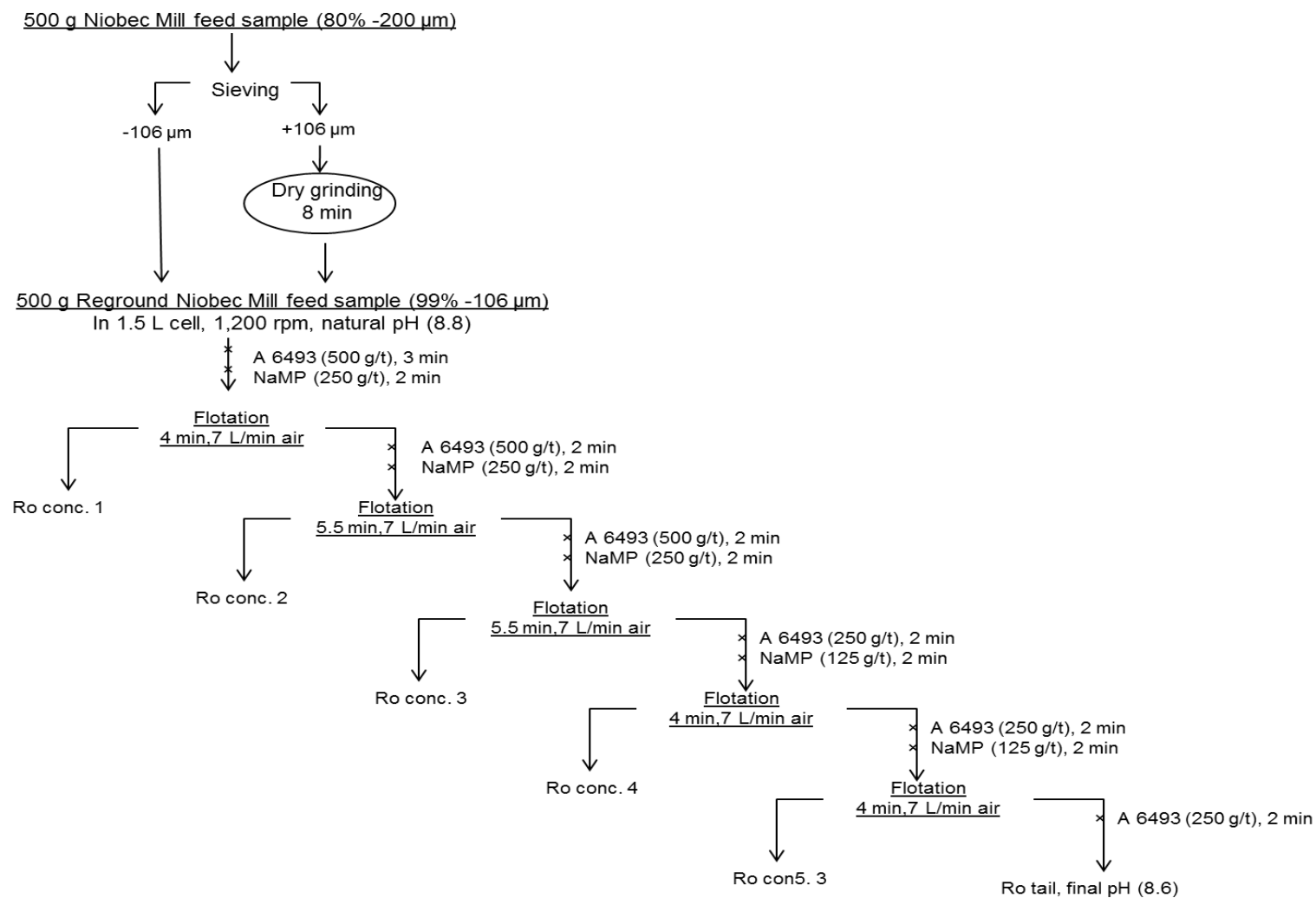


Figure 4.21 Flowsheet of test NP 23.

In tests NP 24 and NP 25, the Mill Feed was floated for 2 rougher stages, and the rougher tail at that point was thickened and re-ground using the same 8" ball mill without prior particle size separation. The ground slurry was diluted and transferred to the flotation cell for two more stages of rougher flotation. Tests NP 24 and NP 25 were exactly the same except that the regrinding time was 30 min in test NP 24 and 20 min in NP 25. The flowsheet of test NP 25 is shown in Figure 4.22.

The results seemed that regrinding of the rougher tail could liberate more pyrochlore which could not be collected in previous tests. After regrinding the rougher tail and two more stages of rougher flotation, the total pyrochlore recovery increased to around 95% in both tests NP 24 and 25. The difference in the total recovery between these two tests was 1% (Figure 4.23), which indicates that the results were reproducible and that 20 min regrinding of the rougher tail was sufficient to release most of the un-liberated pyrochlore from gangue minerals. It is also worthwhile to point out that our reagent combination was more tolerant to fine particles than the current reagents used in industry, so that the desliming stage, which is currently used, will not be necessary when the hydroxamic acid collector is used.

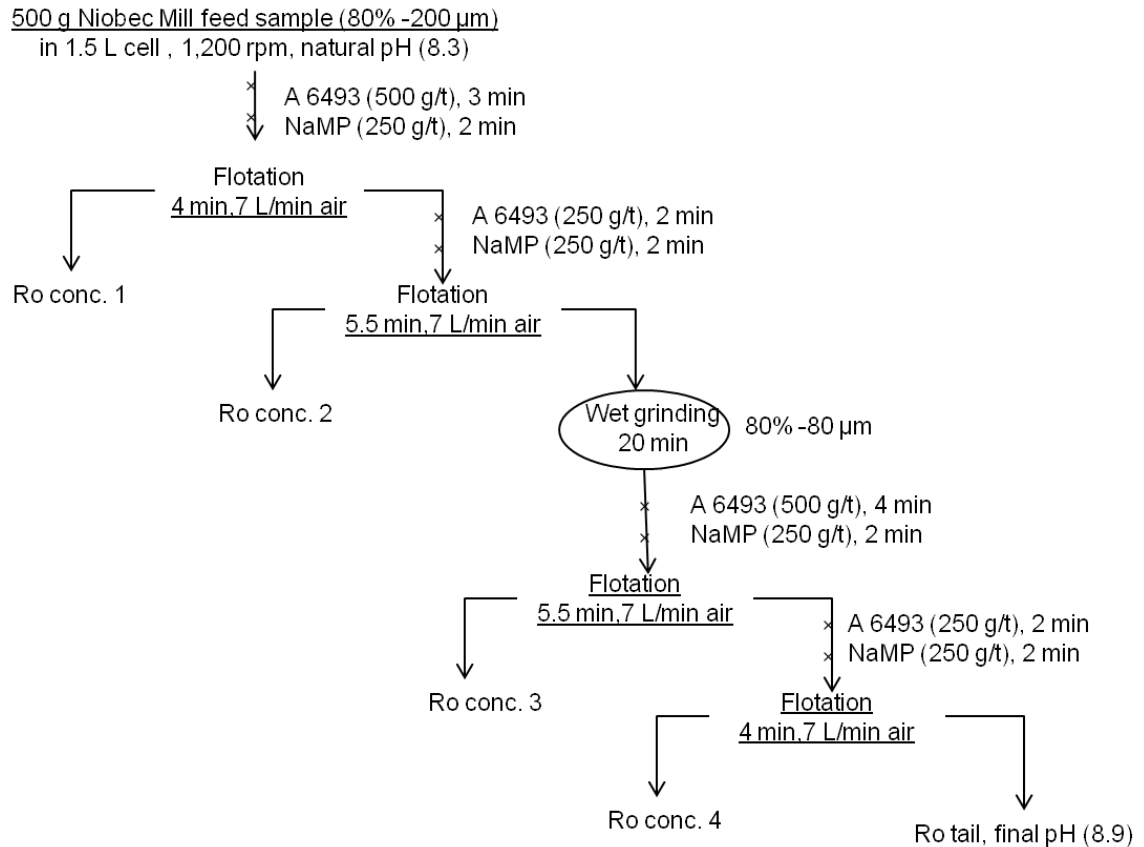


Figure 4.22 Flowsheet of test NP 25.

Figure 4.23 summarizes the total rougher pyrochlore recovery of tests NP 12, and NP 22 to NP 25. The rougher pyrochlore recovery in tests NP 24 and NP 25 was deemed satisfactory so that the rougher flotation procedures of these two tests were used in the subsequent cleaning flotation tests.

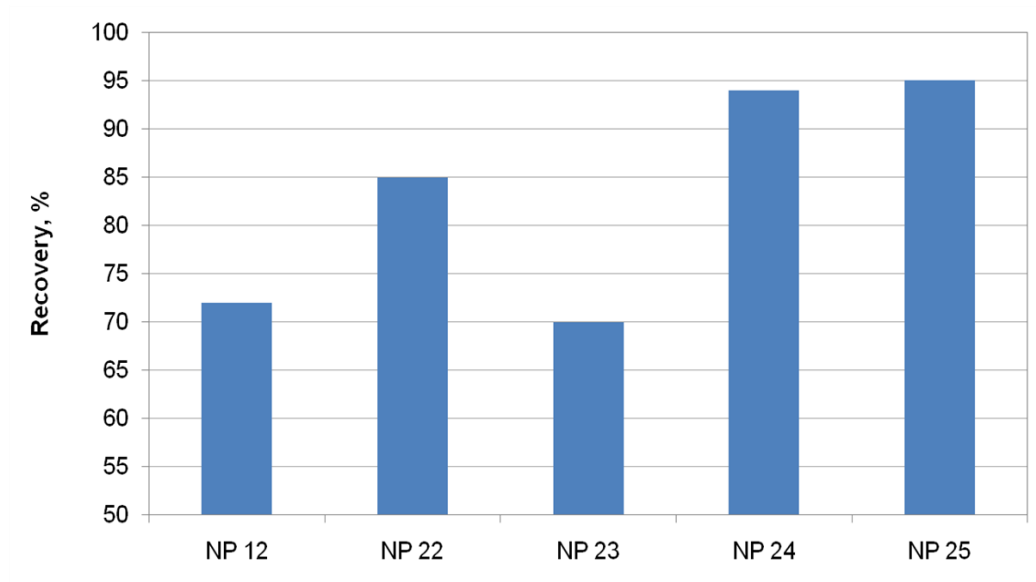


Figure 4.23 Comparison of total rougher pyrochlore recovery in tests NP 12, and NP 22 to NP 25.

4.5. Cleaner flotation

The major objective of cleaner flotation is to obtain high grade concentrates by removing gangue minerals that are trapped in the rougher concentrate. Usually in the cleaner flotation, only frother is used to maintain the froth layer thickness if necessary. The solid concentration in the pulp is lower than that of rougher flotation to give sufficient dilution of the pulp to release the trapped particles. In order to study whether the developed reagent combination could further concentrate pyrochlore to a higher grade, cleaner flotation was carried out. The limited quantity of the rougher concentrate from each batch flotation had limited the total number of cleaner stages that could be carried out. However, this would still be able to show the trend of niobium oxide grade along the cleaner stages.

In the three batch flotation tests (NP 26 to NP 28) where cleaner flotation was carried out, the rougher procedures followed the optimized rougher flotation procedure, which was similar to NP 25: the reagents were added progressively; three rougher stages were conducted in total with rougher tail regrinding after the 1st rougher stage. In test NP 26, two stages of cleaner flotation were carried out with a flotation time of 7 and 5 min, respectively, and final concentrate grade reached 8.11 % Nb₂O₅.

In tests NP 27 and NP 28, one stage of reverse pyrite flotation was carried out before rougher flotation (Figure 4.24). For this purpose, 100 g/t KAX-41 (an amyl xanthate collector from Charles & Tennant) was used and the reverse flotation was carried for 4 min. After the reverse pyrite flotation, the remainder of the rougher flotation was the same as test NP 26. Two cleaner flotation stages were carried out in test NP 27, and five stages of cleaning flotation was carried out in test NP 28.

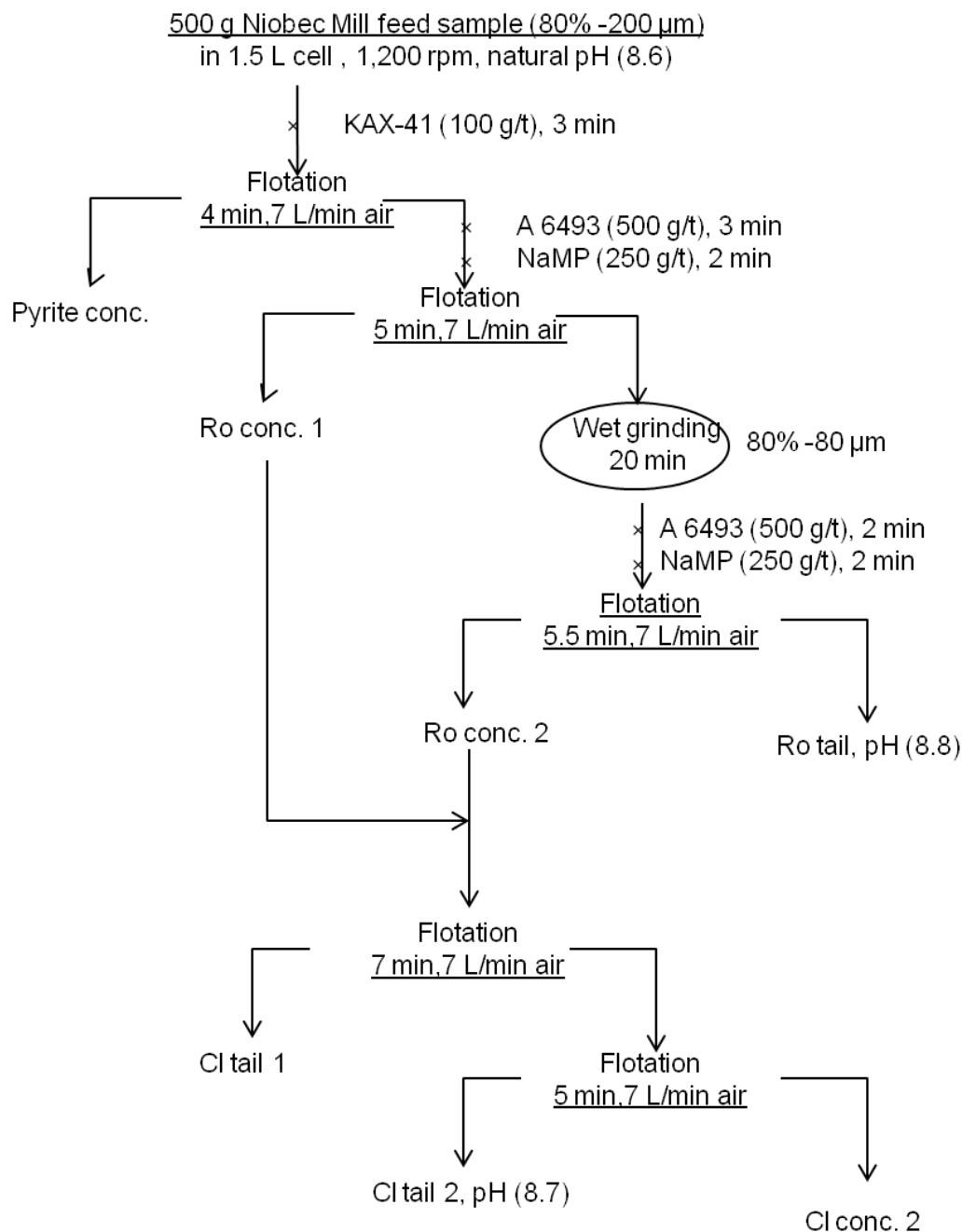
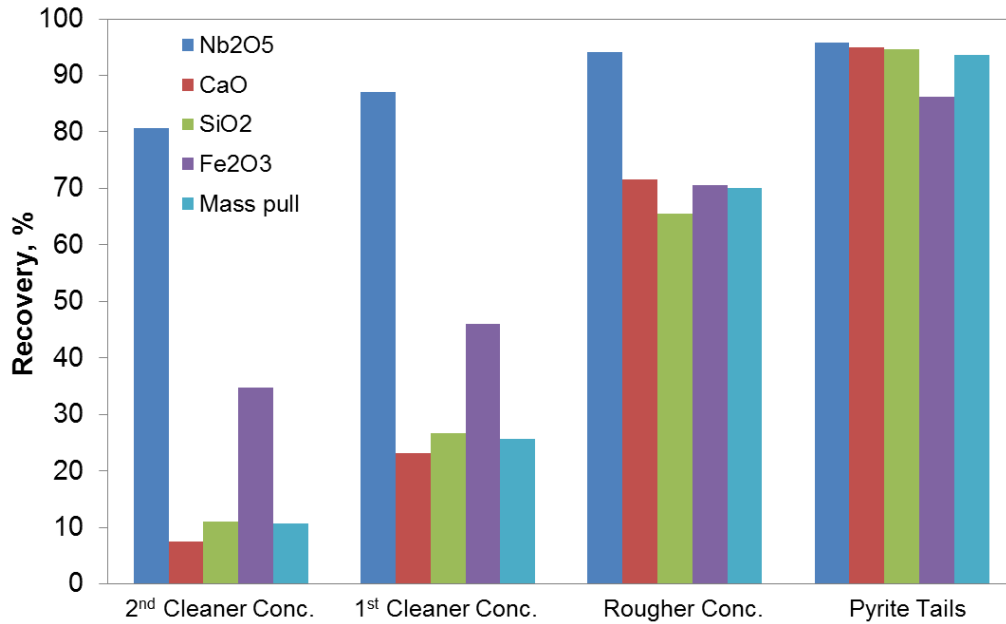


Figure 4.24 Flowsheet of test NP 27.

In test NP 27, the reverse pyrite flotation removed about 14 % of the iron (Figure 4.25 (a)). However, the grade of iron was still very high in the final concentrates

(31.70% compared with 47.70% of test NP 26 (Appendix A), which pyrite was not floated before pyrochlore flotation). The grade of niobium oxide (5.8%) was not improved compared with 8.11% of test NP 26 in the final concentrates, either (Figure 4.25 (b)). It most likely due to iron oxide was not removed in the feed after pyrite reverse flotation such as hematite and magnetite.



(a)

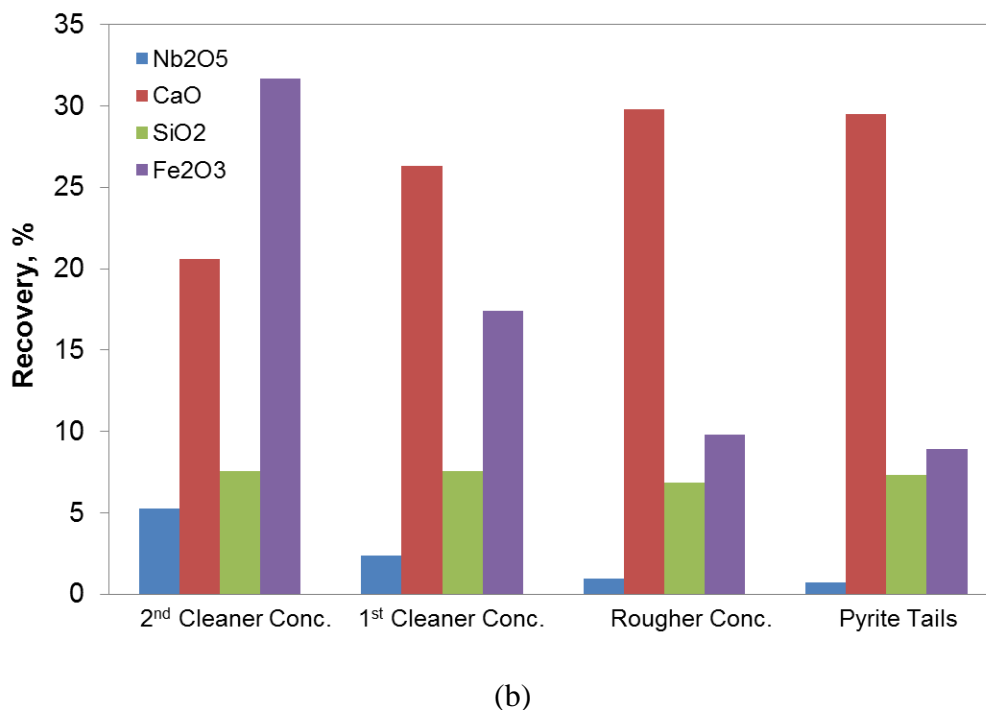
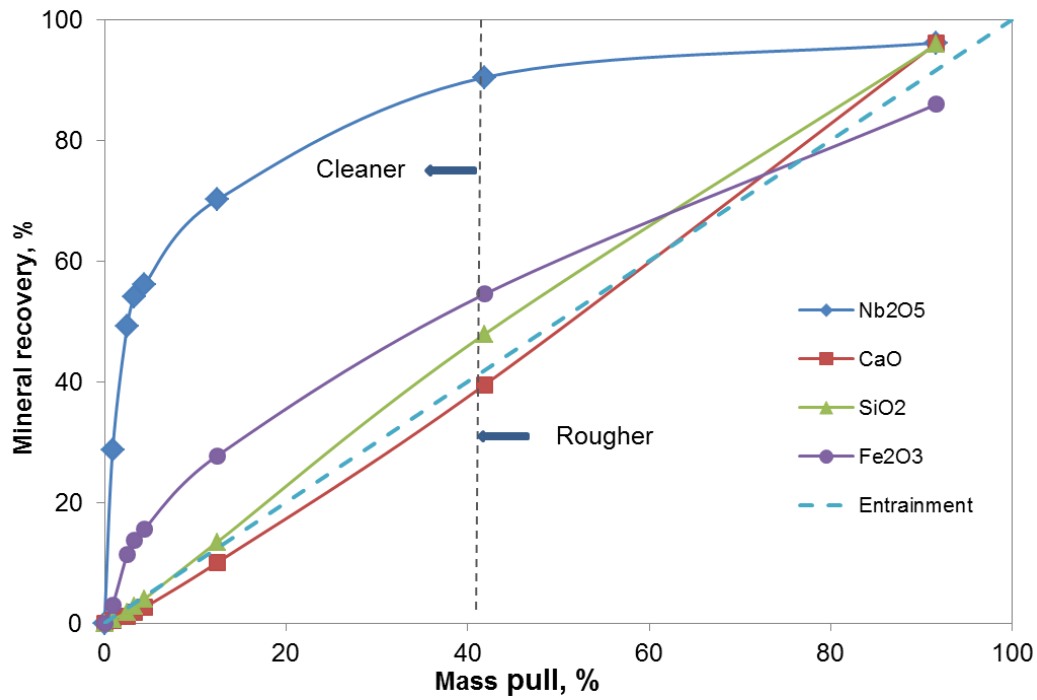
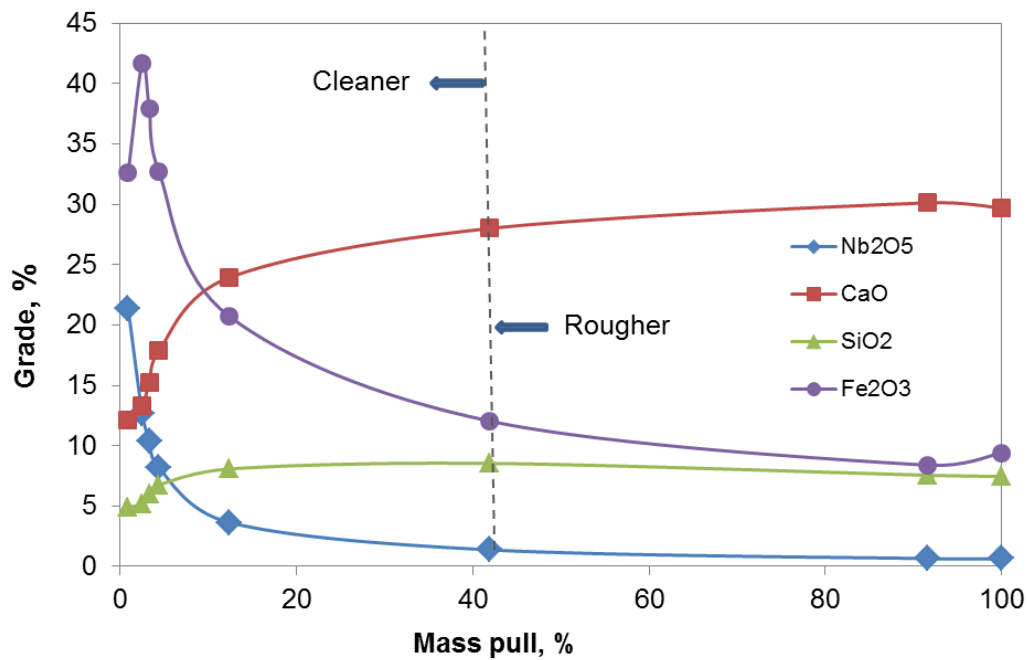


Figure 4.25 Recovery (a) grade (b) in the flotation stages of test NP 27.

Five cleaner flotation stages were carried out in test NP 28. The grade of niobium oxide in the final concentrate reached over 20%, over thirty times higher than that of Mill Feed. Iron oxide grade in the final concentrate reached over 30% while carbonate and silicate grade was lowered to roughly 12 % and 5%, respectively. About 24% of the iron was removed in the pyrite reverse flotation stage. Test NP 28 showed that pyrochlore could be concentrated through repeated cleaning flotation (Figure 4.26). The reason of iron content drop in the final concentrates is not sure at this point, it might be caused by natural selectivity of hydroxamic acid between niobium and iron containing minerals in extensive cleaning stages.



(a)



(b)

Figure 4.26 Mineral recovery (a) Mineral grade (b) and solid recovery in cleaner stages of NP 28.

Iron oxide gangue was collected throughout the rougher and cleaner stages in all batch flotation tests. As the iron oxide gangue is less of a concern compared to carbonate and silicate (the Niobec Mine makes ferroniobium as its final product), the process development has not been focused on the removal of iron oxide gangue.

4.6. Batch flotation using pure hydroxamic acid

Besides commercial product Aero 6493, batch flotation tests were also conducted using synthesized octyl hydroxamic acid (OHA). This was to rule out the effect of other chemicals in the commercial product Aero 6493, and also provide flotation data for the adsorption mechanisms study which was performed using octyl hydroxamic acid. OHA is the major ingredient in Aero 6493 as indicated by Cytec. Since OHA shows strong frothing ability, no additional frother was needed. Plus, it was found that the pure OHA is much powerful in terms of dosage, 100 g/t OHA is capable to recover over half pyrochlore. No depressant was used in order to show the natural selectivity of the collector. In tests NP 30 and 32, only rougher flotation was conducted. The original Pyrochlore Float Feed was used in both tests but in one of them, the magnetite gangue was removed prior to flotation (Table 4.3). No depressant was used.

Salicylhydroxamic acid (SHA) was tested in tests NP 33 to NP 35, on Pyrochlore Float Feed without using any depressant. However for SHA, 40 g/L DF 250 was

needed to keep the froth layer thickness and progressively added into the flotation pulp. Salicylhydroxamic acid has one more hydroxyl group on the benzene ring. Recent research (Jiang et al, 2010, Jiang et al, 2010) indicated that additional bonding groups in hydroxamic acid could increase its selectivity between diaspore and clays. But their conclusion was only based on small-scale flotation tests.

Table 4.3 Collector dosage and feed samples in batch flotation using pure collector.

Test	Feed type	Collector	Collector Dosage, g/t	DF 250 dosage g/t
NP 30	Pyrochlore Feed	OHA	100	
NP 32	Magnetite removed Feed	OHA	100	
NP 33	Pyrochlore Feed	SHA	500	
NP 34	Magnetite removed Feed	SHA	500	40
NP 35	Pyrochlore Feed	SHA	1,000	40

In test NP 30 and 32, it floated roughly 30% solids which containing 85% niobium oxide in the rougher stage. However, iron oxide content in 1st concentrate is 23.70% in NP 32, which is lower than that of NP 30 whose feed the magnetite was not removed. Niobium oxide in 1st concentrate is 18.50% in NP 32, which is higher than that of NP 30. This indicated that removing the magnetite is an effective way to lower the iron content in concentrates.

Unlike the slimy frother using OHA, the frother using SHA was quite clear. No frother was used in NP 33, SHA only recovered 12.8% Nb₂O₅ with 3% mass pull. With 40 g/t DF 250, SHA recovered half of niobium oxide with 10% mass pull in NP 34. Further increasing the SHA dosage to 1,000 g/t, the niobium recovery is

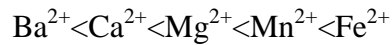
not increased in NP 35. Though the selectivity of SHA is better than OHA, the recovery from tests using SHA is far from satisfying. No further cleaner flotation was carried out. To better compare the selectivity of two collectors, it was quantified by selectivity ratio (Table 4.4) for different minerals.

Table 4.4 Selectivity ratio for different minerals in batch flotation using pure collector.

Test	Collector	S_{Nb}	S_{Fe}	S_{Ca}	S_{Si}
NP 30	OHA	2.60	1.37	1.05	0.68
NP 32	OHA	2.59	1.04	1.07	0.64
NP 34	SHA	5.18	1.54	1.12	0.41

Selectivity ratio of both collectors follows order: Nb>Fe>Ca>Si. Silicate was not floated at all. Niobium and iron were truly concentrated in the rougher flotation tests. It is obvious that hydroxamic acid could float niobium oxide minerals away from carbonate gangue without the need of depressant. Comparing the behavior of OHA and SHA, the selectivity ratio of SHA for niobium (V) oxide was twice that of OHA, indicating that SHA was a more selective collector for pyrochlore. This was also observed for iron gangue, but the difference between OHA and SHA on iron gangue was not as large as that on niobium oxide (Table 4.4). The outstanding selectivity of SHA may be due to the phenol groups which provide extra bonding site for niobium (V) atoms forming stronger chelation complexes. For calcium carbonate, there seems to be no difference in selectivity between the two collectors (Table 4.4).

For metal ions in solution, the stability of chelation complexes is affected by the coordination bonding site formed as well as the central metal ions. Irving-Williams series (Irving and Williams, 1953) summarizes the relative complex stabilities formed from M^{2+} ions as following:



It is worth to note that this series is insensitive to the choice of ligands which indicates that the transition metal ions could form stronger chelation complexes than alkaline earth metals. Plus, Transition metals (d-block) have various oxidation states. Usually the higher oxidation numbered metal ions can form more stable complexes (Lawrence, 2010). This may be due to the smaller size along with higher charge facilitating shorter metal-ligand distances and stronger interaction.

Selectivity ratios in Table 4.4 follow the Irving-Williams series, which implies that selectivity of hydroxamic acid in flotation originates from the interaction strength between hydroxamic acid and surface metallic sites. Further investigation will be carried out in section 4.8.

4.7. Effect of neutral oil

Kerosene as a neutral oil is used in flotation to collect fine particles by shear flocculation flotation (Lu and Song, 1991; Song et al., 2001). Intensive stirring of the system with immiscible organic oil that can wet the dispersed particles may lead to agglomeration or bridging particles by the oil, this is also known as agglomerate flotation (Laskowski and Ralston, 1992). In tests NP 16-21 kerosene was used with Aero 6493/NaMP, and in some of these tests the agitation speed was increased from 1,200 rpm to 1,750 rpm. Results of these tests are listed in Table 4.5 together with two blank tests NP 12 and NP 48 in which no kerosene was used.

Unfortunately, the synergy effect was not observed in any of the tests with kerosene, even worse, the recovery of niobium oxide was in fact depressed after adding kerosene. The intensive agitation (1,750 rpm) coupled with kerosene completely suppressed pyrochlore recovery.

Table 4.5 Batch flotation results of Niobec feed sample using kerosene

Test #	Feed	A 6493, g/t	OHA, g/t	NaMP, g/t	Kerosene, g/t	Stirring speed, rpm	Solid recovery, %	Nb ₂ O ₅ recovery, %
NP 12	Mill Feed	1,000		500		1,200	19.0	74.1
NP 16	Mill Feed	1,000		500	250	1,200	12.2	49.7
NP 17	Mill Feed	1,000		500	250	1,750	6.2	5.1
NP 18	Mill Feed	1,000		500	2,000	1,200	14.1	65.1
NP 19	Mill Feed	1,000		500	5,000	1,200	16.2	43.8
NP 20	Mill Feed	1,000		500	2,000	1,750	10.0	10.1
NP 21	Mill Feed	1,000		500	5,000	1,750	20.7	22.4
NP 48	Carbonate		100			1,200	43.9	66.9
NP 49	Carbonate		100		500	1,750	6.7	4.6

To rule out the effects of other reagents in Aero 6493 and better study the behaviors of kerosene in flotation, kerosene was used with only pure OHA in test NP 49. Figure 4.27 illustrates the particle size distribution of NP 48 rougher tail, NP 49 rougher tail and the flotation feed, i.e., Carbonate Feed. For test NP 48, it can be seen from Figure 4.30 that OHA mostly collected particles that were smaller than 75 μm . Only about 25% of particles in NP 48 rougher tail passed 75 μm compared with approximately 50% in feed. This explained our previous results why further grinding the rougher tails could increase the niobium oxide recovery, because more pyrochlore particles were liberated and collected after regrinding. It also proved that the optimum particle size range for OHA was smaller than the cationic collectors currently used. In both Carbonate Feed and NP 49 rougher tail, the percentage of particles smaller than 75 μm was about 50%. And the particle size distribution of NP 49 was very similar to the feed since the mass pull was very low (only 6.9% compared with 43.9% of NP 48). This showed that adding kerosene in test NP 49 brought significant negative effect: OHA lost its power to collect the fine particles. The reason for this unexpected behavior is not clear at this point. It might be related to the defrothing effect of kerosene.

Since hydroxamic acid itself was a good collector for fine particles, further investigation using other auxiliary collector to collect fine particles was not pursued.

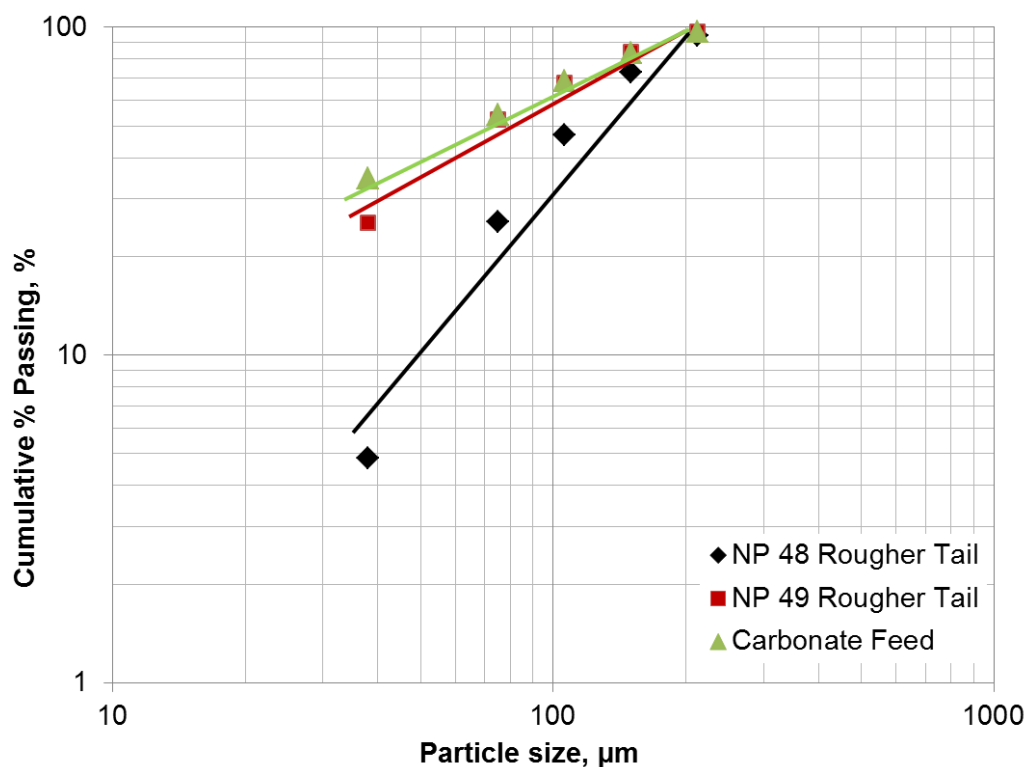


Figure 4.27 Particle size distribution of test NP 48 and 49 rougher tail and their feed.

4.8. Adsorption mechanism studies

4.8.1. Infrared spectroscopy analysis

The types of bonds of adsorbed reagents on mineral surfaces can be identified by infrared spectra (Bellamy, 1975). The appearance of the alkyl groups at 2924 and 2856 cm^{-1} on the OHA treated calcite indicated that the hydroxamic acid molecules were adsorbed on the mineral surface (Figure 4.28). The carbonyl group frequency only shifted by 15 cm^{-1} to the lower wavenumber. The O-H and

N-H stretch can also be seen at higher than $3,000\text{ cm}^{-1}$ wavenumbers. This demonstrates that the carbonyl group and hydroxyl group did not change significantly after adsorption. Therefore, the adsorption of the OHA on calcite was probably more of a physical nature.

Adsorption of hexametaphosphate on the calcite surface was not observed. The characteristic peaks of HMP group include: P=O at 1280 cm^{-1} , P-O at 1097 cm^{-1} and 991 cm^{-1} , and P-O-P at 876 cm^{-1} (Socrates, 1980). None of them can be seen on the treated calcite surface. This might be caused by the complexes formed could be easily washed away by distilled water when preparing the sample. Further investigation using XPS will be described in a later section.

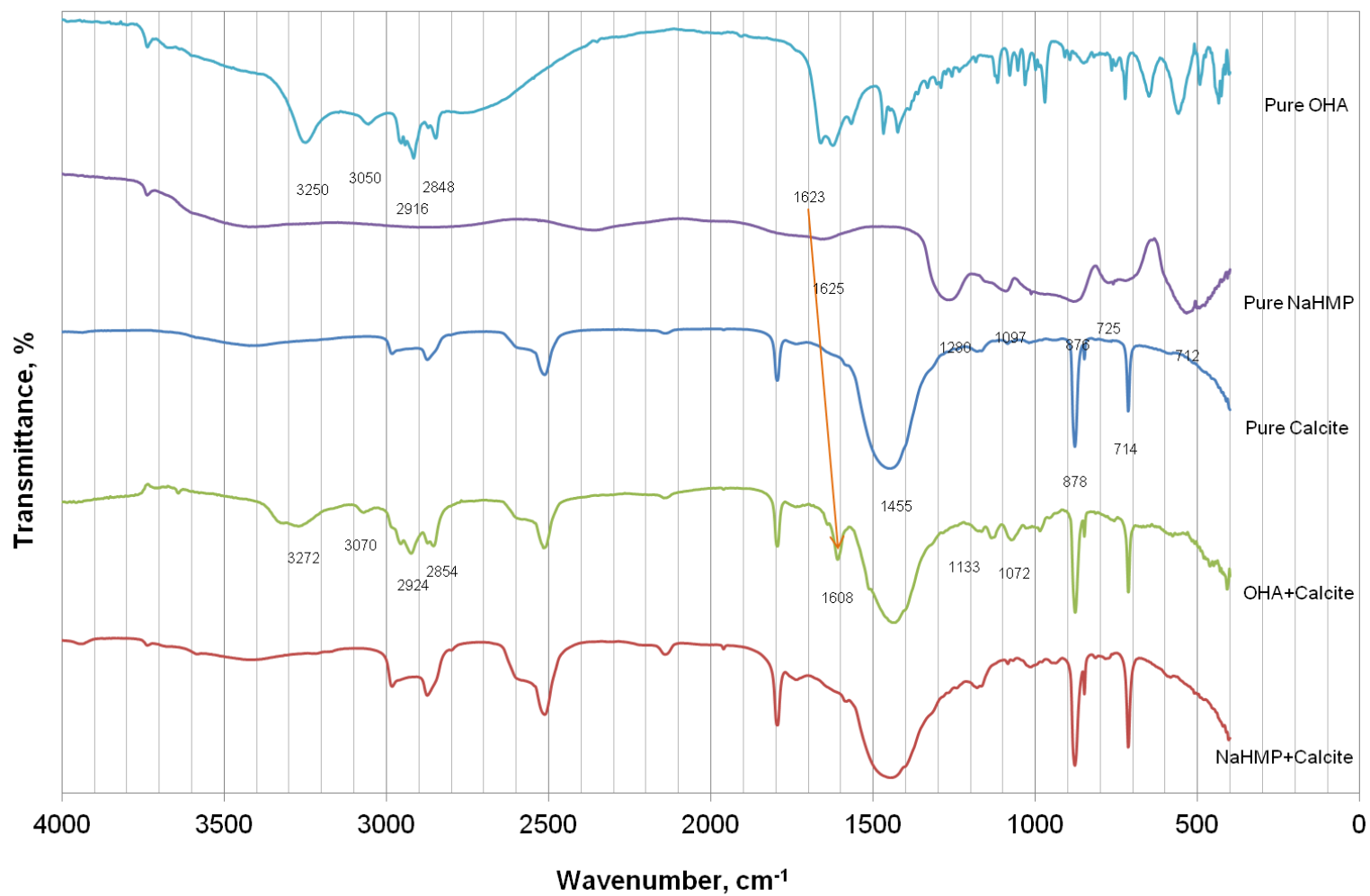


Figure 4.28 The infrared spectra of normal octyl hydroxamic acid, sodium hexametaphosphate, metaphosphate treated calcite, hydroxamic acid treated calcite and pure calcite surface.

The FTIR spectra of high purity OHA, pyrochlore and OHA treated pyrochlore is shown in Figure 4.30. The appearance of the alkyl groups at 2924 and 2856 cm^{-1} on the OHA treated pyrochlore also indicated that the hydroxamic acid molecules were adsorbed on the mineral surface as well. The peak at 1531 cm^{-1} might be the vibrational frequency of carbonyl group of the adsorbed hydroxamic acid, which moved to the lower wavenumber by 92 cm^{-1} from 1623 cm^{-1} . This indicated that the carbonyl oxygen participated in the adsorption by donating its lone pair electrons to form chemical complex with the metal ions on the pyrochlore surface. The broad O-H stretching of pure hydroxamic acid cannot be seen on the treated pyrochlore surface, indicating that the OH group probably also participated in the adsorption process. Therefore, the hydroxamic acid shows a higher affinity to niobium oxide minerals. The formed Nb-OHA chelate structure is shown in Figure 4.29.

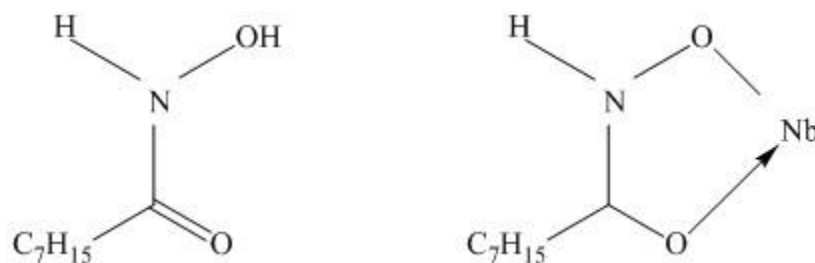


Figure 4.29 Structures of octyl hydroxamic acid and its metal chelates.

The adsorption of hexametaphosphate on the pyrochlore is not observed either (Figure 4.30).

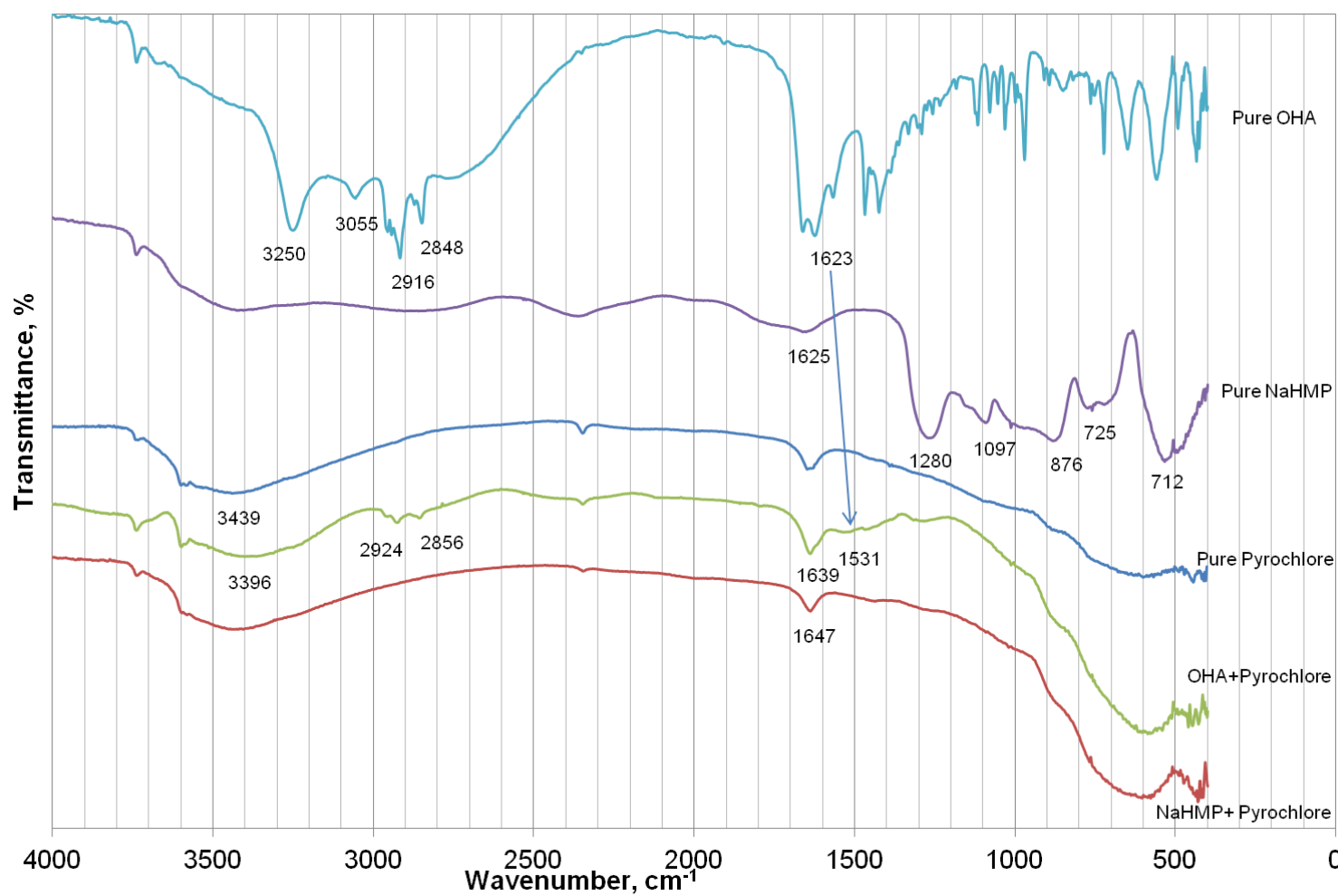


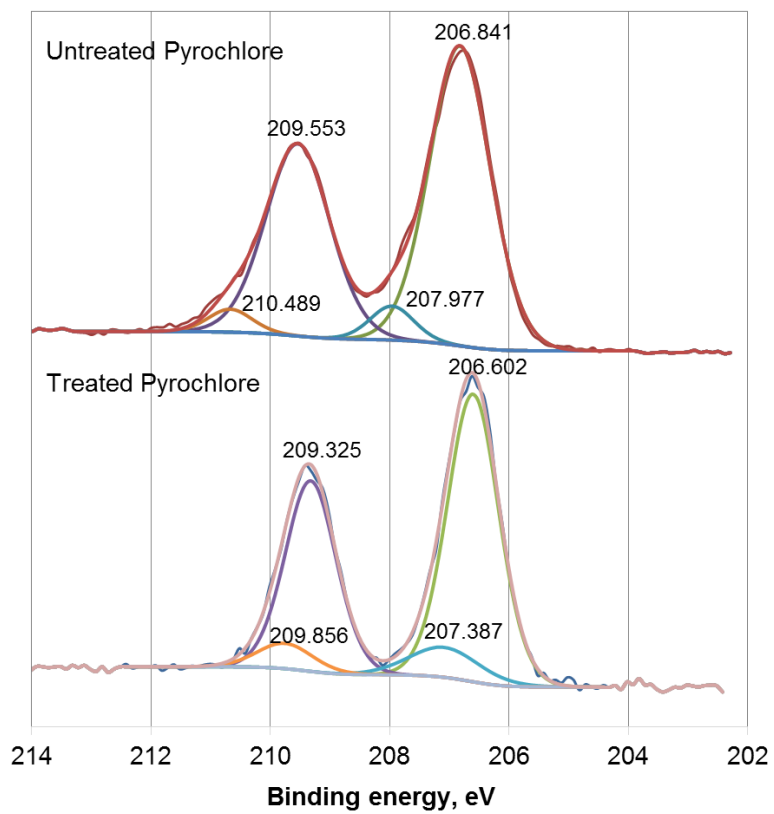
Figure 4.30 The infrared spectra of normal octyl hydroxamic acid, sodium hexametaphosphate, hexametaphosphate treated pyrochlore, hydroxamic acid treated pyrochlore and pure pyrochlore surfaces.

4.8.2. X ray photoelectron spectroscopy analysis of OHA treated minerals

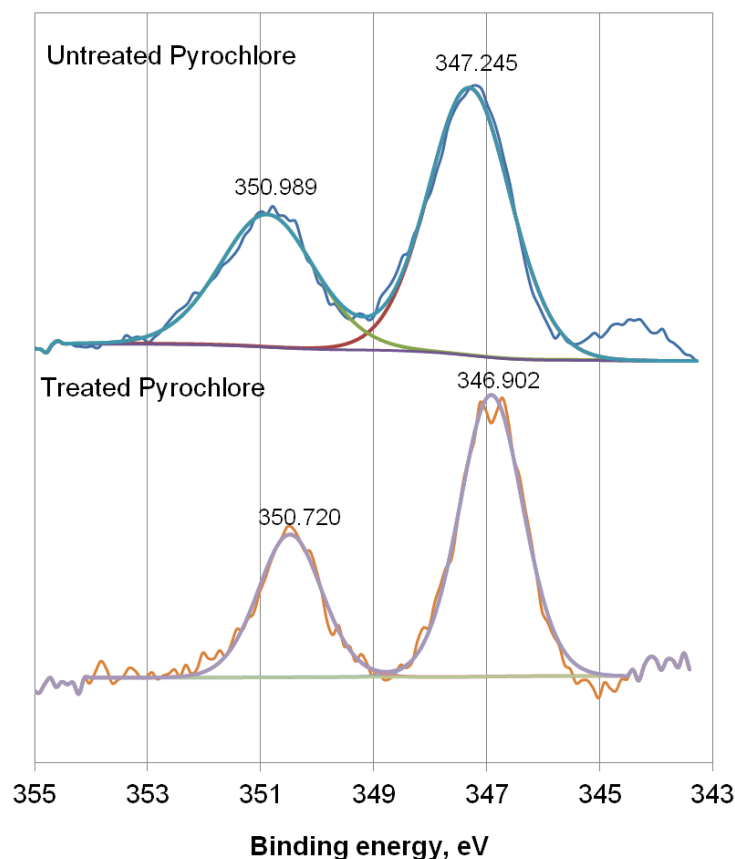
The chemisorption entails a change in the chemical environment surrounding the atoms involved, causing a chemical shift of the electron binding energies, which can be detected by a X-ray photoelectron spectrometer. Figure 4.31 shows the original and de-convoluted binding energy spectra of Nb 3d and Ca 2p electrons on pyrochlore, respectively, before and after reaction with octyl hydroxamic acid.

Figure 4.31(a) shows two pairs of Nb 3d doublets. This may be due to the existence of small amount of columbite (which also contains niobium) in the pyrochlore sample. The ratio of integral areas of these two doublets is approximately 8:1, compared with 10:1 from mineralogical assay. The deviation might be because XPS is a surface analysis technique, while the mineralogical analysis results was a bulk assay.

After OHA adsorption, the binding energy of one Nb 3d^{5/2} electron on OHA treated pyrochlore surface was decreased by 0.24 eV from 206.84 eV to 206.60 eV while that of the other Nb 3d^{5/2} had decreased by 0.59 eV from 207.98 eV to 207.39 eV. This might indicate that columbite shows stronger affinity for OHA. The binding energy of Ca 2p^{3/2} on pyrochlore was decreased by 0.35 eV from 347.25 eV to 346.90 eV after OHA adsorption (Figure 4.31 (b)).



(a)



(b)

Figure 4.31 XPS spectra of (a) Nb 3d (b) Ca 2p of untreated and OHA treated pyrochlore.

However, for the calcium atoms on the OHA treated calcite surface, the binding energy of the Ca 2p^{3/2} electrons dropped by only 0.18 eV from 346.65 eV to 346.47 eV (Figure 4.32). The decrease of the electronic binding energies of the respective cations on the mineral surface indicated that these cations accepted electron clouds after OHA adsorption, i.e., that they were reduced. This was likely caused by the donation of the lone pair electrons on the carbonyl oxygen as discussed earlier, i.e., chemisorption. Therefore, both the calcium and niobium

atoms on pyrochlore surface could be active sites for hydroxamic acid to form chemical bonds, while the adsorption of OHA on calcite was of a weaker interaction in view of the smaller chemical shift observed.

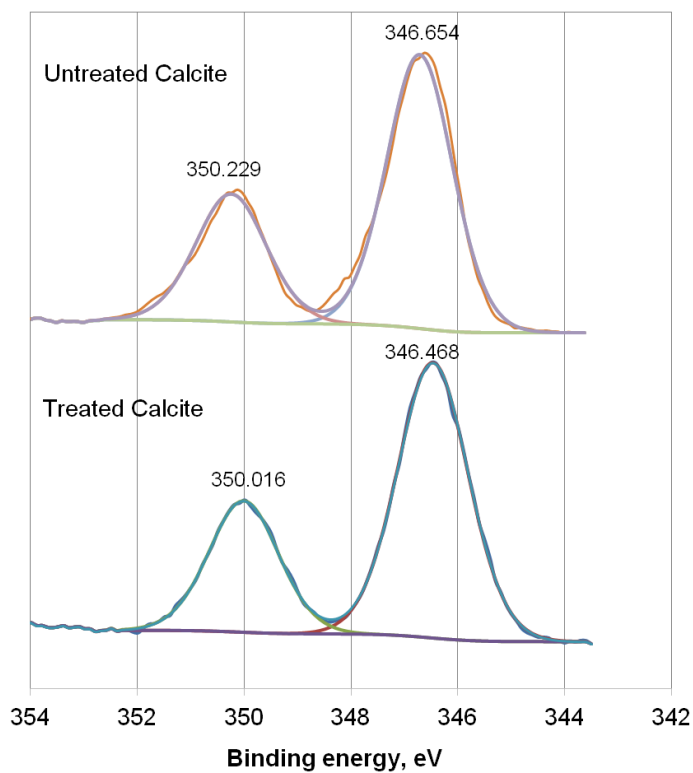


Figure 4.32 XPS spectra of Ca 2p of untreated and OHA treated calcite.

The relative atomic ratios on the OHA treated and untreated pyrochlore and calcite surfaces are listed in Table 4.6. The increase of C/Nb, N/Nb ratios, and C/Ca, N/Ca ratios on both mineral surfaces after OHA treatment shows that the OHA was adsorbed on the mineral surfaces.

Table 4.6 Relative atomic ratio on the pure and OHA treated surfaces.

Sample	C/Nb	N/Nb	Sample	C/Ca	N/Ca
Pyrochlore	6.65	0.00	Calcite	3.20	0.00
OHA treated pyrochlore	10.26	0.66	OHA treated calcite	8.22	0.68

The presence of adsorbed hydroxamic acid on the mineral surface can be best shown by comparing the binding energies of N 1s electrons from the XPS spectra. N 1s signal is also the best indicator of chemical state of atoms in OHA molecules since the other two elements, oxygen and carbon, in OHA is easily overlapped by signals from substrate and/or contaminates. High resolution spectra of N 1s of the OHA as well as on the treated and untreated minerals are shown in Figure 4.33. As can be seen, on both untreated pyrochlore and calcite, no obvious N 1s peaks were detected. However, after treatment by OHA, the N 1s peaks were observed on both minerals. After the N 1s spectra were de-convoluted into components, different adsorption mechanisms on the two minerals were revealed.

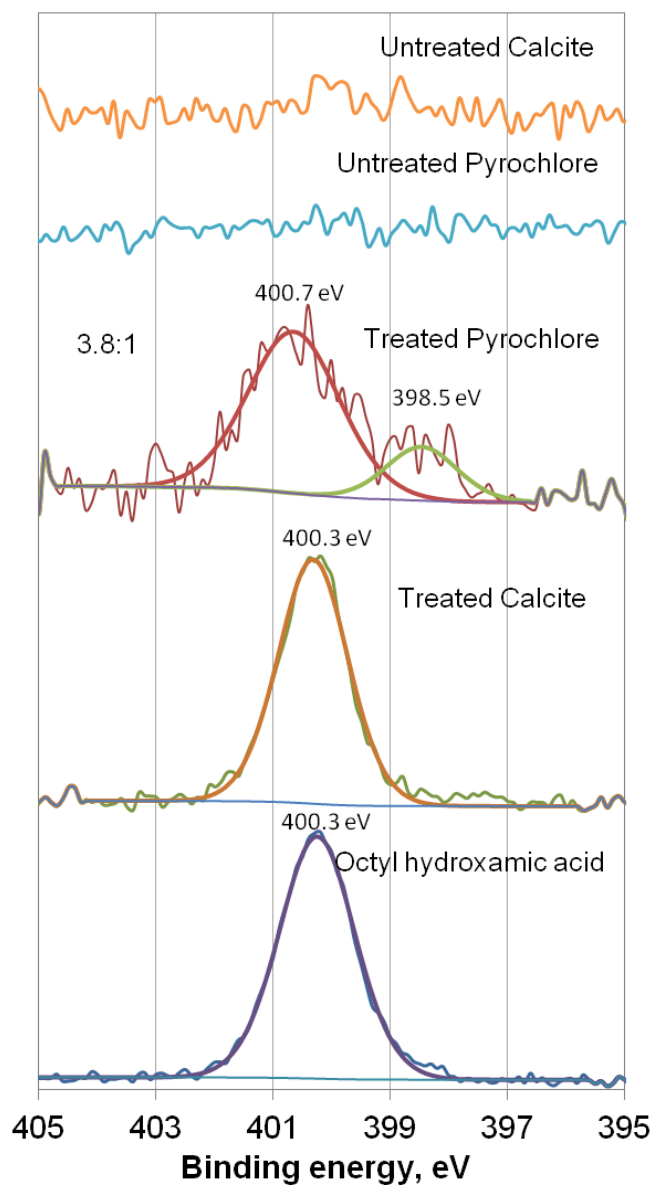


Figure 4.33 N 1s spectra of OHA, untreated and treated pyrochlore and calcite by 50 mL 31 mmol/L OHA solution at pH 8.5.

On OHA treated pyrochlore surface, the N 1s spectrum was made of two components: one at 398.5 eV and the other at 400.7 eV. The one at 400.7 eV was attributed to nitrogen atoms in the neutral molecules, i.e., the protonated (neutral)

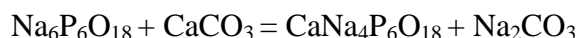
form of the hydroxamic acid, R-CO-NH-OH , and the peak at 398.5 eV was due to the nitrogen in the deprotonated hydroxamate groups, R-CO-NH-O^- (Alagta et al., 2008). Since deprotonation is the first step of chemisorption of the hydroxamic acid on the mineral surface, the peak at 398.5 eV was attributed to chemically adsorbed octyl hydroxamic acid molecules. The integrated area ratio between these two peaks is 3.8:1, indicating that the ratio of physically adsorbed OHA to chemically adsorbed OHA was about 3.8 to 1. XPS analysis (Folkers et al., 1995) of adsorbed hydroxamic acid monolayer on metal oxides indicated that on titanium oxide and aluminum oxide, the deprotonated molecules were also observed, and the ratios of protonated versus deprotonated OHA were 2.5:1 and 2.3:1, respectively. On the other hand, on the treated calcite surface, only a single peak was detected at 400.3 eV, which matches exactly the single N 1s peak in the original protonated OHA. The peak at 398.5 eV was absent.

Therefore, the XPS spectra of OHA treated pyrochlore indicated chemical shift of binding energies of electrons in the atoms in both adsorbate (nitrogen in OHA) and adsorbent (niobium and calcium in pyrochlore) after adsorption. In contrast, the chemical shift of the N 1s in OHA could not be found on treated calcite surface, and the chemical shift of Ca 2p on treated calcite was also subtle. This indicated that OHA was likely adsorbed on calcite by physical adsorption whereas on pyrochlore by chemisorption.

Transitional metal (especially higher valence) ions in solution could form stable complexes with OHA while calcium and magnesium could not (Khalil and Fazary, 2004; Khalil and Mahmoud, 2008). These complexes formed in the bulk solution are different from those formed on mineral surface (by chemisorbed OHA). The stability constant of niobium-OHA interaction formed on pyrochlore surface is difficult to measure by current technologies. However, XPS and FTIR spectrum indicated that interaction between adsorbed OHA and cations on pyrochlore was stronger than that on calcite. Hence, chemisorption of OHA on pyrochlore should draw more OHA adsorbed than on calcite which based on weak physical adsorption. The adsorption density on high purity minerals and their mixture will be studied in the later sections.

4.8.3. X-ray photoelectron spectroscopy analysis of NaHMP treated minerals

It is reported that 100 g NaHMP in solution could dissolve 16.2 g of calcium carbonate (Thomson, 1936), which implied the following chemical reaction:



According to this equation, the theoretical dissolvable calcite weight by 5 g NaHMP in solution should be 0.810 g. We verified that 100 ml 50 g/L NaHMP (5 g totally) in solution dissolved 0.805 g calcite by measuring the weight difference before and after hexametaphosphate addition. The aforementioned chemical reaction equation is valid.

The complex formed between calcium and metaphosphate is soluble and most of them were washed away when the sample was prepared. Thus they were not detected in FTIR. But XPS is a more sensitive technique for surface and interface, signals of some residual complexes were detected. P 2p electron can be easily detected on the full scan of the NaHMP treated minerals (Figure 4.34). Detailed high resolution spectrum will be discussed later.

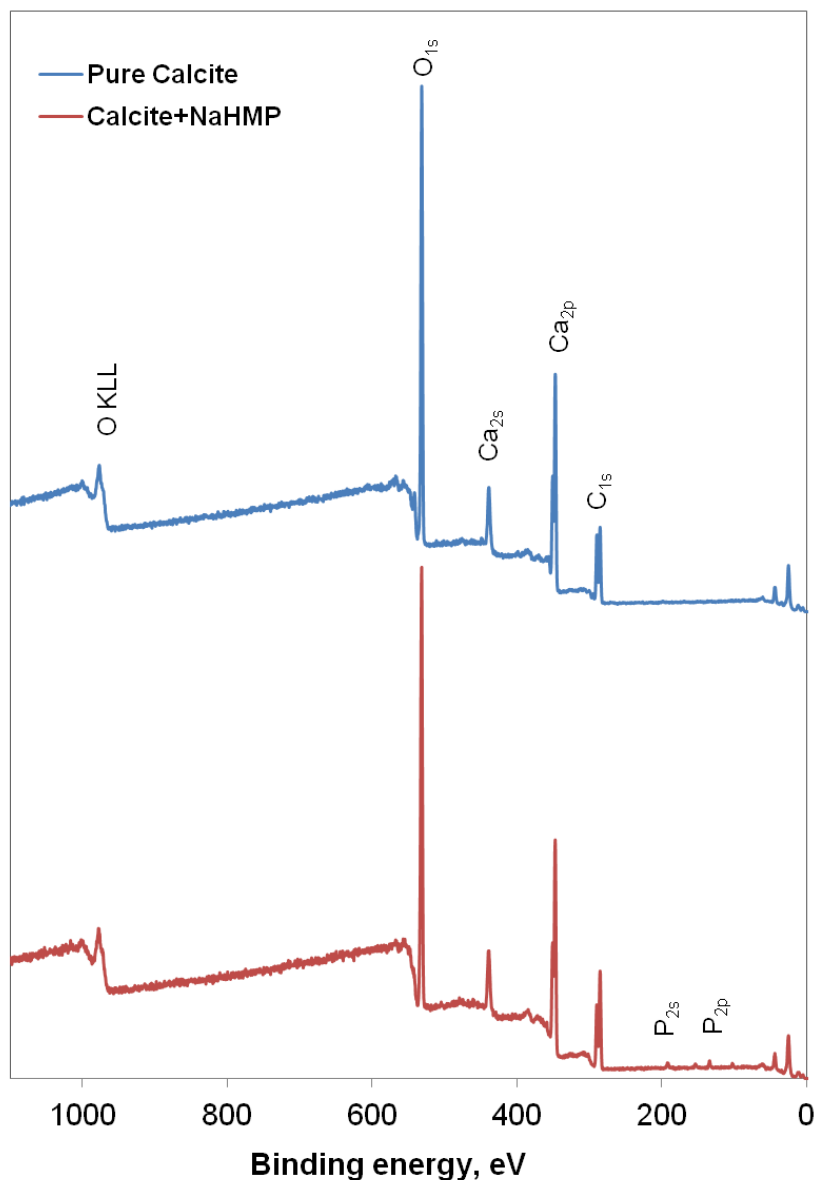
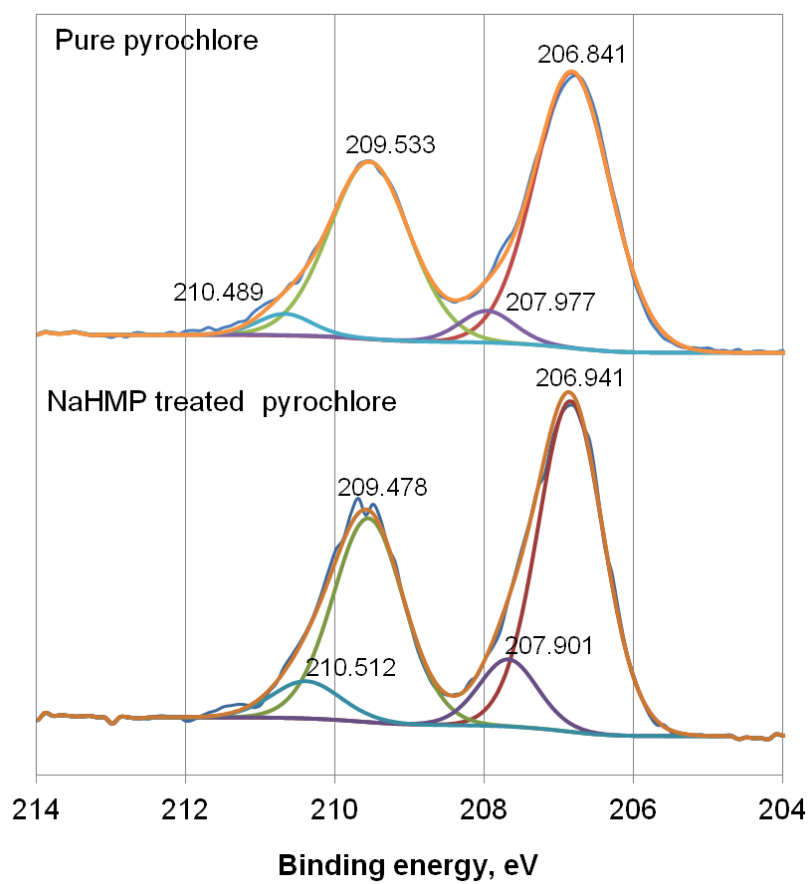
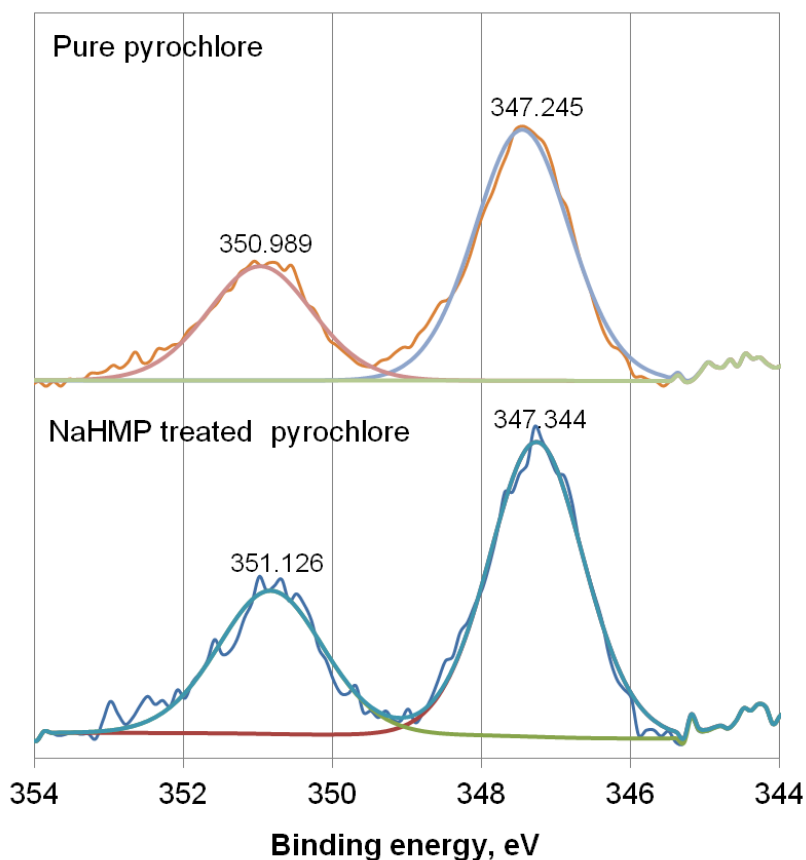


Figure 4.34 XPS spectra of pure and NaHMP treated calcite.

For NaHMP, The binding energy of Nb $3d^{5/2}$ (Figure 4.35) on NaHMP treated pyrochlore surface was increased by 0.10 eV from 206.84 eV to 206.94 eV while that of Ca $2p^{3/2}$ was increased by 0.10 eV from 347.24 eV to 347.34 eV after treatment.



(a)



(b)

Figure 4.35 XPS spectra of (a) Nb 3d (b) Ca 2p of untreated and NaHMP treated pyrochlore.

However, for the calcium atoms on the NaHMP treated calcite surface, the binding energy of the Ca 2p^{3/2} electrons increased by 0.24 eV from 346.65 to 346.90 eV (Figure 4.36). This indicated that the hexametaphosphate group could form stronger chemical complex with the metallic sites on the calcite surface but not on pyrochlore surfaces. This explains the selectivity of NaMP in the flotation tests.

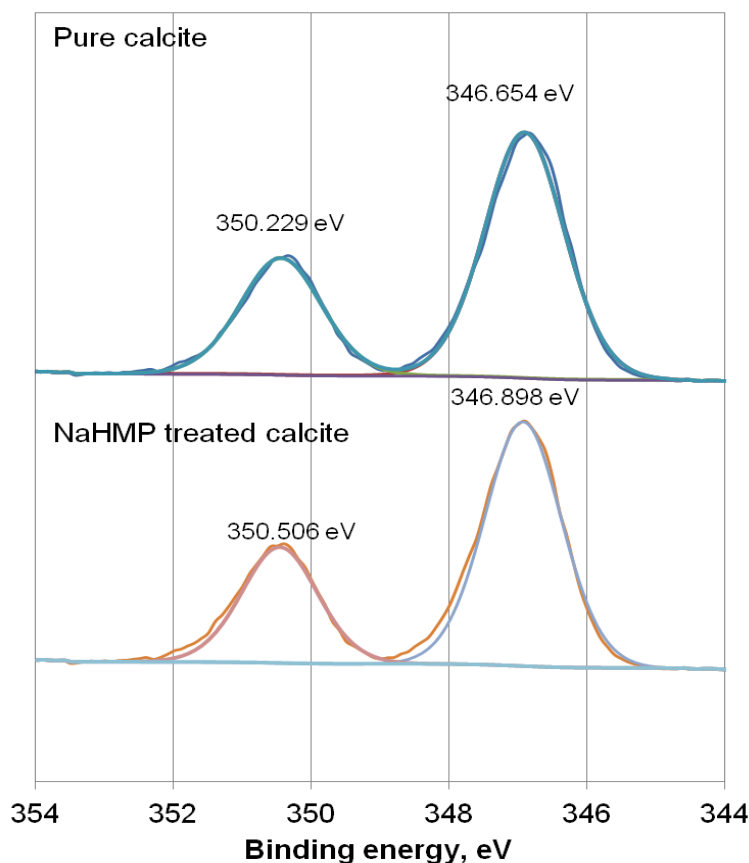


Figure 4.36 XPS spectra of Ca 2p on pure calcite and NaHMP treated calcite.

The relative atomic ratios on the NaHMP treated and untreated pyrochlore and calcite surfaces are listed in Table 4.7. The P/Nb ratio did not increase on the treated pyrochlore. However, P/Ca ratio increased somewhat on the treated calcite. This indicates that calcium hexametaphosphate can be washed away, only little can be left on the treated surface. It is interesting to note that the C/Nb ratio decreased significantly NaHMP-treated pyrochlore, which shows a cleaning action of hexametaphosphate group on the pyrochlore surface. Since more carbon contaminants were removed, more niobium and calcium atoms on the surface can be exposed, which will facilitate hydroxamic acid adsorption.

Table 4.7 Relative atomic ratio on the pure and NaHMP treated surfaces.

Sample	C/Nb	P/Nb	Sample	C/Ca	P/Ca
Pyrochlore	6.65	0.41	Calcite	3.20	0.00
NaHMP treated pyrochlore	2.08	0.34	NaHMP treated calcite	3.28	0.03

The presence of adsorbed hexametaphosphate ions on the mineral surface can be best shown by comparing the P 2p signals from the XPS spectra. The high purity pyrochlore sample shows P 2p electrons, which may be due to contaminants such as apatite (Figure 4.37). The shape and peak location of P 2p electron on pyrochlore was hardly changed after NaHMP treatment.

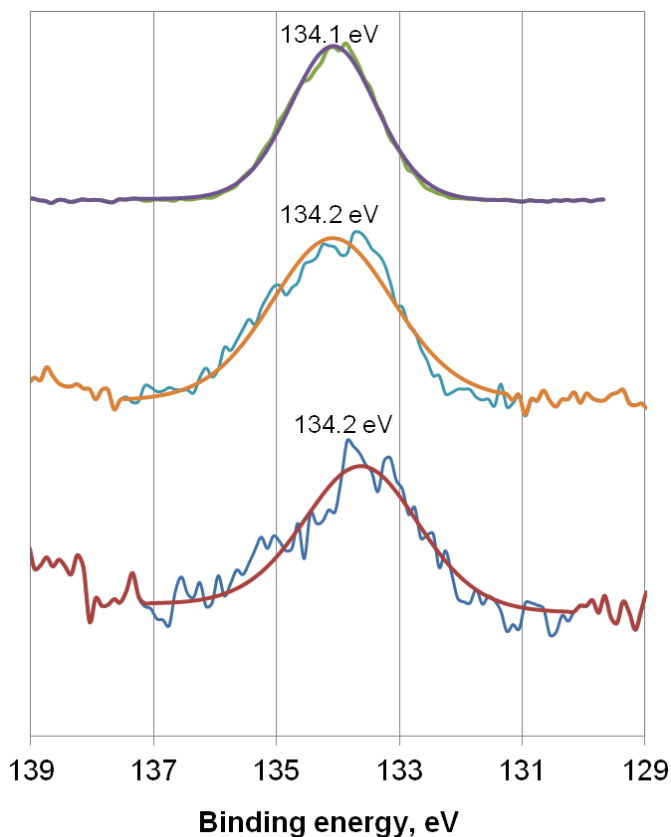


Figure 4.37 P 2p spectra of NaHMP, untreated and treated pyrochlore.

High resolution spectra of P 2p of high purity NaHMP as well as on the treated and untreated calcite are shown in Figure 4.38. As can be seen, on untreated calcite, no obvious P 2p peaks were detected. However, after treatment by NaHMP, the P 2p peak was observed on calcite. P 2p binding energy dropped by 0.2 eV. This may be caused by phosphate groups that formed a complex with the surface calcium ions.

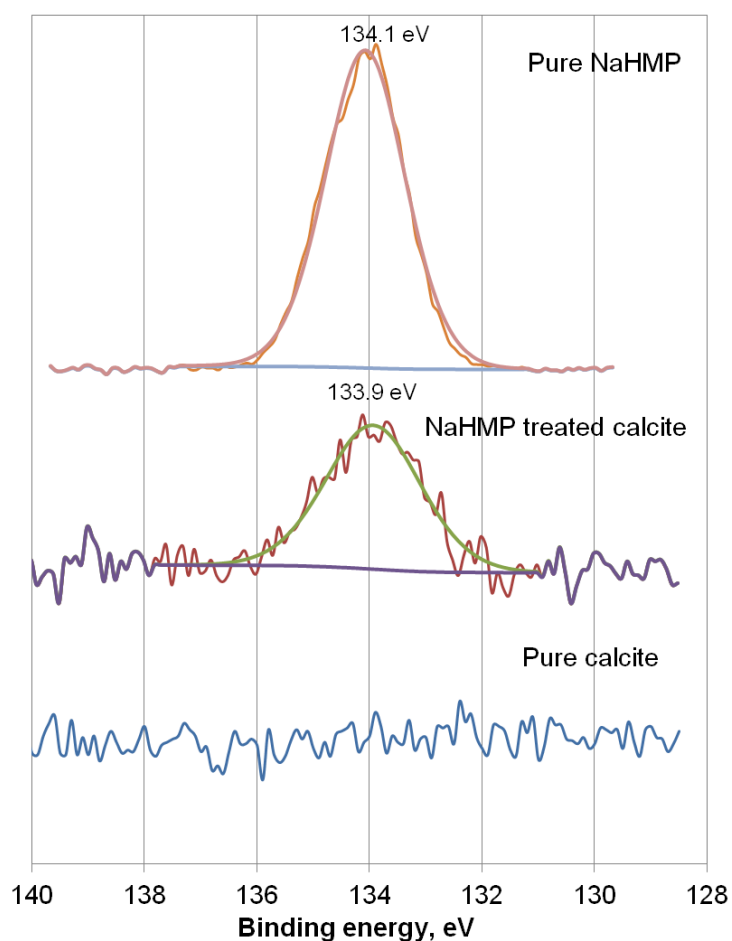


Figure 4.38 XPS spectra of P 2p on pure calcite, pure NaHMP and NaHMP treated calcite.

4.8.4. The adsorption of hydroxamic acid on mineral surfaces

In batch flotation, OHA showed the natural selectivity for niobium oxide minerals in both rougher and cleaner stages (NP 43 in Appendix A). By utilizing this selectivity, we may use OHA as the only flotation reagent to separate niobium oxide minerals from other gangues. So the adsorption of OHA on high purity minerals deserves more in-depth studies. In previous sections, we found that OHA interact stronger with metallic sites on pyrochlore than those on calcite. NaHMP is opposite. Thus, more OHA should adsorb onto pyrochlore at low concentrations than calcite before first monolayer is saturated. To verify this, the adsorption isotherm of OHA on each mineral was measured in this section.

The adsorption density of octyl hydroxamic acid (OHA) on high purity pyrochlore and calcite were measured at room temperature. The adsorption isotherm of OHA on calcite is shown in Figure 4.39. The stepwise increase in the adsorption density was observed for OHA adsorption on calcite at low OHA concentrations. It was proposed that adsorbed OHA molecules on calcite surface could have different orientations (Pradip and Fuerstenau, 1985): at low concentrations, the molecules tend to lie flat on the surface whereas at high concentration, they tend to form close-pack until reaching a dense packing corresponding to an edge-on vertical monolayer surface coverage. Based on this hypothesis, the adsorption densities corresponding to a horizontal or a vertical monolayer orientation were calculated, using the lengthwise and cross-sectional

area size of OHA of 55 and 20.5 Å², respectively. The calculated values of horizontal and vertical monolayer adsorption densities are 3 and 8 μmol/m², respectively (Note: as the number of adsorbed monolayers = molecule size (m²) × adsorption density (mol/m²) × Avogadro Number (6.02×10²³), it follows that the adsorption density (mol/m²) at one monolayer coverage is the inverse of molecule size (m²) times the Avogadro Number, where the molecular size is either 55 or 20.5 Å², for lengthwise and cross-sectional areas of the OHA). By examining the data in Figure 4.39, it can be seen that the horizontal oriented monolayer of OHA was observed below an equilibrium OHA concentration of 1 mmol/L on calcite. However, it is less certain if the vertical oriented monolayer was established on calcite surface. It is suggested that physically adsorbed surfactants may not organize into close-packed vertically oriented monolayer at low concentrations (Auqulis et al., 2004; Giangregorio et al., 2011; Lee et al., 2011). At higher OHA concentrations (>1.5 mmol/L), the adsorption density on calcite increased drastically, indicating random stacking of OHA molecules on top of the initial adsorption layers.

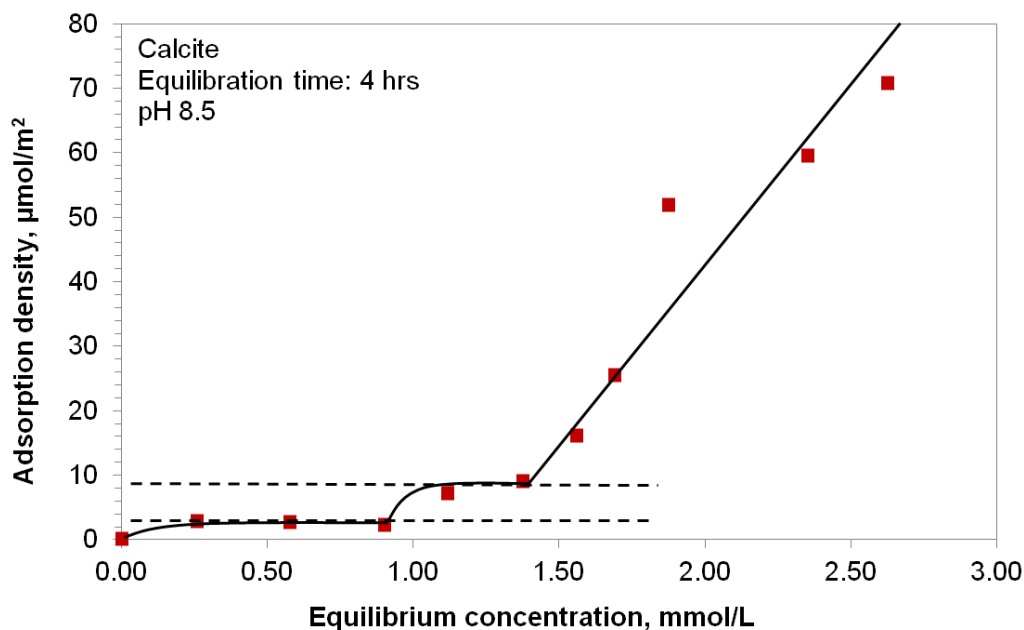


Figure 4.39 Adsorption isotherm of OHA on calcite at pH 8.5 (dashed lines: calculated horizontal orientation and vertical orientation monolayer adsorption density).

The adsorption isotherm of OHA on pyrochlore surface is shown in Figure 4.40. Unlike on calcite surface, it seems that there was no horizontal oriented OHA monolayer on the pyrochlore. Even at very low equilibrium OHA concentrations, vertical oriented OHA monolayers formed on the pyrochlore surface. This may be due to the strong chemisorption of OHA on the pyrochlore. These stable complexes could be formed even at a low concentration until the active sites on the surface were completely occupied. As OHA concentration increases, a second plateau was observed on the adsorption isotherm. This should be the multilayer formed by the physically adsorbed OHA molecules on top of the first chemically adsorbed monolayer. It is interesting to note that based on the adsorption density

data in Figure 4.40, the ratio of chemically adsorbed OHA to physically adsorbed OHA was 1:4. This matches with XPS results, which showed that the ratio was 1:3.8 as discussed earlier (section 4.8.2).

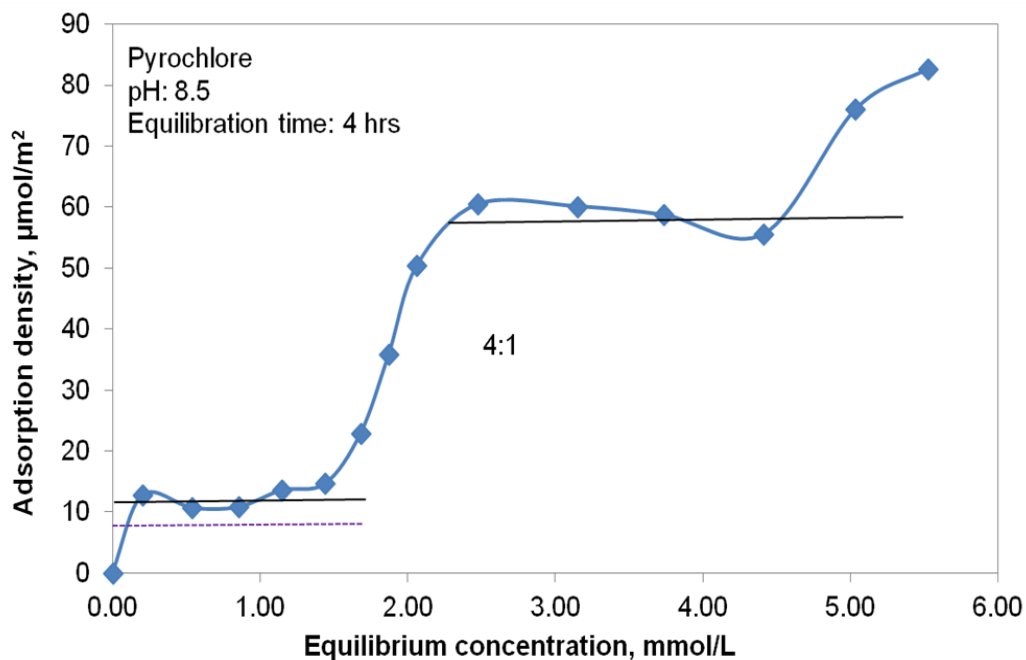


Figure 4.40 Adsorption isotherm of OHA on pyrochlore at pH 8.5 (solid lines: averaged adsorption densities at these two plateaus. Dashed line: calculated vertical orientation saturation adsorption density for chemically adsorbed monolayer).

Figure 4.41 shows a comparison of the adsorption densities of OHA on pyrochlore and calcite at low equilibrium concentrations (which was used in the batch flotation tests). A vertical line indicates the exact starting OHA concentration in the batch flotation tests, and the adsorption density of OHA on pyrochlore was higher than that on calcite at this concentration.

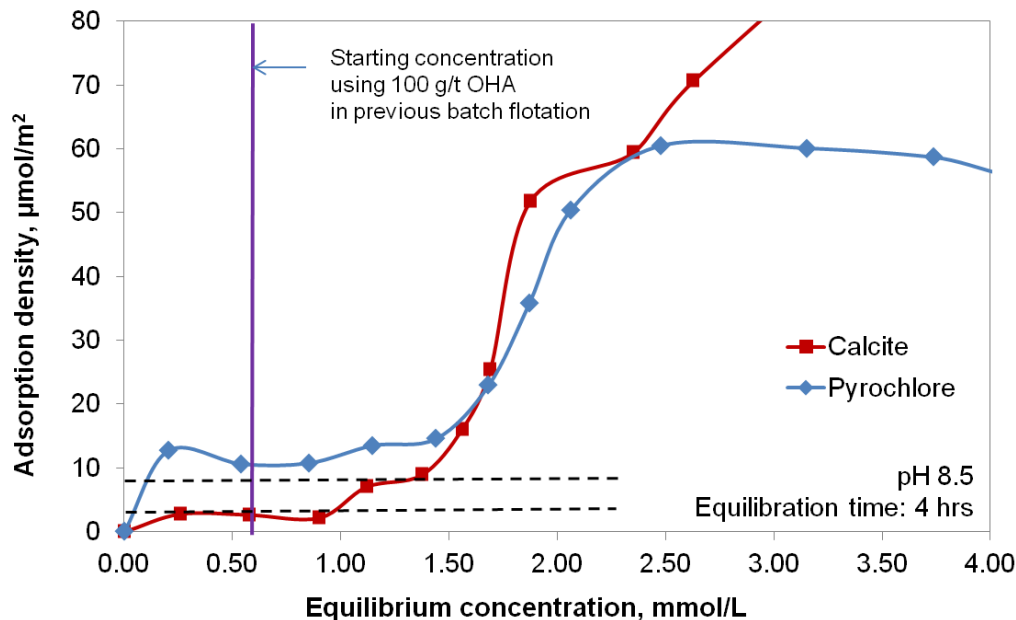


Figure 4.41 Adsorption isotherm at low OHA dosage on pyrochlore and calcite at pH 8.5 (dashed lines: calculated horizontal orientation and vertical orientation monolayer adsorption density).

A stable self-assembled monolayer at low adsorbate concentration on a substrate may be facilitated by chemisorption of reagents on the surface. The adsorption densities difference at low OHA concentrations were due to the higher affinity of OHA to pyrochlore which caused a vertical orientation of the OHA on pyrochlore. But they were in a horizontal orientation on the calcite surface, this horizontal orientation on calcite surface prevented more OHA molecules from being adsorbed. The vertical orientation on the pyrochlore surface not only led to higher adsorption density, but also to higher surface hydrophobicity as the hydrocarbon tail of the OHA is oriented outwards to the bulk aqueous solution (Figure 4.42).

At high concentrations, the adsorption density of OHA on the calcite surface increased faster than that on pyrochlore surface. This explained why simply increasing OHA dosage would have a negative effect on niobium flotation selectivity previously observed in batch flotation (section 4.3.5).

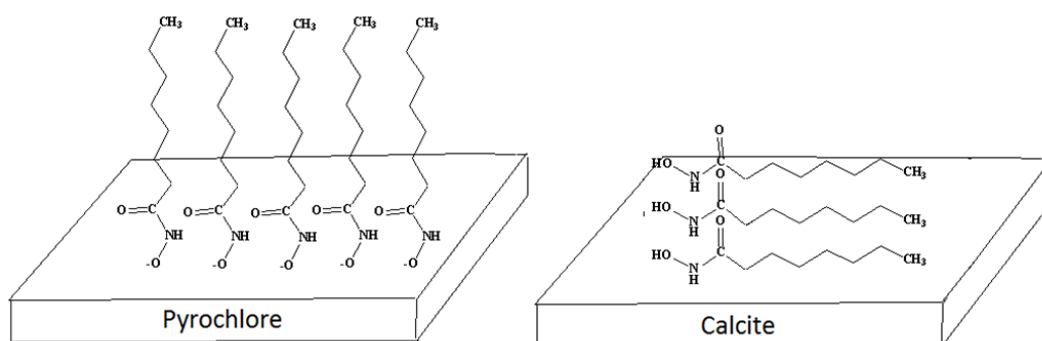


Figure 4.42 Proposed self-assembled monolayer of OHA on pyrochlore and horizontal oriented monolayer on calcite at low OHA concentrations.

4.8.5. ToF-SIMS imaging analysis

The adsorption density measurements were carried out on high purity single minerals and while they showed the relative affinity of OHA to the minerals, they did not show the competitive adsorption when both minerals were present in the flotation pulp where OHA was added. Competitive adsorption of OHA onto the mineral mixtures was studied using time of flight secondary ions mass spectroscopy (ToF-SIMS). Image acquisitions using spectra of positive ions Ca^+ , Nb^+ , $\text{C}_8\text{H}_{17}\text{NO}_2^+$ were carried out (Figure 4.43). Positive ion Nb^+ (Figure 4.43a)

was selected to identify pyrochlore (and columbite) distribution in the mineral mixtures. Signals of Ca^+ ion (Figure 4.43b) can be detected on both pyrochlore and calcite surface since they both contain calcium. However, its intensity was higher on calcite as calcite had higher content of calcium (58.34% CaO) than that of pyrochlore (10.5% CaO). Positive ion $\text{C}_8\text{H}_{17}\text{NO}_2^+$ (Figure 4.43c) was used to determine the distribution of OHA on the mineral mixtures. It can be seen that the pattern of Figure 4.43c is very similar to Figure 4.43a, indicating that higher OHA fragment ion intensity corresponded to higher Nb intensity, which shows that OHA was adsorbed mostly on the pyrochlore.

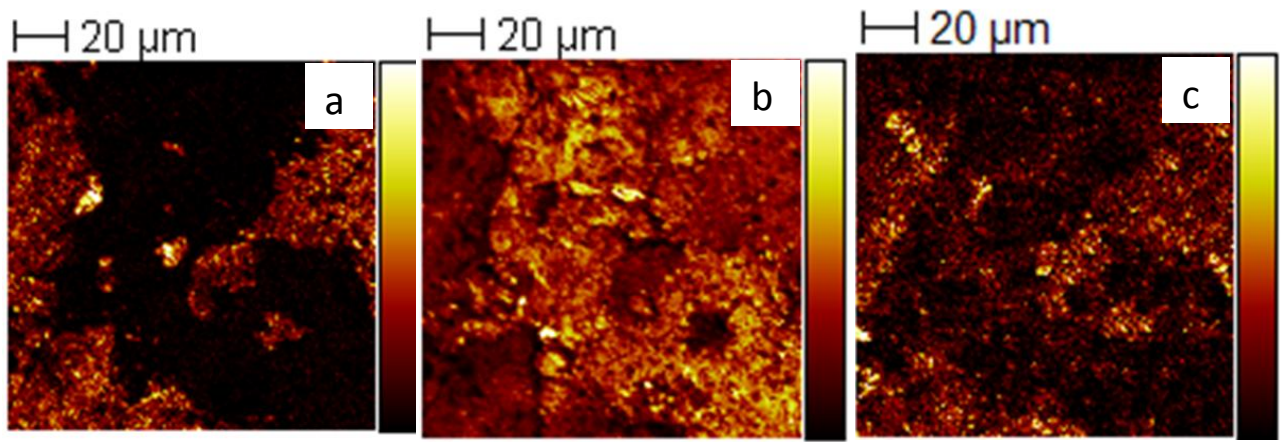


Figure 4.43 Positive ion intensity images of $136.2 \times 136.2 \mu\text{m}^2$ size on OHA treated pyrochlore and calcite mixture (weight ratio 1:1) (a) Nb^+ ; (b) Ca^+ ; (c) $\text{C}_8\text{H}_{17}\text{NO}_2^+$.

ToF-SIMS imaging reveals competitive adsorption of OHA on pyrochlore in the mixture with calcite. It is closer to the realistic situation in our flotation tests than the adsorption isotherms on high purity single minerals. Both of them indicate

that at low concentration, OHA could preferably adsorb on pyrochlore than that on calcite due to the stronger chemisorption.

4.9. More in-depth studies on the adsorption of hydroxamic acid on pyrochlore

The adsorption density (section 4.8.4) and XPS measurements (section 4.8.2) on OHA treated pyrochlore demonstrated that the first monolayer was chemically adsorbed OHA in a vertical orientation, while the layer(s) beyond the first monolayer were physically adsorbed OHA possibly in a random orientation. The binding energy of the N 1s electrons in octyl hydroxamic acid showed a single symmetrical peak at 400.3 eV. Upon adsorption on calcite the peak remained single and symmetrical at 400.3 eV. However, after adsorption on pyrochlore, the N 1s peak split into two peaks, one at 400.5 eV and the other at 398.5 eV, and these were assigned to the neutral R-CO-NH-OH and ionized R-CO-NH-O⁻, respectively (Alagta et al., 2008). The ratio of the integrated areas of the two peaks at 400.7 eV and 398.5 eV turned out to be 3.8:1 (Figure 4.33), matching almost exactly the ratio of adsorption densities of the two plateaus observed on pyrochlore (Figure 4.40).

Therefore, it seems that the split of the N 1s binding energy peak can be used to characterize the type of adsorption of octyl hydroxamic acid on mineral surfaces. For instance, at very low concentrations of octyl hydroxamic acid, the octyl

hydroxamic acid molecules chemisorb on pyrochlore surface forming a vertically oriented monolayer. If this is the case, the binding energy spectra of N 1s should only show the chemisorbed OHA with a peak at around 398.5 eV, with very low peak at 400.7 eV. Test was conducted at two low starting OHA concentrations, 1 mmol/L and 2 mmol/L, and the XPS spectra are shown in Figure 4.44 together with the spectrum from a higher starting concentration (31 mmol/L) reported earlier.

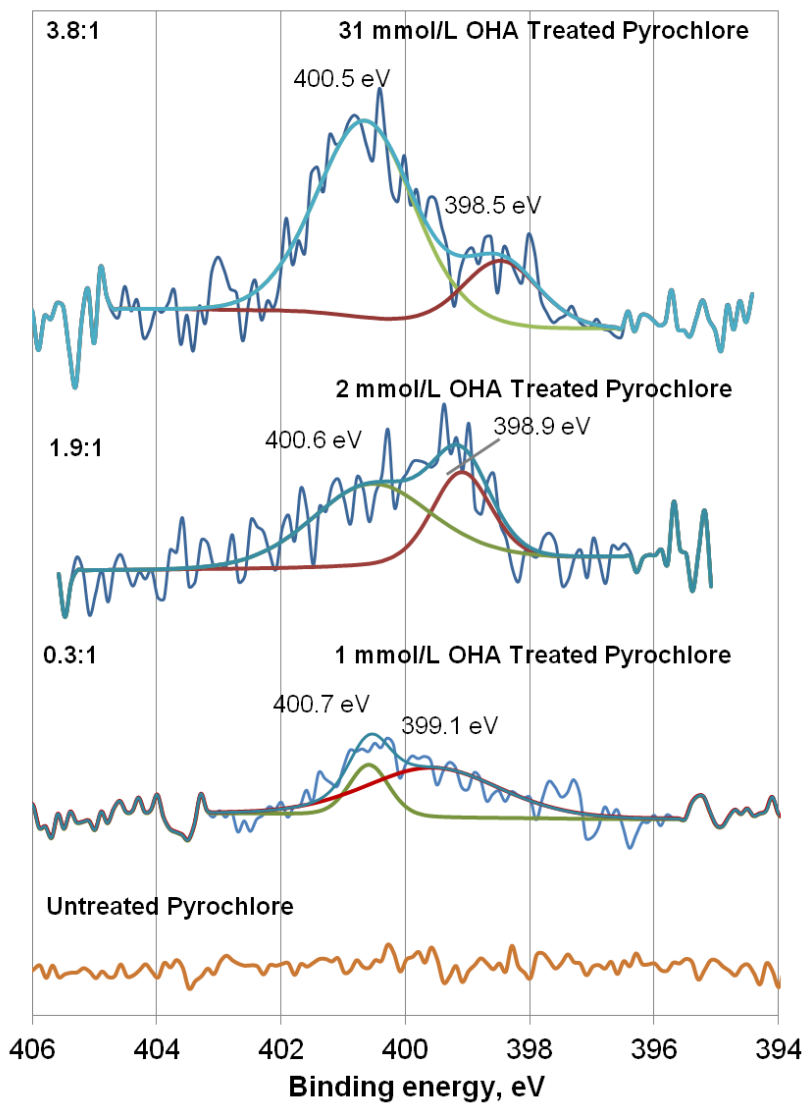


Figure 4.44 N 1s spectra of untreated and OHA treated pyrochlore with various concentration.

As can be seen from Figure 4.44, the N 1s spectra could be detected on all treated pyrochlore sample including at the lowest OHA concentration. The spectra could be de-convoluted into two peaks. The binding energy of one peak was around 399 eV, the other was higher than 400 eV. As discussed before, the peak above 400

eV was attributed to nitrogen atoms in the neutral molecules, i.e., the protonated form of the hydroxamic acid, R-CO-NH-OH, and the peak around 399 eV was due to the nitrogen in the deprotonated hydroxamate groups, R-CO-NH-O⁻ (Folkers et al., 1995; Alagta et al., 2008). When the OHA concentration was 1 mmol/L, only a small peak of physically adsorbed OHA (400.7 eV) could be detected, indicating that at this concentration, the majority of the OHA were chemically adsorbed on the pyrochlore (399.1 eV). When the concentration of OHA was 2 mmol/L, the peak due to physically adsorbed OHA (400.6 eV) was significantly more intense than at lower concentrations. The ratio of the integrated peak areas of the physically adsorbed (protonated) and chemically adsorbed (deprotonated) OHA increased with the increasing OHA concentration. It is interesting to note that the integrated peak area ratio obtained from N 1s spectra of 1 mmol/L and 2 mmol/L OHA treated pyrochlore, at 0.3:1 and 1.9:1, respectively, matches the adsorption isotherm (shown in Figure 4.45). At the starting concentration of 1 mmol/L and 2 mmol/L OH, the equilibrium OHA concentration was found to be 0.85 mmol/L and 1.80 mmol/L, respectively, which were shown in Figure 4.45 as the two vertical lines. Based on previous data, the adsorption density of OHA corresponding to a theoretical calculated vertically oriented monolayer on pyrochlore is 8 $\mu\text{mol}/\text{m}^2$. As can be seen from Figure 4.45, the adsorption densities at an equilibrium concentration of 0.85 and 1.80 mmol/L OHA are approximately 11 $\mu\text{mol}/\text{m}^2$ and 23 $\mu\text{mol}/\text{m}^2$, respectively. Therefore, the ratios of physically adsorbed OHA to chemisorbed OHA were $(11-8)/8 = 0.4:1$

and $(23-8)/8 = 1.9:1$, respectively. These results matched almost exactly with the XPS results shown in Figure 4.44.

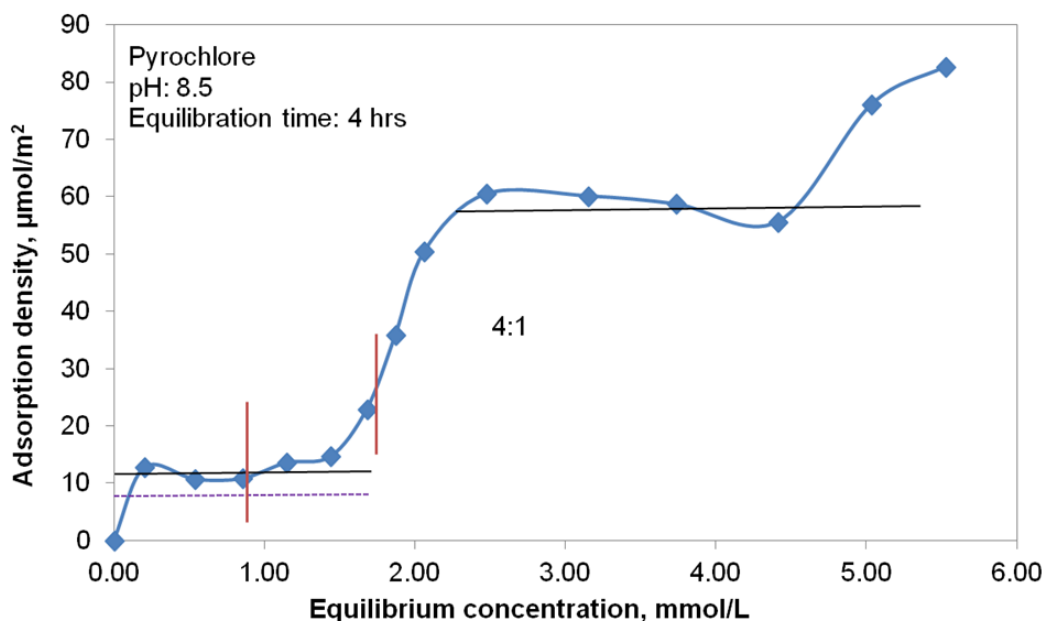


Figure 4.45 Adsorption isotherm of OHA on pyrochlore at pH 8.5 (solid lines: averaged adsorption densities at these two plateaus. Dashed line: calculated vertical orientation saturation adsorption density for chemically adsorbed monolayer. Red vertical lines: equilibrium concentration corresponding to a starting concentration of 1 mmol/L and 2 mmol/L OHA).

However, the XPS results shown in Figure 4.44 indicated that at the high OHA concentration of 31 mmol/L, the physically adsorbed OHA remained to be about 4 times the chemisorbed OHA, i.e., the physically adsorbed OHA should be about

32 $\mu\text{mol}/\text{m}^2$, and the total adsorption density of OHA (physically adsorbed and chemisorbed) should be about 40 $\mu\text{mol}/\text{m}^2$. On the other hand, Figure 4.45 shows that at high equilibrium concentrations, the adsorption density followed a different trend and was much more than 40 $\mu\text{mol}/\text{m}^2$.

The discrepancy was probably caused by the differences in the experimental procedures. The pyrochlore samples used in XPS measurements were filtered and washed, whereas the pyrochlore samples in the adsorption density measurement were only filtered, and the supernatant was used to determine the equilibrium OHA concentration. It was possible that the physisorbed OHA beyond the second plateau could be easily desorbed and washed away. To verify this, more adsorption density studies were carried out at a starting concentration of 10 mmol/L. After equilibration, the slurry was filtered and the mineral solids were washed with 5 aliquots of 50 mL distilled water at the same pH (8.5). The wash solution was carefully collected and measured to determine the amount of OHA that was washed off. Details of the test procedure and the results are shown below.

In the test, 0.5121 g of the pyrochlore sample was treated for 1 h in 50 mL of a solution containing 10.265 mmol/L OHA at pH 8.5. After filtration, the equilibrium concentration of OHA was determined to be 9.577 mmol/L. As the specific surface area of the pyrochlore was 0.88 m^2/g , the adsorption density was calculated to be 76.3 $\mu\text{mol}/\text{m}^2$. Therefore, at the equilibrium concentration of 9.6

mmol/L, the ratio of physically and chemically adsorbed OHA was about 8.5:1 (i.e., (76.3-8) divided by 8).

The mineral solids were washed with 50 mL distilled water at pH 8.5. It was found that the wash solution contained 0.2849 mmol/L of OHA. The amount of OHA that was washed off corresponded to $31.6 \mu\text{mol}/\text{m}^2$ from the pyrochlore surface. Therefore, the OHA remaining adsorbed on pyrochlore after the 1st wash was $44.7 \mu\text{mol}/\text{m}^2$. Subsequent wash of the pyrochlore did not release any more of the OHA molecules.

It follows that after washing, the ratio of physically and chemically adsorbed OHA on pyrochlore was 4.6:1. The residual adsorbed OHA on pyrochlore was also very close to the second plateau ($\sim 50 \mu\text{mol}/\text{m}^2$) on the adsorption isotherm. This verified that the octyl hydroxamic acid adsorbed above this adsorption density ($\sim 50 \mu\text{mol}/\text{m}^2$) on pyrochlore could be washed off, so that the amount of physically adsorbed octyl hydroxamic acid on pyrochlore stayed at about four times the amount of chemisorbed octyl hydroxamic acid. At this point, we do not have an explanation why the ratio stayed at 4. However, Folkers et al. (1995) proposed that this ratio was related to the properties of the metal oxides, esp. the isoelectric points (iep). He found that the lower the iep of metal oxide substrates, the higher the ratio. For instance, the iep of titanium and copper oxide was reported to be around 5 and 9 (Folkers et al., 1995), and the corresponding ratio was 2.5 and 0.125, respectively. Since the iep of the pyrochlore used in this work

was about 2, a ratio of physically over chemisorbed OHA on pyrochlore of 4 seemed to be in line with their hypothesis.

The above washing tests were also carried out on 10 mmol/L OHA treated calcite. The adsorption density at corresponding equilibrium concentration (7.68 mmol/L) was found to be about 160 $\mu\text{mol}/\text{m}^2$. After the 1st wash, the amount of OHA that was washed off corresponded to approximately 116 $\mu\text{mol}/\text{m}^2$ with respect to initial calcite particle size. Unfortunately, we could not calculate the residual adsorption density with respect to unit area after washing the calcite. Since calcite is a semi-soluble mineral, certain amount of calcite could be dissolved after extensive washing changing specific area. However, the calcite particles treated with 10 mmol/L OHA and then washed with 400 mL distilled water were collected and dried for XPS measurement. The XPS results are shown in Figure 4.46. As can be seen, only small and symmetrical physically adsorbed OHA peak could be observed on the calcite surface.

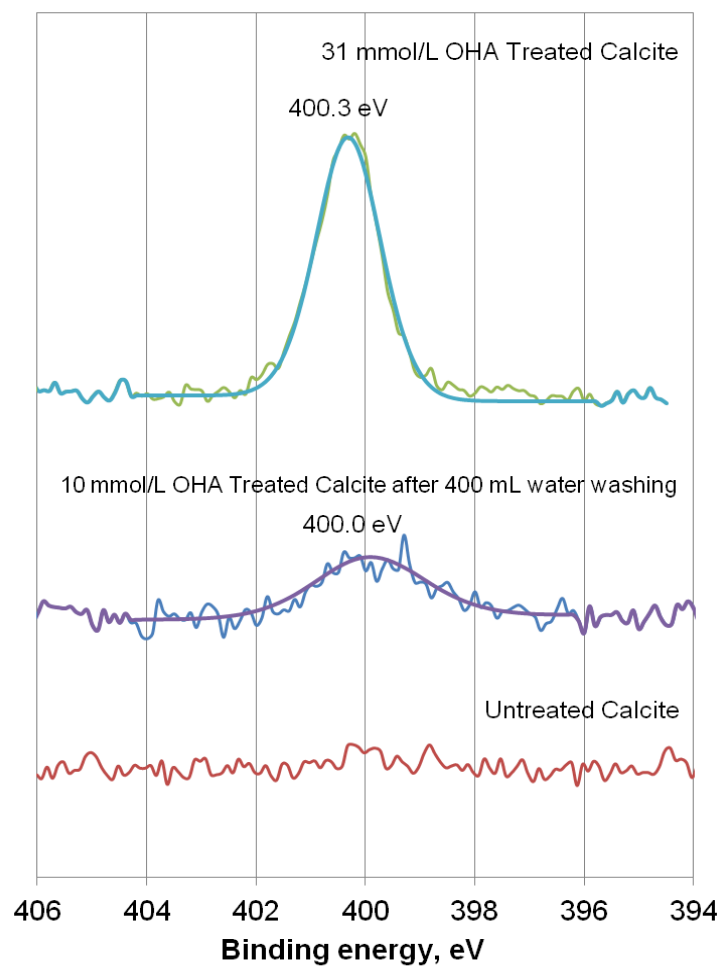


Figure 4.46 N 1s spectra of untreated and OHA treated calcite with and without washing.

5. Conclusions and recommendations

5.1. Summary of Major Findings

- Hydroxamic acid (Aero 6493) and diphosphonic acid both showed good collecting power towards niobium oxide mineral pyrochlore in small-scale single mineral flotation (Nb recovery >90%). However, only hydroxamic acid was further tested in the batch flotation because diphosphonic acid only floated the pyrochlore at acidic pulp condition (pH 4), which is unsuitable for Niobec ores. Hydroxamic acid floated the pyrochlore in a broad pH range from slightly acidic to strongly alkaline. The combination of Aero 6493 and NaMP could separate pyrochlore from carbonate in small-scale mineral mixture flotation.
- Hydroxamic acid (either as a commercial product Aero 6493 or in the high purity form) was proven to be a selective collector for the Niobec ore samples in the batch rougher and cleaner flotation tests. At dosages less than 2 kg/t it resulted in over 95% recovery of pyrochlore in rougher flotation with medium and low recoveries for carbonate and silicate, respectively, at less than 47% mass recovery. The hydroxamic acid collected fine particles effectively as the Aero 6493 was used to float the Mill Feed directly without desliming or reverse carbonate flotation. Moreover, the use of hydroxamic acid did not require any pH adjustment

and all the batch flotation tests were conducted at the natural pulp pH (8-9). Sodium metaphosphate was verified as a selective depressant for the carbonate gangue. The combination of hydroxamic acid and sodium metaphosphate concentrated the pyrochlore in tests with rougher and extensive cleaner flotation stages from the Niobec Mill Feed. Preliminary cleaning flotation results showed that the grade of niobium oxide in the final concentrate reached 21.40% Nb_2O_5 , which was over thirty times higher than that of the Mill Feed. Pure octyl hydroxamic acid (OHA) also could concentrate the pyrochlore through three stages of cleaner flotation. The grade of niobium oxide in final concentrate reached 22.30% Nb_2O_5 . It is anticipated that with better control of cleaning flotation conditions, more cleaning stages and recycling of the cleaner tails, niobium mineral recovery could be kept relatively high while increasing the concentrate grade. However in these tests, minerals containing iron was also concentrated through the process. Removal of the iron-bearing gangue minerals such as pyrite, magnetite and hematite is necessary for further upgrading of the pyrochlore concentrate.

- Selectivity ratio was used to quantify the selective collecting power of collector in the batch flotation test. The results indicated that hydroxamic acid has the highest affinity for niobium oxide, followed by iron-bearing gangue minerals, carbonate and silicate, in that order. SHA showed better selectivity for niobium containing minerals than OHA.

- Adsorption mechanism studies were carried out to delineate the nature of the interaction between hydroxamic acid and the primary value mineral, pyrochlore, and the primary gangue mineral, calcite. FTIR measurements showed a shift of the vibrational frequencies of the carbonyl group in hydroxamic acid after adsorption on pyrochlore (92 cm^{-1}) and calcite (15 cm^{-1}). XPS results indicated a lowering of the binding energies (chemical shift) of Nb $3d^{5/2}$ and Ca $2p^{3/2}$ electrons on hydroxamic acid treated pyrochlore (0.24 and 0.35 eV, respectively), and the lowering of the binding energies of Ca $2p^{3/2}$ electrons on collector treated calcite (0.19 eV), but the chemical shift was more pronounced on NaHMP treated calcite (0.24 eV) than treated pyrochlore (0.1 eV). The results indicated that hydroxamic acid formed stronger complexes with pyrochlore than with calcite, but NaHMP formed stronger complexes with calcite than with pyrochlore. The binding energy spectra of N 1s electrons on hydroxamic acid treated pyrochlore samples could be de-convoluted into two peaks: one at a binding energy of around 399 eV (chemically adsorbed OHA), and the other at a binding energy between 400 and 401 eV (physically adsorbed OHA). As the concentration of the octyl hydroxamic acid was increased, the ratio between the integrated areas of the N 1s peak for physically adsorbed OHA over that of chemisorbed OHA indeed increased from nearly zero to about 4. The results coincided well with the adsorption isotherm that showed at low OHA concentration (1 or 2 mmol/L), the pyrochlore surface was covered by mostly chemisorbed OHA that formed

a vertically oriented monolayer. An increase in OHA concentration brought more octyl hydroxamic acid molecules to the pyrochlore surface that was only physically adsorbed. But at high OHA concentration (31 mmol/L), the ratio of physically adsorbed to chemically adsorbed OHA obtained from XPS measurement was lower than that from adsorption isotherm. It was verified that the octyl hydroxamic acid adsorbed beyond the second plateau ($\sim 50 \mu\text{mol}/\text{m}^2$) of the adsorption isotherm on pyrochlore could be washed off, so that the amount of physically adsorbed octyl hydroxamic acid on pyrochlore stayed at about four times the amount of chemisorbed octyl hydroxamic acid. Only small and symmetrical physically adsorbed OHA peak could be observed on OHA treated calcite after extensive washing, indicating a physisorption mechanism.

- In conclusion, the strong chemisorption of the OHA on pyrochlore surface led to a vertical head-on orientation of the molecules so that the pyrochlore was strongly hydrophobized even at low OHA concentrations, whereas the weak adsorption of OHA on calcite led to a horizontal orientation of the adsorbed OHA molecules with low adsorption density and low imparted surface hydrophobicity. This was confirmed by both adsorption isotherm measurements on the high purity single minerals of pyrochlore and calcite and ToF-SIMS imaging data on the mixtures of the two minerals. The results explain the observed selectivity of hydroxamic acid in the flotation of Niobec ores.

5.2. Original contributions

- The work done in this thesis showed that alkyl hydroxamic acid was an effective collector for niobium oxide minerals in the carbonatite niobium ores. The optimum pH of flotation recovery matched with the natural pulp pH for this type of ores, and the collector was more efficient in collecting fine particles. Hydroxamic acid is therefore a potential replacement for the cationic collectors currently used in Niobec Mine as well as other niobium oxide flotation plants.
- Contrary to literature, it was observed that hydroxamic acid could not be with kerosene to improve fine particle flotation. While the exact mechanisms require further study, the observation was important as neutral oil such as kerosene was typically assumed to benefit fine particle recovery. It was found in this work that this depended on the collectors used.
- The adsorption mechanisms studies not only proved that hydroxamic acid chemisorbed onto niobium containing minerals while physisorbed onto carbonate gangues, they also showed that the chemisorption was the driving force for the configurational change and the compact head-on vertically oriented monolayer of adsorbed OHA. The chemisorption on pyrochlore surface led to higher adsorption density than on calcite surface, thus stronger hydrophobicity.

5.3. Recommendations for future work

Hydroxamic acid is known to be an efficient collector for many oxide ores. However, it has not been used in the commercial flotation of niobium ores. The results of this thesis project provide an alternative for Niobec Mines, as well as other niobium producers in the world such as Araxa and Catalao in Brazil, to solve their problems in the ore dressing flowsheet. In order to achieve this objective, the following further research work is deemed necessary:

Rejection of the major gangue minerals such as carbonates and silicates is mainly achieved in this work. Other gangue minerals, most noticeably magnetite, pyrite and apatite, have not been closely followed. Obviously these gangue minerals should receive attention as well if hydroxamic acid is to be used as a collector for the niobium minerals. Rejection of these gangue minerals may necessitate the use of additional selective depressants.

The ore sample tested in this work contained both pyrochlore and columbite as value Nb minerals, although pyrochlore is the main component. Unfortunately at this point, we are not capable of generating a separate high purity columbite mineral to study its response to hydroxamic acid and NaMP. However, mineralogical analyses on selected flotation products (concentrates and tails) from the batch flotation tests should reveal information about the responses of columbite to the reagents.

Other ways to depress the gangue minerals need to be tested, especially in terms of reducing the mechanical/hydraulic entrainment of the gangue minerals. Starch phosphate is particularly interesting because starch itself is known to be a good depressant to calcite, while phosphate was found to be a good selective depressant for carbonate gangue in this work. Starch is also a good depressant for iron oxide minerals, which is a problem in Niobec ore. The work on starch phosphate in this thesis project is very preliminary and more work can be directed toward this direction.

The reason why kerosene cannot be used together with hydroxamic acid to improve niobium oxide flotation needs to be investigated. Currently the price of hydroxamic acid is still high in the market, so that searching for a cheaper flotation agent to reduce the consumption of hydroxamic acid is highly desirable. More studies in this area also could reveal more insights into the distribution, adsorption behavior and solution chemistry of hydroxamic acid both in flotation pulp and on mineral surfaces.

Finally, more selective collectors in the hydroxamic acid family should be considered. The results reported in this work indicated that introducing another active group (phenolic hydroxyl group) into hydroxamic acid molecules could increase its selectivity for niobium oxide, although it may negatively affect recovery. Is it possible to synthesize hydroxamic acid with different hydrocarbon

chains to achieve better selectivity while maintaining recovery? Systematic studies are required.

References

- Abeidu, A. M. (1974) *Journal of Applied Chemistry & Biotechnology*, 24, n 8, 425-35
- Abouzeid, A. M. (2008) *International Journal of Mineral Processing*, 85, 59-84
- Adamson, A. M., Gast, A. P. (1997) *Physical chemistry of surfaces*, 308-15
- Agar, G. E., Khan, F., Markovich, B., Shea, A., Kelly, C. (1996) *Minerals Engineering*, 9 (12), 1215-1226
- Anderson, A. (2000) Mineral Processing Technology Roadmap, US Department of Energy
- http://www1.eere.energy.gov/manufacturing/industries_technologies/mining/pdfs/mptroadmap.pdf
- Aral H., Bruckard, W. J. (2008) *Mineral Processing and Extractive Metallurgy*, 117, n 4, 193-204
- Auqulis, R., Vliokas, R., Liedberg, B., Rotomskis, R. (2004) *Diffusion and Defect Data Part B*, 97-98, 195-200
- Bellamy, L. J. (1975) *The infrared spectra of complex molecules*, 3rd ed., Chapman & Hall, Wiley, New York, USA, 381-392
- Belzile, E. (2009) *NI 43-101 Technical Report for Niobec Mine*
- Biss, R. (1982) *Canadian Mining Journal*, 103, n 8, 17-18, 21-22, 24-5
- Brookhaven Instruments Corporation, 1999, *Instruction Manual for ZetaPALS, Zeta Potential Analyzer*

- Buckley, A. N., Woods, R., Wouterlood, H. J. (1989) *International Journal of Mineral Processing*, 26, 1-2, 29-49
- Bulatovic, S. M. (2007) *Handbook of Flotation Reagents*, Elsevier
- Bulatovic, S. M. (2010) *Handbook of Flotation Reagents Volume 2*, Elsevier, 114-116
- Burks, H.G. (1958) *British Patent GB 800717*
- Cao, J., Gan, J., He, D., He, K., Lin, L., Linghu, J., Liu, D., Liu, Y., Luo, J., Ren, C., Wang, F., Wang, Y., Yuan, Q., Zhang, M., Zhang, R., Zhao, W., Zhou, W., Zhou, Y. (2010) *Chinese patent application*, CN 101786038 A
- Cap, M., Machovic, V. (1962) *Rudy*, 10, 124-126
- Chaki, A., Purohit, R. K., Mamallan, R. (2011) *Energy Procedia*, 7, 153-157
- Chen, G. L., Tao, D., Ren, H., Ji, F. F., Qiao, J. K. (2005) *International Journal of Mineral Processing*, 76, 111-22
- Chowdhury, R. (2012) *Proceeding of International Mineral Processing Congress 2012*, paper 1140
- Crichton, R. R. (2012) *Biological Inorganic Chemistry: A New Introduction to Molecular Structure and Function* (2nd ed.), Elsevier
- Drelich, J., Kim, J. H., Payne, T., Miller, J. D., Kobler, R. W. (1999) *Separation and Purification Technology*, 15, 9-17
- Dutta, R. L., Ghosh, S. (1967) *Journal of Indian Chemical Society*, 44, 10, 820
- Espinosa-Gomez, R., Finch, J. A., Laplante, A.R. (1987) *Colloids and Surfaces*, 26, 333-50
- Faucher, J.A.R. (1964) *AIME transactions*, 229, 255-258

- Folkers, J. P., Gorman, C. B., Laibinis, P. E., Buchholz, S., Whitesides, G. M., Nuzzo, R. G. (1995) *Langmuir*, 11, 813-824
- Fuerstenau, D. W., Herrera-Urbina, R., McGlashan, D. W. (2000) *International Journal of Mineral Processing*, 58, 15-33
- Giangregorio, M. M., Losurdo, M., Bianco, G. V., Operamolla, A., Dilonardo, E., Sacchetti, A., Capezzuto, P., Babudri, F., Bruno, G. (2011) *Journal of Physical Chemistry C*, 115, 19520-19528
- Grau, R. A., Laskowski, J. S., Heiskanen, K. (2005) *International Journal of Mineral Processing*, 76, 225-233
- Grill, R., Gnadenberger, A. (2006) *International Journal of Refractory Metals & Hard Materials*, 24, 275-82
- Guimaraes, H. N., Weiss, R. A. (2001) *Niobium, Science and Technology*, 37-51
- Hampel, C. A. (1961) *Industrial and Engineering Chemistry*, 53, 2, 90-96
- Hanna, H. S., Somsundaran, P. (1976) in: Fuerstenau M. C., *Flotation-A. M. Gaudin Memorial Volume*, AIME, New York, USA, 1, 197-272
- Havens, R., Nissen, W. I. (1964) *Bureau of Mines Report of Investigations*, 6386, 3, 18
- Hebda, J. (2001) *Niobium Science & Technology: Proceeding of the International Symposium Niobium 2001*, Orlando, Florida, USA
- Herrera-Urbina, R., Sotillo, F. J., Fuerstenau, D. W. (1999) *International Journal of Mineral Processing*, 55, 3, 157-170
- Herrera-Urbina, R. (2003) *Mineral Processing and Extractive Metallurgy Review*, 24, 139-182

- Higgins, F. S., Magliocco, L. G., Colthup, N. B. (2006) *Applied Spectroscopy*, 60, 3, 279-287
- Hirva, P., Tikka, H. (2002) *Langmuir*, 18, 5002-5006
- Irannajad, M., Ejtemaei, M., Gharabaghi, M. (2009) *Minerals Engineering*, 22, 9-10, 766-771
- Irving, H. M. N. H., Williams, R. J. P. (1953) *Journal of the Chemical Society*, 3192-3210
- Jiang, C., Parekh, B. K., Leonard, J. W., Wang, X. (1999) *Advances in Filtration and Separation Technology*, 13A, 227-241
- Jiang, Y., Zhao, B., Zhou, X., Zhou, L. (2010) *Hydrometallurgy*, 104, 112-118
- Jiang, Y., Zhou, L., Zhou, X., Zhao, B. (2010) *Separation Science and Technology*, 45, 2475-2480
- Kawatra, S. K., Seitz, R. A. (1993) *Flotation Plants: Are They Optimized?* D. Malhotra (ed.), SME, 137-146
- Khalil, M. M., Fazary, A. E. (2004) *Monatshefte fur Chemie*, 135, 1455-1474
- Khalil, M. M., Mahmoud, R. K. (2008) *Journal of Chemical Engineering Data*, 53, 2318-2327
- Khmeleva, T. N., Chapelet, J. K., Skinner, W. M., Beattie, D. A. (2006) *International Journal of Mineral Processing*, 79, 1, 61-75
- Klimpel, R. R., Fee, B. F. (1993) *Flotation Plant: Are They Optimized?* D. Malhotra, (ed.), SME, 55-67
- Largman, T., Sifniades, S. (1983) *Extraction of Uranium from Phosphoric acid using supported extractants*, US Patent 4,402,917

- Laskowski, J. S., Ralston, J. (1992) *Colloids chemistry in mineral processing*, Elsevier, 361
- Lawrance, G. A. (2010) *Introduction to coordination chemistry*, Wiley, Hoboken, NJ, USA, 41-82
- Lee, J. S., Nagaraj, D. R., Coe, J. E. (1998) *Minerals Engineering*, 11, n 10, 929-39
- Lee, S., Yoon, J. H., Yoon, S. (2011) *Journal of Physical Chemistry C*, 115, 12501-12507
- Lee, T. J., Chung, Y. C., Chun, B. C. (2002) *Reactive and Functional Polymers*, 52, 43-51
- Liu, Y., Liu, Q. (2004) *Minerals Engineering*, 17, 855-863
- Long, J., Drelich, J., Xu, Z., Masliya, J. H. (2007) *Canadian Journal of Chemical Engineering*, 85, 5, 726-738
- Lu, S., Song, S. (1991) *Colloids and Surfaces*, 57, 49-60
- Lu, Y., Zhang, M., Feng, Q., Long, T., Ou, L., Zhang, G. (2011) *Transactions of Nonferrous Metals Society of China*, 21, 208-213
- MacDonald, Wm. T. (1937) *Mining and Metallurgy*, 18, 285-286
- Majumdar, A. K. (1972) *N-benzoylphenylhydroxylamine and its analogues*, Pergamon, Oxford
- Marabini, A. M., Barbaro, M., Alesse, V. (1991) *International Journal of Mineral Processing*, 33 (1-4), 291-306
- Marinakakis, K. I., Kelsall, G. H. (1987) *Colloids and Surfaces*, 26, 243-55

- Mohammadkhani, M., Noaparast, M., Shafaei, S. Z., Amini, A., Amini, E., Abdollahi, H. (2011) *International Journal of Mineral Processing*, 100, 3-4, 157-165
- Moon, Th., Nagarajan, R. (1998) *Colloids and Surfaces A: Physicochemical and Engineering Aspects*, 132, 275-288
- Mulleneers, H. A. E., Koopal, L. K., Swinkels, G. C. C., Bruning, H., Rulkens, W. H. (1999) *Colloids and Surfaces A: Physicochemical and Engineering Aspects*, 151, 293-301
- Natarajan, R., Nirdosh, I. (2003) *International Journal of Mineral Processing*, 71, 113-29
- Natarajan, R., Sharma, J., Nirdosh, I. (2010) *Adsorption*, 16:541-548
- Nanthakumar, B., Grimm, D., Pawlik, M. (2009) *International Journal of Mineral Processing*, 92, 1-2, 49-57
- Nekhoroshev, N. E., Popov, R. L., Abramov, A. A., Sushentsev, V. A. (1978) *Tsventnye Metally*, 7, 101-110
- Oliveira, J. F., Saraiva, S. M., Pimenta, J. S., Oliveira, A. P. A. (2001) *Mineral Engineering*, 14, n1, 99-105
- Ozbayoglu, G., Akgok, Y. Z. (1995) *Proceedings of the XIX International Mineral Processing Congress*, 4, 147-149
- Papp, J. F. (2009) *U. S. Geological Survey, Mineral Commodity Summaries*
- Park, D. P., Sung, J. H., Kim, C. A., Choi, H. J., Jhon, M. S. (2003) *Journal of Applied Polymer Science*, 91, 1770-1773

Parsonage, P., Melven, D., Healey, A. F., Watson, D. (1984) *Inst of Mining and Metallurgy*, London, 33-40

Parolis, L. A. S., van der Merwe, R., van Leerdam, G. C., Prins, F. E., Smeink, R. G. (2007) *Minerals Engineering*, 20, 10, 970-978

Passauer, L., Bender, H., F., Fischer, S. (2010) *Carbohydrate Polymers*, 82, 809-814

Patel, Z., Khul'ka, K. (2001) *Metallurgist*, 45, 11-12, 477-80

Pavlor, D. A. (1976) *Tsvetnie Metally*, 8

Peck, A. S., Wadsworth, M. E. (1965) *Transactions of AIME*, 156, 174-185

Pradip, D. W. Fuerstenau (1985) *Colloids and Surfaces*, 15, 137-146

Pradip (1991) *Metals, Materials and Processes*, 3 (1), 15-36

Poliyo, E. and Hirvonen, Y. (1976) *Finnish Patent FI 51822*

Quast, K. B. (2000) *Minerals Engineering*, 13, n 13, 1361-76

Ren, J., Lu, S., Song, S., Niu, J. (1997) *Minerals Engineering*, 10, n 12, 1395-404

Ren, H., Ji, F. F., Chen G. L., Tao, D., Qiao, J. K. (2004) *International Journal of Mineral Processing*, 74, 271-279

Rao, S.R., Espinosa-Gomez, R., Finch, J. A., Biss, R. (1988) *Mineral Engineering*, 1, n 3, 189-202

Rubio, J., Souza, M. L., Smith, R. W. (2002) *Minerals Engineering*, 15, 139-155

Scales, M. (2003) *Canadian Mining Journal*, August, 16-18

Shapovalov, G.M., Pol'kin, S.I. (1958) *Tsvetnykh. Metal. I Zolota*, n 31, 256-68

Shcherbakov, O. K. (1964) *Tr. Nauchn. Issled, I Proektn, Inst. "Uralsmekhanobr"*, 11, 25-28

- Shen, H., Pugh, R. J., Forssberg, E. (2002) *Colloids and Surfaces A: Physicochemical and Engineering Aspects*, 196, 63-70
- Shogren, R. L. (2009) *Carbohydrate Polymers*, 76, 639-644
- Socrates, G., 1980. Infrared characteristic group frequencies, Wiley, New York, USA
- Somasundaran, P. (1969) *Journal of Colloid and Interface Science*, 31, 4, 557-565
- Song, S., Lopez-Valdivieso, A., Reyes-Bahena, J. L., Lara-Valenzuela, C. (2001) *Minerals Engineering*, 14, 1, 87-98
- Sreenivas, T., Padmanabhan, N. P. H. (2002) *Colloids and Surfaces A*, 205, 47-59
- Thiers, P., Thiers, G. (2001) Mining chemicals, *SCUP Reports*, SRI consulting
- Thomson, R. T. (1936) "Some properties of sodium hexametaphosphate", *Analyst*, 61, 320-323
- van de Ven, T. G. M., Sauve, C. P., Garnier, G. (2001) "Deinking of recycled fibers in a flotation flow loop", *Colloids and Surfaces A: Physicochemical and Engineering Aspects*, 192, 53-60
- Vickerman, J. C., Briggs, D. (2001) TOF-SIMS: Surface analysis by mass spectrometry, IM publications, West Sussex, UK
- Wang, X., Nguyen, A. V., Miller, J. D. (2006) *International Journal of Mineral Processing*, 78, 122-30
- Watts, J. F., Wolstenholme, J. (2003) *An Introduction to Surface Analysis by XPS and AES*, New York, NY, US
- Webster online dictionary, froth flotation, www.webster-online-dictionary.org

Wills, B. A. (1997) *Minerals Processing Technology* 6th Version, Butterworth-Heinemann, Burlington, MA, US

Yale, H. L. (1993) *Chemical Review*, 33, 209-256

Zheng, X. P., Misra, M., Smith, R. W., Qiao, J. K. (1996) *Minerals Engineering*, 9, n 3, 331-41

Zheng, Y. Y., Zhao, C. C. (1993) *Separation Science and Technology*, 28 (5), 1233-1240

Appendix A: Bench-scale flotation tests

Figure 1. Test procedure and metallurgical balance for NP 01.

Test No:		NP01												
Sample:		Carbonate flotation feed						Project:		CRDPJ379600-08				
Grind size:		plant condition						Date:		Jan 19, 2010				
Pulp density:		31	% solids								Operator:		Xiao Ni	
Objective:		Scoping bench flotation test of pyrochlore flotation feed using A6493												
		Aero 6493 added to pulp directly												
TEST PROCEDURE														
STAGE		TIME (min)	pH	ADDITION		COMMENTS						Conc pulp weight, g		
				Reagent	g/tonne									
Slurry			8.3			JKTeck flotation machine, 1200 rpm 500 g sample in 1.5 L stainless steel cell								
Condition		3	8.4	Aero 6493	500	250 milligrams of Aero 6493 added directly								
Rougher flotation														
Rougher float 1		2				air flowrate at scale 7-9 on the flowmeter						504.26		
Rougher float 2		3				Scrap until froth is barren						142.22		
			8.2			Final pH								
						tailings pulp						1136.92		
METALLURGICAL BALANCE														
Product		Solid weight		Water weight		Assay (%)				Distribution (%)				
		(g)	(%)	(g)		Nb2O5	Fe2O3	CaO	SiO2	Nb2O5	Fe2O3	CaO	SiO2	
Rougher concentrate 1		191.8	34.5	312.5		1.24	9.29	33.1	3.02	61.2	38.0	38.3	13.8	
Rougher concentrate 2		48.6	8.7	93.7		1.28	10.70	31.9	2.79	16.0	11.1	9.3	3.2	
Rougher conc. 1+2		240.4	43.2	406.1		1.25	9.57	32.9	2.97	77.2	49.1	47.6	17.0	
Float tail		316.2	56.8	820.7		0.28	7.54	27.5	11.00	22.8	50.9	52.4	83.0	
Total		556.6	100.0	1226.8		0.70	8.42	29.8	7.53	100.0		100.0	100.0	
Measured						0.67		29.2	7.56					

Figure 2. Test procedure and metallurgical balance for NP 02

Test No: NP02																																																																																																																																																																																																																																																																																																																																																																																																																																																																																																																																																																																																																																																																																																																																																																																																																																																																																																																																																																																																																																																																																																																																																																																																																																																																																																																																																																																																																															
----------------------	--	--	--	--	--	--	--	--	--	--	--	--	--	--	--	--	--	--	--	--	--	--	--	--	--	--	--	--	--	--	--	--	--	--	--	--	--	--	--	--	--	--	--	--	--	--	--	--	--	--	--	--	--	--	--	--	--	--	--	--	--	--	--	--	--	--	--	--	--	--	--	--	--	--	--	--	--	--	--	--	--	--	--	--	--	--	--	--	--	--	--	--	--	--	--	--	--	--	--	--	--	--	--	--	--	--	--	--	--	--	--	--	--	--	--	--	--	--	--	--	--	--	--	--	--	--	--	--	--	--	--	--	--	--	--	--	--	--	--	--	--	--	--	--	--	--	--	--	--	--	--	--	--	--	--	--	--	--	--	--	--	--	--	--	--	--	--	--	--	--	--	--	--	--	--	--	--	--	--	--	--	--	--	--	--	--	--	--	--	--	--	--	--	--	--	--	--	--	--	--	--	--	--	--	--	--	--	--	--	--	--	--	--	--	--	--	--	--	--	--	--	--	--	--	--	--	--	--	--	--	--	--	--	--	--	--	--	--	--	--	--	--	--	--	--	--	--	--	--	--	--	--	--	--	--	--	--	--	--	--	--	--	--	--	--	--	--	--	--	--	--	--	--	--	--	--	--	--	--	--	--	--	--	--	--	--	--	--	--	--	--	--	--	--	--	--	--	--	--	--	--	--	--	--	--	--	--	--	--	--	--	--	--	--	--	--	--	--	--	--	--	--	--	--	--	--	--	--	--	--	--	--	--	--	--	--	--	--	--	--	--	--	--	--	--	--	--	--	--	--	--	--	--	--	--	--	--	--	--	--	--	--	--	--	--	--	--	--	--	--	--	--	--	--	--	--	--	--	--	--	--	--	--	--	--	--	--	--	--	--	--	--	--	--	--	--	--	--	--	--	--	--	--	--	--	--	--	--	--	--	--	--	--	--	--	--	--	--	--	--	--	--	--	--	--	--	--	--	--	--	--	--	--	--	--	--	--	--	--	--	--	--	--	--	--	--	--	--	--	--	--	--	--	--	--	--	--	--	--	--	--	--	--	--	--	--	--	--	--	--	--	--	--	--	--	--	--	--	--	--	--	--	--	--	--	--	--	--	--	--	--	--	--	--	--	--	--	--	--	--	--	--	--	--	--	--	--	--	--	--	--	--	--	--	--	--	--	--	--	--	--	--	--	--	--	--	--	--	--	--	--	--	--	--	--	--	--	--	--	--	--	--	--	--	--	--	--	--	--	--	--	--	--	--	--	--	--	--	--	--	--	--	--	--	--	--	--	--	--	--	--	--	--	--	--	--	--	--	--	--	--	--	--	--	--	--	--	--	--	--	--	--	--	--	--	--	--	--	--	--	--	--	--	--	--	--	--	--	--	--	--	--	--	--	--	--	--	--	--	--	--	--	--	--	--	--	--	--	--	--	--	--	--	--	--	--	--	--	--	--	--	--	--	--	--	--	--	--	--	--	--	--	--	--	--	--	--	--	--	--	--	--	--	--	--	--	--	--	--	--	--	--	--	--	--	--	--	--	--	--	--	--	--	--	--	--	--	--	--	--	--	--	--	--	--	--	--	--	--	--	--	--	--	--	--	--	--	--	--	--	--	--	--	--	--	--	--	--	--	--	--	--	--	--	--	--	--	--	--	--	--	--	--	--	--	--	--	--	--	--	--	--	--	--	--	--	--	--	--	--	--	--	--	--	--	--	--	--	--	--	--	--	--	--	--	--	--	--	--	--	--	--	--	--	--	--	--	--	--	--	--	--	--	--	--	--	--	--	--	--	--	--	--	--	--	--	--	--	--	--	--	--	--	--	--	--	--	--	--	--	--	--	--	--	--	--	--	--	--	--	--	--	--	--	--	--	--	--	--	--	--	--	--	--	--	--	--	--	--	--	--	--	--	--	--	--	--	--	--	--	--	--	--	--	--	--	--	--	--	--	--	--	--	--	--	--	--	--	--	--	--	--	--	--	--	--	--	--	--	--	--	--	--	--	--	--	--	--	--	--	--	--	--	--	--	--	--	--	--	--	--	--	--	--	--	--	--	--	--	--	--	--	--	--	--	--	--	--	--	--	--	--	--	--	--	--	--	--	--	--	--	--	--	--	--	--	--	--	--	--	--	--	--	--	--	--	--	--	--	--	--	--	--	--	--	--	--	--	--	--	--	--	--	--	--	--	--	--	--	--	--	--	--	--	--	--	--	--	--	--	--	--	--	--	--	--	--	--	--	--	--	--	--	--	--	--	--	--	--	--	--	--	--	--	--	--	--	--	--	--	--	--	--	--	--	--	--	--	--	--	--	--	--	--	--	--	--	--	--	--	--	--	--	--	--	--	--	--	--	--	--	--	--	--	--	--	--	--	--	--	--	--	--	--	--	--	--	--	--	--	--	--	--	--	--	--	--	--	--	--	--	--	--	--	--	--	--	--	--	--	--	--	--	--	--	--	--	--	--	--	--	--	--	--	--	--	--	--	--	--	--	--	--	--	--	--	--	--	--	--	--	--	--	--	--	--	--	--	--	--	--	--	--	--	--	--	--	--	--	--	--	--	--	--	--	--	--	--	--	--	--	--	--	--	--	--	--	--	--	--	--	--	--	--	--	--	--	--	--	--	--	--	--	--	--	--	--	--	--	--	--	--	--	--	--	--	--	--	--	--	--	--	--	--	--	--	--	--	--	--	--	--	--	--	--	--	--	--	--	--	--	--	--	--	--	--	--	--	--	--	--	--	--	--	--	--	--	--	--	--	--	--	--	--	--	--	--	--	--	--	--	--	--	--	--	--	--	--	--	--	--	--	--	--	--	--	--	--	--	--	--	--	--	--	--	--	--	--	--	--	--	--	--	--	--	--	--	--	--	--	--	--	--	--	--	--	--	--	--	--	--	--	--	--	--	--	--	--	--	--	--	--	--	--	--	--	--	--	--	--	--	--	--	--	--	--	--	--	--	--	--	--	--	--	--	--	--	--	--	--	--	--	--	--	--	--	--	--	--	--	--	--	--	--	--	--	--	--	--	--	--	--	--	--	--	--	--	--	--	--	--	--	--	--	--	--	--	--	--	--	--	--	--	--	--	--	--	--	--	--	--	--	--	--	--

Figure 3. Test procedure and metallurgical balance for NP 03.

Test No: NP03													
Sample: Carbonate flotation feed						Project:		CRDPJ379600-08					
Grind size: plant condition						Date:		Jan 20th, 10					
Pulp density: 31 % solids						Operator:		Xiao Ni					
Objective: Scoping bench flotation test of pyrochlore flotation feed using A6493 and NaMP													
Same as NP01 but added 250 g/t NaMP													
TEST PROCEDURE													
STAGE	TIME (min)	pH	ADDITION			COMMENTS						Conc pulp weight, g	
			Reagent	g/tonne									
Slurry		8.6				JKTeck flotation machine, 1200 rpm 500 g sample in 1.5 L stainless steel cell							
Condition	3	8.6	Aero 6493	500		250 milligrams of Aero 6493 added directly							
Rougher flotation Condition	2	8.8	NaMP	250		12.5 mL 1% solution of NaMP							
Rougher float 1	2					air flowrate at scale 7-9 on the flowmeter						156.08	
Rougher float 2	3					Scrap until froth is barren						158.7	
		8.8				Final pH							
						tailings pulp						1514.67	
METALLURGICAL BALANCE													
Product	Solid weight		Water weight	Assay (%)				Distribution (%)					
	(g)	(%)	(g)	Nb2O5	Fe2O3	CaO	SiO2	Nb2O5	Fe2O3	CaO	SiO2		
Rougher concentrate 1	40.3	7.8	115.8	4.73	22.50	26.9	4.05	55.6	21.1	7.0	4.2		
Rougher concentrate 2	12.7	2.5	146.0	2.15	15.20	27.0	7.50	7.9	4.5	2.2	2.5		
Rougher conc. 1+2	52.9	10.3	261.8	4.11	20.75	26.9	4.88	63.5	25.6	9.3	6.7		
Float tail	463.4	89.7	1051.3	0.27	6.88	30.1	7.79	36.5	74.3	90.7	93.3		
Total	516.3	100.0	1313.1	0.66	8.31	29.8	7.49	100.0	96.8	100.0	100.0		
Measured				0.67		29.2	7.56						

Figure 4. Test procedure and metallurgical balance for NP 04.

Test No:	NP04									
Sample:	Carbonate flotation feed						Project:	CRDPJ379600-08		
Grind size:	plant condition						Date:	Jan 20th, 10		
Pulp density:	31	% solids					Operator:	Xiao Ni		
Objective:	Scoping bench flotation test of pyrochlore flotation feed using A6493 and NaMP									
	Same as NP02 but added 250 g/t NaMP									
TEST PROCEDURE										
STAGE	TIME (min)	pH	ADDITION		COMMENTS					Conc pulp weight, g
			Reagent	g/tonne						
Slurry		8.4			JKTeck flotation machine, 1200 rpm 500 g sample in 1.5 L stainless steel cell					
Condition	3	8.4	Aero 6493	500	250 milligrams of Aero 6493, blended with 200 mL water					
Rougher flotation										
Condition	2	8.6	NaMP	250	12.5 mL 1% solution of NaMP					
Rougher float 1	2				air flowrate at scale 7-9 on the flowmeter					96.78
Rougher float 2	3				Scrap until froth is barren					165.96
		8.8			Final pH					
					tailings pulp					1508.94
METALLURGICAL BALANCE										
Product	Solid weight		Water weight		Assay (%)			Distribution (%)		
	(g)	(%)	(g)		Nb2O5	CaO	SiO2	Nb2O5	CaO	SiO2
Rougher concentrate 1	11.9	2.4	84.9		3.06	26.4	4.44	10.3	2.0	1.4
Rougher concentrate 2	12.0	2.4	153.9		1.55	28.2	6.22	5.3	2.2	1.9
Rougher conc. 1+2	23.9	4.9	238.8		2.30	27.3	5.33	15.5	4.2	3.3
Float tail	468.3	95.1	1040.7		0.64	31.5	7.95	84.5	95.8	96.7
Total	492.2	100.0	1279.5		0.72	31.3	7.82	100.0	100.0	100.0
Measured					0.67	29.2	7.56			

Figure 5. Test procedure and metallurgical balance for NP 05.

Test No: NP05															
Sample:		Carbonate flotation feed								Project:		CRDPJ379600-08			
Grind size:		plant condition								Date:		March 2nd, 2010			
Pulp density:		33	% solids						Operator:		Xiao Ni				
Objective:		Scoping bench flotation test of pyrochlore flotation feed using A6493 and NaMP Same as NP03 but with increase dosage of NaMP													
TEST PROCEDURE															
STAGE		TIME (min)	pH	ADDITION		COMMENTS								Conc pulp weight, g	
				Reagent	g/tonne										
Slurry						JKTeck flotation machine, 1200 rpm 500 g sample in 1.5 L stainless steel cell if natural pH is between 6 and 10, don't adjust									
Condition		3	8.5	Aero 6493	500	250 milligrams of Aero 6493 added directly									
Rougher flotation Condition		2	8.5	NaMP	500	25 mL 1% solution of NaMP									
Rougher float 1		2				air flowrate at 7-9								77.1	
Rougher float 2		3				scrap until froth is barren								64.76	
			8.9			Record final pH									
						tailings pulp								1441.54	
METALLURGICAL BALANCE															
Product		Solid weight		Water weight		Assay (%)				Distribution (%)					
		(g)	(%)	(g)	Nb2O5	Fe2O3	CaO	SiO2	Nb2O5	Fe2O3	CaO	SiO2			
Rougher concentrate 1		18.3	3.5	58.8	7.54	30.10	24.0	3.01	39.7	12.7	2.8	1.4			
Rougher concentrate 2		6.5	1.3	58.2	5.44	25.30	23.7	4.86	10.2	3.8	1.0	0.8			
Rougher conc. 1+2		24.8	4.8	117.0	6.99	28.84	23.9	3.50	50.0	16.5	3.8	2.2			
Float tail		496.5	95.2	945.0	0.35	7.30	30.6	7.67	50.0	83.5	96.2	97.8			
Total Measured		521.4	100.0	1062.0	0.67	8.33	30.3	7.47	100.0	100.0	100.0	100.0			

Figure 6. Test procedure and metallurgical balance for NP 06.

Test No:	NP06								
Sample:	Carbonate flotation feed						Project:	CRDPJ379600-08	
Grind size:	plant condition						Date:	March 3rd, 2010	
Pulp density:	35	% solids					Operator:	Xiao Ni	
Objective:	Scoping bench flotation test of pyrochlore flotation feed using A6493 and NaMP Same as NP03 but with increased dosage of NaMP and AERO 6493								
TEST PROCEDURE									
STAGE	TIME (min)	pH	ADDITION		COMMENTS	Conc pulp weight, g			
			Reagent	g/tonne					
Slurry					JKTeck flotation machine, 1200 rpm 500 g sample in 1.5 L stainless steel cell				
Condition	3	8.2	Aero 6493	1000	500 milligrams of Aero 6493 added directly				
Rougher flotation									
Condition	2	8.3	NaMP	500	25 mL 1% solution of NaMP				
Rougher float 1	2				air flowrate at 7-9	167.43			
Rougher float 2	3				Scrap until froth is barren	59.78			
		8.9			Record final pH				
					tailings pulp	1254.33			
METALLURGICAL BALANCE									
Product	Solid weight		Water weight (g)	Assay (%)			Distribution (%)		
	(g)	(%)		Nb2O5	CaO	SiO2	Nb2O5	CaO	SiO2
Rougher concentrate 1	62.5	12.2	105.0	2.72	34.0	2.26	50.2	13.9	3.6
Rougher concentrate 2	12.8	2.5	47.0	3.30	31.6	3.35	12.5	2.6	1.1
Rougher conc. 1+2	75.3	14.7	151.9	2.82	33.6	2.45	62.6	16.5	4.7
Float tail	436.4	85.3	817.9	0.29	29.3	8.50	37.4	83.5	95.3
Total Measured	511.7	100.0	969.8	0.66	29.93	7.61	37.4	83.5	95.3

Figure 7. Test procedure and metallurgical balance for NP 07.

Test No:		NP07									
Sample:		Carbonate flotation feed				Project:		CRDPJ379600-08			
Grind size:		plant condition				Date:		March 19th, 2010			
Pulp density:		34	% solids		Operator:		Xiao Ni				
Objective:		Scoping bench flotation test of pyrochlore flotation feed using A6493 and SP (Starch phosphate)									
TEST PROCEDURE											
STAGE		TIME	pH	ADDITION		COMMENTS				Conc pulp	
		(min)		Reagent	g/tonne					weight, g	
Slurry						JKTeck flotation machine, 1200 rpm 500 g sample in 1.5 L stainless steel cell					
Condition		3	8.4	Aero 6493	500	250 milligrams of Aero 6493, blended with					
Rougher flotation											
Condition		2	8.7	Starch phosphate	250	0.125g SP stirred in distilled water for half an hour before using					
Rougher float 1		2				air flowrate at 7-9				195.43	
Rougher float 2		3				Scrap until froth is barren				110.3	
			9.0			final pH					
						tailings pulp				1190.33	
METALLURGICAL BALANCE											
Product		Solid weight		Water weight	Assay (%)			Distribution (%)			
		(g)	(%)	(g)	Nb2O5	CaO	SiO2	Nb2O5	CaO	SiO2	
Rougher concentrate 1		75.7	14.8	119.8	2.69	31.2	2.59	60.3	15.7	4.9	
Rougher concentrate 2		32.2	6.3	78.1	1.52	31.1	2.49	14.5	6.6	2.0	
Rougher conc. 1+2		107.9	21.1	197.9	2.34	31.2	2.56	74.9	22.3	6.9	
Float tail		404.0	78.9	786.4	0.21	29.0	9.20	25.1	77.7	93.1	
Total		511.8	100.0	984.2	0.66	29.5	7.80	100.0	100.0	100.0	
Measured											

Figure 8. Test procedure and metallurgical balance for NP 08.

Test No:	NP08									
Sample:	Carbonate flotation feed						Project:	CRDPJ379600-08		
Grind size:	plant condition						Date:	March 19th, 2010		
Pulp density:	34	% solids					Operator:	Xiao Ni		
Objective:	Scoping bench flotation test of pyrochlore flotation feed using A6493 and SP (Starch phosphate)									
TEST PROCEDURE										
STAGE		TIME (min)	pH	ADDITION		COMMENTS	Conc pulp weight, g			
				Reagent	g/tonne					
Slurry						JKTeck flotation machine, 1200 rpm 500 g sample in 1.5 L stainless steel cell				
Condition		3	8.2	Aero 6493	1000	500 milligrams of Aero 6493 add directly				
Rougher flotation Condition		2	8.6	Starch phosphate	250	0.125g SP stirred in distilled water for half an hour before using				
Rougher float 1		2				Air flowrate at 7-9				362.73
Rougher float 2		3				Scrap until froth is barren				185.86
			8.9			Final pH				
									tailings pulp	940.04
METALLURGICAL BALANCE										
Product	Solid weight		Water weight	Assay (%)			Distribution (%)			
	(g)	(%)	(g)	Nb2O5	CaO	SiO2	Nb2O5	CaO	SiO2	
Rougher concentrate 1	163.0	31.8	199.7	1.27	33.9	3.00	61.8	36.4	12.6	
Rougher concentrate 2	80.0	15.6	105.9	0.93	32.1	3.23	22.2	16.9	6.7	
Rougher conc. 1+2	243.0	47.5	305.6	1.16	33.3	3.08	83.9	53.3	19.3	
Float tail	269.1	52.5	670.9	0.20	26.4	11.60	16.1	46.7	80.7	
Total	512.2	100.0	976.5	0.65	29.7	7.56	100.0	100.0	100.0	
Measured										

Figure 9. Test procedure and metallurgical balance for NP 09.

[illegible]

Figure 10. Test procedure and metallurgical balance for NP 10.

Test No:		NP10											
Sample:		Mill feed						Project:		CRDPJ379600-08			
Grind size:		plant condition						Date:		Apr 28th, 2010			
Pulp density:		28		% solids		Operator:						Xiao Ni	
Objective:		Scoping bench flotation test of mill feed using A6493											
TEST PROCEDURE													
STAGE		TIME (min)	pH	ADDITION		COMMENTS	Conc pulp weight, g						
				Reagent	g/tonne								
Slurry						JKTeck flotation machine, 1200 rpm 500 g sample in 1.5 L stainless steel cell							
Condition		3	8.6	Aero 6493	500	250 milligrams of Aero 6493 add directly							
Rougher flotation Condition		2	8.6	NaHMP	500	25 mL 1% solution of NaHMP							
Rougher float 1		2				Air flow rate at 7	131.26						
Rougher float 2		3				Scrap until froth is barren	197.6						
			9.0			Record final pH							
						tailings pulp	1462.43						
METALLURGICAL BALANCE													
Product		Solid weight		Water weight	Assay (%)				Distribution (%)				
		(g)	(%)	(g)	Nb2O5	Fe2O3	CaO	SiO2	Nb2O5	Fe2O3	CaO	SiO2	
Rougher concentrate 1		22.0	4.4	109.3	3.40	33.80	19.0	4.59	22.0	16.2	3.4	2.8	
Rougher concentrate 2		17.1	3.4	180.5	1.80	17.70	25.1	6.83	9.1	6.6	3.5	3.3	
Rougher conc. 1+2		39.1	7.8	289.8	2.70	26.76	21.7	5.57	31.1	22.8	6.8	6.1	
Float tail		458.6	92.2	1003.9	0.51	7.71	25.1	7.34	68.9	77.2	93.2	93.9	
Total Measured		497.6	100.0	1293.7	0.68	9.21	24.8	7.20	100.0	100.0	100.0	100.0	

Figure 11. Test procedure and metallurgical balance for NP 11.

Test No:	NP11											
Sample:	Pyrochlore flotation feed							Project:	CRDPJ379600-08			
Grind size:	plant condition							Date:	April 29th, 2010			
Pulp density:	29	% solids						Operator:	Xiao Ni			
Objective:	Scoping bench flotation test of carbonate flotation feed using A6493 and NaHMP											
TEST PROCEDURE												
STAGE	TIME (min)	pH	ADDITION			COMMENTS						Conc pulp weight, g
			Reagent	g/tonne								
Slurry		9.0				JKTeck flotation machine, 1200 rpm 500 g sample in 1.5 L stainless steel cell if natural pH is between 6 and 10, don't adjust						
Condition	3	8.9	Aero 6493	500		250 milligrams of Aero 6493 added directly						
Rougher flotation Condition	2	8.7	NaHMP	500		25 mL 1% solution of NaHMP						
Rougher float 1	2					Scrap until froth is barren						197.23
Rougher float 2	3											274.9
		9.0				Record final pH						
						tailings pulp						1602.43
METALLURGICAL BALANCE												
Product	Solid weight		Water weight	Assay (%)				Distribution (%)				
	(g)	(%)	(g)	Nb2O5	Fe2O3	CaO	SiO2	Nb2O5	Fe2O3	CaO	SiO2	
Rougher concentrate 1	29.1	5.8	168.2	10.10	23.80	21.1	7.93	66.7	16.8	4.5	4.1	
Rougher concentrate 2	14.2	2.8	260.7	2.24	13.60	22.4	15.30	7.2	4.7	2.3	3.9	
Rougher conc. 1+2	43.3	8.6	428.9	7.52	20.46	21.5	10.34	73.9	21.5	6.8	8.0	
Float tail	461.3	91.4	1141.2	0.25	7.01	27.8	11.10	26.2	78.5	93.3	92.0	
Total Measured	504.5	100.0	1570.0	0.87	8.17	27.3	11.03	100.0	100.0	100.0	100.0	

Figure 12. Test procedure and metallurgical balance for NP 12.

Test No:		NP12									
Sample:		Mill feed									
Grind size:		plant condition									
Pulp density:		30 % solids		Project:		CRDPJ379600-08					
				Date:		May 20th, 2010					
Operator:		Xiao Ni									
Objective:		Scoping bench flotation test of mill feed using A6493 and NaMP Aero 6493 added to pulp directly									
TEST PROCEDURE											
STAGE	TIME (min)	pH	ADDITION		COMMENTS		Conc pulp weight, g				
			Reagent	g/tonne							
Slurry		8.5			JKTeck flotation machine, 1200 rpm 500 g sample in 1.5 L stainless steel cell						
Condition	3		Aero 6493	1,000	500 milligrams of Aero 6493 added directly						
Rougher flotation Condition	2	8.2	NaMP	500	25 mL 1% solution of NaHMP						
Rougher float 1	2				Air flow rate 7L/min		220.34				
Rougher float 2	3				Scrap until froth is barren		164.85				
		8.6			Final pH						
					tailings pulp		1317.98				
METALLURGICAL BALANCE											
Product	Solid weight		Water weight (g)	Assay (%)				Distribution (%)			
	(g)	(%)		Nb2O5	CaO	Fe2O3	SiO2	Nb2O5	CaO	Fe2O3	SiO2
Rougher concentrate 1	60.7	11.8	159.6	2.41	29.5	16.2	3.94	41.5	12.0	20.8	6.6
Rougher concentrate 2	36.5	7.1	128.4	3.15	24.8	24.6	4.83	32.6	6.1	19.0	4.9
Rougher conc. 1+2	97.2	19.0	288.0	2.69	27.7	19.4	4.27	74.1	18.1	39.8	11.5
Floater tail	415.4	81.0	902.6	0.22	29.4	6.8	7.70	25.9	81.9	60.1	88.5
Total Measured	512.6	100.0	1190.6	0.69	29.1	9.2	7.05	100.0	100.0	99.9	100.0

Figure 13. Test procedure and metallurgical balance for NP 13.

Test No:	NP13									
Sample:	Mill feed							Project:	CRDPJ379600-08	
Grind size:	plant condition							Date:	May 20th, 2010	
Pulp density:	30	% solids						Operator:	Xiao Ni	
Objective:	Scoping bench flotation test of mill feed using A6493 and NaMP Aero 6493 added to pulp directly									
TEST PROCEDURE										
STAGE	TIME (min)	pH	ADDITION		COMMENTS					Conc pulp weight, g
			Reagent	g/tonne						
Slurry					JKTeck flotation machine, 1200 rpm 500 g sample in 1.5 L stainless steel cell					
Condition	3	8.0	Aero 6493	1,500	750 milligrams of Aero 6493 added directly					
Rougher flotation										
Condition	2	8.3	NaMP	500	25 mL 1% solution of NaHMP					
Rougher float 1	2				Air flowrate 7 L/min					343.16
Rougher float 2	3				Scrap until froth is barren					144.89
		8.7			Final pH					
					tailings pulp					1226.95
METALLURGICAL BALANCE										
Product	Solid weight		Water weight	Assay (%)			Distribution (%)			
	(g)	(%)	(g)	Nb2O5	CaO	SiO2	Nb2O5	CaO	SiO2	
Rougher concentrate 1	92.1	18.2	251.1	1.98	30.6	4.32	51.2	19.0	10.9	
Rougher concentrate 2	35.4	7.0	109.5	2.01	29.1	4.61	20.0	7.0	4.5	
Rougher conc. 1+2	127.5	25.2	360.6	1.99	30.2	4.40	71.3	25.9	15.4	
Float tail	378.9	74.8	848.1	0.27	29.0	8.14	28.7	74.1	84.6	
Total Measured	506.4	100.0	1208.7	0.70	29.3	7.20	100.0	100.0	100.0	

Figure 14. Test procedure and metallurgical balance for NP 14.

Test No: NP14																			
Sample: flotation feed																Project: CRDPJ379600-08			
Grind size: Carbonate plant condition																Date: May 26, 2010			
Pulp density: 31 % solids																Operator: Xiao Ni			
Objective: Scoping bench flotation test of pyrochlore flotation feed using A6493, NaMP and Starch																			
TEST PROCEDURE																			
STAGE		TIME (min)	pH	ADDITION		COMMENTS				Conc pulp weight, g									
				Reagent	g/tonne														
Slurry			8.6			JKTeck flotation machine, 1200 rpm 500 g sample in 1.5 L stainless steel cell													
Condition		3	8.7	Aero 6493	500	250 milligrams of Aero 6493 added directly													
Rougher flotation																			
Condition		2		NaMP	250	12.5 mL 1% solution of NaMP													
		2	9.2	Starch (potato)	150	7.5 mL 1% solution of starch													
Rougher float 1		2				Air flowrate at 7 L/min				164.34									
Rougher float 2		3				Scrap until froth is barren				141.45									
			9.0			Record final pH													
						tailings pulp				1546.28									
METALLURGICAL BALANCE																			
Product		Solid weight		Water weight	Assay (%)				Distribution (%)										
		(g)	(%)	(g)	Nb2O5	Fe2O3	CaO	SiO2	Nb2O5	Fe2O3	CaO	SiO2							
Rougher concentrate 1		35.8	6.7	128.6	3.49	16.5	30.6	3.97	36.4	13.6	6.9	3.6							
Rougher concentrate 2		15.0	2.8	126.5	2.25	13.8	29.3	5.6	9.8	4.8	2.8	2.1							
Rougher conc. 1+2		50.7	9.5	255.1	3.12	15.70	30.2	4.45	46.3	18.3	9.7	5.6							
Float tail		484.6	90.5	1061.7	0.38	7.32	29.6	7.78	53.7	81.7	90.3	94.4							
Total Measured		535.3	100.0	1316.8	0.64	8.11	29.7	7.46	100.0	100.0	100.0	100.0							

Figure 15. Test procedure and metallurgical balance for NP 15.

Test No: NP15																	
Sample: Carbonate flotation feed												Project:		CRDPJ379600-08			
Grind size: plant condition												Date:		May 26, 2010			
Pulp density: 28 % solids												Operator:		Xiao Ni			
Objective: Scoping bench flotation test of pyrochlore flotation feed using A6493, NaMP and starch																	
TEST PROCEDURE																	
STAGE		TIME (min)	pH	ADDITION		COMMENTS						Conc pulp weight, g					
				Reagent	g/tonne												
Slurry			8.6			JKTeck flotation machine, 1200 rpm 500 g sample in 1.5 L stainless steel cell											
Condition		3	8.7	Aero 6493	500	250 milligrams of Aero 6493 add directly											
Rougher flotation																	
Condition		2	8.7	NaMP	250	12.5 mL 1% solution of NaMP											
		2	9.8	Starch	500	25 mL 1% solution of starch											
Rougher float 1		2				Air flowrate at 7 L/min						157.72					
Rougher float 2		3				Scrap until froth is barren						170.58					
			9.4			Record final pH											
						tailings pulp						1569.75					
METALLURGICAL BALANCE																	
Product		Solid weight		Water weight		Assay (%)				Distribution (%)							
		(g)	(%)	(g)	Nb2O5	Fe2O3	CaO	SiO2	Nb2O5	Fe2O3	CaO	SiO2					
Rougher concentrate 1		43.2	8.5	114.5	2.68	13	31.2	5.01	36.7	14.0	9.0	5.7					
Rougher concentrate 2		22.1	4.4	148.5	1.68	11	29.5	7.03	11.7	6.0	4.4	4.1					
Rougher conc. 1+2		65.3	12.9	263.0	2.34	12.32	30.6	5.69	48.4	20.0	13.4	9.8					
Float tail		440.6	87.1	1129.2	0.37	7.3	29.4	7.8	51.6	80.0	86.6	90.2					
Total Measured		505.9	100.0	1392.1	0.62	7.95	29.6	7.53	100.0	100.0	100.0	100.0					

Figure 16. Test procedure and metallurgical balance for NP 16.

Test No:		NP16									
Sample:		Mill feed				Project:		CRDPJ379600-08			
Grind size:		plant condition				Date:		June 2nd, 2010			
Pulp density:		31		% solids		Operator:		Xiao Ni			
Objective:		Scoping bench flotation test of mill flotation feed using A6493, NaMP and Kerosene Kerosene emulsified and added to pulp directly									
TEST PROCEDURE											
STAGE	TIME (min)	pH	ADDITION			COMMENTS	Conc pulp weight, g				
			Reagent	g/tonne							
Slurry		8.4				JKTeck flotation machine, 1200 rpm 500 g sample in 1.5 L stainless steel cell					
Condition	3	8.1	Aero 6493	1000		500 milligrams of Aero 6493 added directly					
Rougher flotation											
Condition	2		NaMP	500		25 mL 1% solution of NaHMP					
Condition	1	8.5	Kerosene	250		125 milligrams of kerosene, blended with 200 mL water and 1 drop of DF250					
Rougher float 1	2					Air flowrate at 7 L/min	225.64				
Rougher float 2	3					Scrap until froth is barren	123.83				
		8.9				tailings pulp	1324.48				
METALLURGICAL BALANCE											
Product	Solid weight		Water weight (g)	Assay (%)				Distribution (%)			
	(g)	(%)		Nb2O5	Fe2O3	CaO	SiO2	Nb2O5	Fe2O3	CaO	SiO2
Rougher concentrate 1	44.4	8.6	181.2	2.87	23.30	25.5	5.37	36.2	21.7	7.5	6.4
Rougher concentrate 2	18.6	3.6	105.2	2.55	20.70	25.2	7.18	13.5	8.1	3.1	3.6
Rougher conc. 1+2	63.0	12.2	286.4	2.78	22.53	25.4	5.90	49.7	29.8	10.6	10.0
Rougher concentrate 3											
Rougher conc. 1+2+3	63.0	12.2	286.4	2.78	22.53	25.4	5.90	49.7	29.8	10.6	10.0
Float tail	454.5	87.8	870.0	0.39	7.36	29.6	7.36	50.3	70.2	89.4	90.0
Total Measured	517.6	100.0	1156.4	0.68	9.21	29.1	7.18	100.0	100.0	100.0	100.0

Figure 17. Test procedure and metallurgical balance for NP 17.

Test No:		NP17																	
Sample:		Mill flotation feed								Project:		CRDPJ379600-08							
Grind size:		plant condition								Date:		June 2nd, 2010							
Pulp density:		28		% solids						Operator:		Xiao Ni							
Objective:		Scoping bench flotation test of mill flotation feed using A6493, NaMP and Kerosene Kerosene emulsified, and pulp agitated at high speed																	
TEST PROCEDURE																			
STAGE		TIME	pH	ADDITION		COMMENTS						Conc pulp							
		(min)		Reagent	g/tonne							weight, g							
Slurry			8.6			JKTeck flotation machine, 1200 rpm 500 g sample in 1.5 L stainless steel cell													
Condition		3	8.2	Aero 6493	1000	500 milligrams of Aero 6493 added directly													
Rougher flotation																			
Condition		2	7.9	NaMP	500	25 mL 1% solution of NaHMP													
Condition			8.9	Kerosene	250	125 milligrams of emulsified kerosene 1750 rpm													
		10																	
Rougher float 1		2				1200 rpm. Air flowrate at 7 L/min						152.95							
Rougher float 2		3				Scrap until froth is barren						197.4							
			9.2			tailings pulp						1420.35							
METALLURGICAL BALANCE																			
Product		Solid weight		Water weight	Assay (%)				Distribution (%)										
		(g)	(%)	(g)	Nb2O5	Fe2O3	CaO	SiO2	Nb2O5	Fe2O3	CaO	SiO2							
Rougher concentrate 1		17.1	3.4	135.9	0.57	25.40	21.0	6.74	2.7	9.2	2.5	3.2							
Rougher concentrate 2		13.8	2.7	183.7	0.61	17.90	24.3	7.75	2.4	5.2	2.3	3.0							
Rougher conc. 1+2		30.8	6.2	319.5	0.59	22.05	22.5	7.19	5.1	14.5	4.7	6.2							
Rougher concentrate 3																			
Float tail		469.4	93.8	951.0	0.72	8.54	29.6	7.10	94.9	85.5	95.3	93.8							
Total Measured		500.2	100.0	1270.5	0.71	9.37	29.2	7.11	100.0	100.0	100.0	100.0							

Figure 18. Test procedure and metallurgical balance for NP 18.

Test No:	NP18									
Sample:	Mill feed							Project:	CRDPJ379600-08	
Grind size:	plant condition							Date:		
Pulp density:	28	% solids						Operator:	Xiao Ni	
Objective:	Scoping bench flotation test of mill feed using A6493, kerosene and NaHMP									
TEST PROCEDURE										
STAGE	TIME (min)	pH	ADDITION		COMMENTS				Conc pulp weight, g	
			Reagent	g/tonne						
Slurry		8.4			JKTeck flotation machine, 1200 rpm 500 g sample in 1.5 L stainless steel cell					
Condition	3	8.1	Aero 6493	1,000	500 milligrams of Aero 6493 add directly					
Rougher flotation Condition	2	8.2	NaHMP	500	25mL 1% solution of NaMP					
Condition	1	8.4	Kerosene	2,000	1 grams of kerosene, blended with 200 mL water and 1 drop of DF250					
Rougher float 1	2				Air rate 7l/min				248.24	
Rougher float 2	3								229.74	
Rougher float 3	5				Scrap until froth is barren				255.77	
Rougher float 4										
Rougher float 5										
		8.8			Record final pH					
					tailings pulp				1050.08	
METALLURGICAL BALANCE										
Product	Solid weight		Water weight	Assay (%)			Distribution (%)			
	(g)	(%)	(g)	Nb2O5	CaO	SiO2	Nb2O5	CaO	SiO2	
Rougher concentrate 1	50.3	10.0	198.0	3.94	25.5	3.69	56.6	8.7	5.2	
Rougher concentrate 2	20.8	4.1	209.0	1.43	29.9	6.08	8.5	4.2	3.5	
Rougher conc. 1+2	71.1	14.1	406.9	3.21	26.8	4.39	65.1	12.9	8.7	
Float tail	418.1	83.1	632.0	0.27	29.8	7.58	32.3	84.4	88.4	
Total Measured	503.0	100.0	1280.9	0.70	29.3	7.13	100.0	100.0	100.0	

Figure 19. Test procedure and metallurgical balance for NP 19.

Test No:	NP19									
Sample:	Mill feed							Project:	CRDPJ379600-08	
Grind size:	plant condition							Date:	June 17, 2010	
Pulp density:	24	% solids						Operator:	Xiao Ni	
Objective:	Scoping bench flotation test of mill feed using A6493, kerosene and NaHMP									
TEST PROCEDURE										
STAGE	TIME (min)	pH	ADDITION		COMMENTS	Conc pulp weight, g				
			Reagent	g/tonne						
Slurry		8.6			JKTeck flotation machine, 1200 rpm 500 g sample in 1.5 L stainless steel cell					
Condition	3		Aero 6493	1,000	500 milligrams of Aero 6493 add directly					
Rougher flotation										
Condition	2		NaHMP	500	25 mL 1% solution of NaHMP					
Condition	1	8.8	Kerosene	5,000	2.5 grams of kerosene, blended with 200 mL water and 1 drop of DF250					
Rougher float 1	2				Air flowrate at 7 L/min	237.96				
Rougher float 2	3					207.52				
					tailings pulp	1555.55				
METALLURGICAL BALANCE										
Product	Solid weight		Water weight (g)	Assay (%)			Distribution (%)			
	(g)	(%)		Nb2O5	CaO	SiO2	Nb2O5	CaO	SiO2	
Rougher concentrate 1	53.6	10.7	184.4	1.83	25.9	5.78	28.5	9.5	8.7	
Rougher concentrate 2	26.0	5.2	181.6	2.02	28.3	6.36	15.3	5.0	4.7	
Rougher conc. 1+2	79.6	15.9	365.9	1.89	26.7	5.97	43.8	14.5	13.4	
Rougher concentrate 3	1.7		97.6	1.18	28.2	8.44				
Rougher conc. 1+2+3	81.2	16.2	463.6	1.85	26.1	5.85	43.8	14.5	13.4	
Rougher concentrate 4										
Rougher conc. 1+2+3+4	81.2	16.2	463.6	1.85	26.1	5.85	43.8	14.5	13.4	
Rougher concentrate 5										
Rougher conc. 1+2+3+4+5	81.2	16.2	463.6	1.85	26.1	5.85	43.8	14.5	13.4	
Conc 1										
Conc 2										
Total Measured	501.2	100.0	1599.1	0.69	29.3	7.06	100.0	100.0	100.0	

Figure 20. Test procedure and metallurgical balance for NP 20.

Test No:	NP20									
Sample:	Mill feed						Project:	CRDPJ379600-08		
Grind size:	plant condition						Date:			
Pulp density:	25	% solids					Operator:	Xiao Ni		
Objective:	Scoping bench flotation test of pyrochlore flotation feed using A6493, NaMP and Kerosene									
	Pulp agitated									
TEST PROCEDURE										
STAGE	TIME (min)	pH	ADDITION		COMMENTS				Conc pulp weight, g	
			Reagent	g/tonne						
Slurry					JKTeck flotation machine					
Condition	3		Aero 6493	1,000	500 g sample in 1.5 L stainless steel cell 500 milligrams of Aero 6493 added directly					
Rougher flotation										
Condition	2		NaMP	500	25 mL 1% solution of NaMP					
Condition	1		Kerosene	2,000	1 grams of kerosene add directly					
Agitation	10	8.8			1,750 rpm					
Rougher float 1	2		DF250	15	Air rate 7 L/min					140.72
Rougher float 2	3		DF250	25						224.14
		9.0			Record final pH					
									tailings pulp	1382.28
METALLURGICAL BALANCE										
Product	Solid weight		Water weight	Assay (%)			Distribution (%)			
	(g)	(%)		(g)	Nb2O5	CaO	SiO2	Nb2O5	CaO	
Rougher concentrate 1	16.0	3.2	124.8	0.78	22.7	6.85	3.5	2.4	3.0	
Rougher concentrate 2	16.8	3.3	207.4	0.73	25.0	7.60	3.4	2.8	3.5	
Rougher conc. 1+2	32.7	6.5	332.1	0.75	23.9	7.23	6.9	5.2	6.5	
Rougher concentrate 3	17.9	3.5	293.6	0.66	26.6	8.27				
Rougher conc. 1+2+3	50.6	10.0	625.8	0.72	24.8	7.60	10.1	8.4	10.5	
Rougher concentrate 4										
Rougher conc. 1+2+3+4	50.6	10.0	625.8	0.72	24.8	7.60	10.1	8.4	10.5	
Rougher concentrate 5										
Rougher conc. 1+2+3+4+5	50.6	10.0	625.8	0.72	24.8	7.60	10.1	8.4	10.5	
Float tail	455.1	90.0	927.2	0.71	30.2	7.20	89.9	91.6	89.5	
Total	505.7	100.0	1553.0	0.71	29.7	7.24	100.0	100.0	100.0	
Measured										

Figure 21. Test procedure and metallurgical balance for NP 21.

Test No:	NP21									
Sample:	Mill feed							Project:	CRDPJ379600-08	
Grind size:	plant condition							Date:		
Pulp density:	21	% solids						Operator:	Xiao Ni	
Objective:	Scoping bench flotation test of pyrochlore flotation feed using A6493, NaMP and Kerosene									
	Pulp agitated									
TEST PROCEDURE										
STAGE	TIME (min)	pH	ADDITION		COMMENTS				Conc pulp weight, g	
			Reagent	g/tonne						
Slurry					JKTeck flotation machine					
Condition	3		Aero 6493	1000	500 g sample in 1.5 L stainless steel cell 500 milligrams of Aero 6493, add directly					
Rougher flotation										
Condition	2		NaMP	500	25 mL 1% solution of NaMP					
Condition	1	8.7	Kerosene	5,000	2.5 grams of kerosene add directly					
Agitation	10				1,750 rpm					
Rougher float 1	2		DF250	400	Air rate 7 L/min				391.96	
Rougher float 2	3								474.42	
		9.2			Record final pH					
					tailings pulp				1160.85	
METALLURGICAL BALANCE										
Product	Solid weight		Water weight (g)	Assay (%)			Distribution (%)			
	(g)	(%)		Nb2O5	CaO	SiO2	Nb2O5	CaO	SiO2	
Rougher concentrate 1	43.7	8.5	348.3	0.89	24.9	6.92	10.6	7.3	8.3	
Rougher concentrate 2	38.1	7.4	436.3	0.72	27.6	7.62	7.5	7.0	8.0	
Rougher conc. 1+2	81.8	15.9	784.6	0.81	26.2	7.25	18.0	14.3	16.3	
Rougher concentrate 3	24.6	4.8	437.8	0.65	27.7	7.81				
Rougher conc. 1+2+3	106.4	20.7	1222.4	0.77	26.5	7.38	22.4	18.8	21.6	
Rougher concentrate 4										
Rougher conc. 1+2+3+4	106.4	20.7	1222.4	0.77	26.5	7.38	22.4	18.8	21.6	
Rougher concentrate 5										
Rougher conc. 1+2+3+4+5	106.4	20.7	1222.4	0.77	26.5	7.38	22.4	18.8	21.6	
Float tail	408.5	79.3	752.3	0.70	29.8	6.99	77.6	81.2	78.4	
Total	514.9	100.0	1974.7	0.72	29.1	7.07	100.0	100.0	100.0	
Measured										

Figure 22. Test procedure and metallurgical balance for NP 22.

Test No: NP22																				
Sample: Mill Feed																				
Grind size: plant condition																				
Pulp density: 17 % solids																				
Objective: Progressive additions of A6493 and NaMP to maximize Nb2O5 recovery from Mill Feed																				
TEST PROCEDURE																				
STAGE		TIME (min)	pH	ADDITION			COMMENTS					Conc pulp weight, g								
				Reagent	g/tonne															
Slurry			8.4				JKTeck flotation machine, 1200 rpm 500 g sample in 1.5 L stainless steel cell													
Condition		3		Aero 6493	500		250 milligrams of Aero 6493 add directly													
Rougher flotation Condition		2	8.5	NaMP	250		12 mL 1% solution of NaMP													
Rougher float 1		4					Air flow rate at 7, scrap until froth is barren					282.84								
Condition		2		Aero 6493	500															
		2		NaMP	250															
Rougher float 2		5.5					Scrap until froth is barren					307.16								
Condition		2		Aero 6493	250															
		2		NaMP	125															
Rougher float 3		5.5					Scrap until froth is barren					453.02								
Condition		2		Aero 6493	250															
		2		NaMP	125															
Rougher float 4		4					Scrap until froth is barren					297.16								
Rougher float 5		4		Aero 6493	250		Scrap until froth is barren					212.02								
			8.7				Record final pH													
											tailings pulp	1320.55								
METALLURGICAL BALANCE																				
Product		Solid weight		Water weight		Assay (%)				Distribution (%)										
		(g)	(%)	(g)		Nb2O5	Fe2O3	CaO	SiO2	Nb2O5	Fe2O3	CaO	SiO2							
Rougher concentrate 1		59.6	11.9	223.3		4.07	28.10	21.9	5.31	69.5	36.7	8.9	8.8							
Rougher concentrate 2		35.3	7.1	271.9		1.24	13.60	26.1	9.67	12.5	10.5	6.3	9.5							
Rougher conc. 1+2		94.8	19.0	495.2		3.02	22.71	23.5	6.93	82.1	47.2	15.2	18.3							
Rougher concentrate 3		48.1	9.6	405.0		0.17	6.44	28.0	10.80	2.3	6.8	9.2	14.4							
Rougher conc. 1+2+3		142.9	28.7	900.1		2.06	17.23	25.0	8.23	84.4	54.0	24.4	32.7							
Rougher concentrate 4		17.4	3.5	279.7		0.09	6.02	27.7	9.65	0.5	2.3	3.3	4.7							
Rougher conc. 1+2+3+4		160.3	32.2	1179.9		1.85	16.02	25.3	8.39	84.9	56.3	27.7	37.4							
Rougher concentrate 5		15.2	3.0	196.9		0.07	5.53	28.4	9.67	0.3	1.8	2.9	4.1							
Rougher conc. 1+2+3+4+5		175.5	35.2	1376.7		1.69	15.11	25.6	8.50	85.2	58.1	30.7	41.5							
Float tail		323.1	64.8	997.5		0.16	5.92	31.4	6.52	14.8	41.9	69.3	58.5							
Total Measured		498.6	100.0	2374.2		0.70	9.15	29.3	7.22	100.0	100.0	100.0	100.0							

Figure 23. Test procedure and metallurgical balance for NP 23.

[illegible]

Figure 24. Test procedure and metallurgical balance for NP 24.

[illegible]

Figure 25. Test procedure and metallurgical balance for NP 25.

[illegible]

Figure 26. Test procedure and metallurgical balance for NP 26.

[illegible]

Figure 27. Test procedure and metallurgical balance for NP 27.

[illegible]

Figure 28. Test procedure and metallurgical balance for NP 28.

[illegible]

Figure 29. Test procedure and metallurgical balance for NP 29.

[illegible]

Figure 30. Test procedure and metallurgical balance for NP 30.

[illegible]

Figure 31. Test procedure and metallurgical balance for NP 31.

[illegible]

Figure 32. Test procedure and metallurgical balance for NP 32.

[illegible]

Figure 33. Test procedure and metallurgical balance for NP 33.

[illegible]

Figure 34. Test procedure and metallurgical balance for NP 34.

[illegible]

Figure 35. Test procedure and metallurgical balance for NP 35.

[illegible]

Figure 36. Test procedure and metallurgical balance for NP 36.

[illegible]

NP 37,39-41,42 are several exploratory batch flotation tests using higher dosage of pure OHA or combination of SHA and OHA, which all the feed particles were collected, while no tails were able to be collected.

Figure 37. Test procedure and metallurgical balance for NP 38.

[illegible]

NP 44-47 are several exploratory tests using sodium silicate as depressant under various conditions, none of which had good solid recovery (mass pull <1g) for assaying.

Figure 38. Test procedure and metallurgical balance for NP 43.

Test No: NP43															
Sample: Pyrochlore Feed										Project: CRDPJ379600-08					
Grind size: plant condition										Date: Feb 1, 2012					
Pulp density: 16 % solids										Operator: Xiao Ni					
Objective: Rougher and cleaner flotation (4 stages) of pyrochlore feed using OHA without depressant															
TEST PROCEDURE															
STAGE		TIME (min)	pH	ADDITION			COMMENTS						Conc pulp weight, g		
				Reagent	g/tonne										
Hand magnetite removal Slurry							JKTeck flotation machine, 1200 rpm								
Rougher flotation							500 g sample in 1.5 L stainless steel cell								
Condition		3	8.8	OHA	50		25mL 1g/L OHA								
							Repeating three times and combining four rougher concentrates								
Rougher float 1		3					Air flow rate at 7, scrap until froth is barren								
Cleaner flotation															
Condition															
Cleaner float 1		1					Cleaner tails 1						1584.63		
Condition							Transfer the Cleaner concentrate 1 into the cell and add make-up water								
Cleaner float 2		1					Cleaner tails 2						793.92		
Condition				DF 250	2		Cleaner tail 3						861.08		
Cleaner float 3		1													
Condition				DF 250	2		Cleaner Tail 4						1203.2		
Cleaner float 4		1					Cleaner Concent. 4						107.79		
			8.50				Record final pH								
							tailings pulp						5064		
METALLURGICAL BALANCE															
Product		Solid weight		Water weight		Assay (%)				Distribution (%)					
		(g)	(%)	(g)	Nb2O5	Fe2O3	CaO	SiO2	Nb2O5	Fe2O3	CaO	SiO2			
Cleaner Concentrate 4		7.2	0.5	100.6	22.30	38.90	10.00	3.30	13.8	2.3	0.2	0.2			
Cleaner tail 4		3.6	0.2	1199.6	12.60	30.00	17.20	6.43	3.9	0.9	0.1	0.2			
Cleaner Concentrate 3		10.8	0.7	1300.2	19.06	35.93	12.40	4.35	17.7	3.2	0.3	0.3			
Cleaner tail 3		3.9	0.3	857.2	6.90	22.80	21.80	8.39	2.3	0.7	0.2	0.2			
Cleaner Concentrate 2		14.6	1.0	2157.5	15.85	32.46	14.89	5.41	20.0	3.9	0.5	0.5			
Cleaner tail 2		12.4	0.8	781.5	8.96	24.90	20.00	6.79	9.6	2.6	0.6	0.6			
Cleaner Concentrate 1		27.0	1.8	2939.0	12.68	28.99	17.24	6.05	29.7	6.5	1.1	1.1			
Cleaner tail 1		124.5	8.2	1460.1	1.78	8.66	28.80	8.09	19.2	9.0	8.5	6.7			
Rougher concentrate		151.6	10.0	4399.1	3.72	12.29	26.74	7.73	48.8	15.5	9.6	7.8			
Rougher tail		1353.6	88.9	3710.4	0.37	6.70	28.10	10.20	43.3	75.4	90.0	91.9			
Magnetic tail		1505.2	98.8		0.71	7.26	27.96	9.95	92.2	90.8	99.6	99.7			
Megnetic concentrate		17.8	1.2		5.08	62.10	9.89	2.78	7.8	9.2	0.4	0.3			
Total		1522.9	100.0	8109.5	0.76	7.90	27.75	9.87	100.0	100.0	100.0	100.0			
Measured															

Figure 39. Test procedure and metallurgical balance for NP 48.

Test No:	NP48								
Sample:	Carbonate feed					Project:	CRDPJ379600-08		
Grind size:	plant condition					Date:	Sep 7, 2012		
Pulp density:	22	% solids				Operator:	Xiao Ni		
Objective:	Scoping bench flotation test of carbonate feed using OHA solution								
TEST PROCEDURE									
STAGE	TIME (min)	pH	ADDITION		COMMENTS	Conc pulp weight, g			
			Reagent	g/tonne					
Slurry					JKTeck flotation machine				
Condition	3		OHA solution	100	500 g sample in 1.5 L stainless steel cell 50 ml OHA solution added directly 1,200 rpm				
Rougher flotation									
		8.8							
Rougher float 1	2				Air rate 7 L/min	443.59			
Rougher float 2	3					449.81			
		9.0			Record final pH				
					tailings pulp	1521.7			
METALLURGICAL BALANCE									
Product	Solid weight		Water weight (g)	Assay (%)			Distribution (%)		
	(g)	(%)		Nb2O5	CaO	SiO2	Nb2O5	CaO	SiO2
Rougher concentrate 1	171.0	32.2	272.6	0.53	30.8	3.22	53.0	34.1	14.2
Rougher concentrate 2	62.4	11.7	387.4	0.38	29.0	6.53	13.9	11.7	10.5
Rougher conc. 1+2	233.4	43.9	660.0	0.49	30.3	4.11	66.9	45.8	24.7
Rougher concentrate 3									
Rougher conc. 1+2+3	233.4	43.9	660.0	0.49	30.3	4.11	66.9	45.8	24.7
Rougher concentrate 4									
Rougher conc. 1+2+3+4	233.4	43.9	660.0	0.49	30.3	4.11	66.9	45.8	24.7
Rougher concentrate 5									
Rougher conc. 1+2+3+4+5	233.4	43.9	660.0	0.49	30.3	4.11	66.9	45.8	24.7
Float tail	298.0	56.1	1223.7	0.19	28.1	9.81	33.1	54.2	75.3
Total	531.4	100.0	1883.7	0.32	29.1	7.30	100.0	100.0	100.0
Measured									

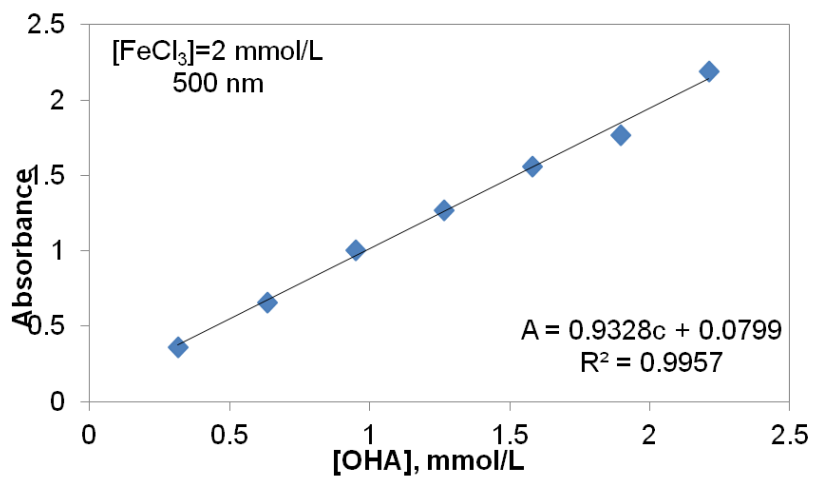
Figure 40. Test procedure and metallurgical balance for NP 49.

Test No: NP49										
Sample: Carbonate feed						Project: CRDPJ379600-08				
Grind size: plant condition						Date: Sep 7, 2012				
Pulp density: 22 % solids						Operator: Xiao Ni				
Objective: Scoping bench flotation test of carbonate feed using OHA solution and kerosene										
TEST PROCEDURE										
STAGE		TIME (min)	pH	ADDITION		COMMENTS			Conc pulp weight, g	
				Reagent	g/tonne					
Slurry						JKTeck flotation machine 500 g sample in 1.5 L stainless steel cell				
Condition		3		OHA solution	100	50 ml 1% OHA solution added directly				
Condition		1		Kerosene	500	0.25 grams of kerosene add directly				
Agitation		10	9.1			1,750 rpm				
Rougher flotation										
Rougher float 1		2				Air rate 7 L/min			242.41	
Rougher float 2		3							59.14	
						Record final pH				
						tailings pulp			1945	
METALLURGICAL BALANCE										
Product		Solid weight		Water weight	Assay (%)			Distribution (%)		
		(g)	(%)	(g)	Nb2O5	CaO	SiO2	Nb2O5	CaO	SiO2
Rougher concentrate 1		27.5	5.6	215.0	0.53	28.7	5.69	4.6	5.6	4.3
Rougher concentrate 2		5.6	1.1	53.5						
Rougher conc. 1+2		33.1	6.7	268.5	0.44	23.8	4.72	4.6	5.6	4.3
Rougher concentrate 3										
Rougher conc. 1+2+3		33.1	6.7	268.5	0.44	23.8	4.72	4.6	5.6	4.3
Rougher concentrate 4										
Rougher conc. 1+2+3+4		33.1	6.7	268.5	0.44	23.8	4.72	4.6	5.6	4.3
Rougher concentrate 5										
Rougher conc. 1+2+3+4+5		33.1	6.7	268.5	0.44	23.8	4.72	4.6	5.6	4.3
Float tail		460.4	93.3	1484.6	0.66	29.0	7.59	95.4	94.4	95.7
Total		493.5	100.0	1753.1	0.65	28.7	7.40	100.0	100.0	100.0
Measured										

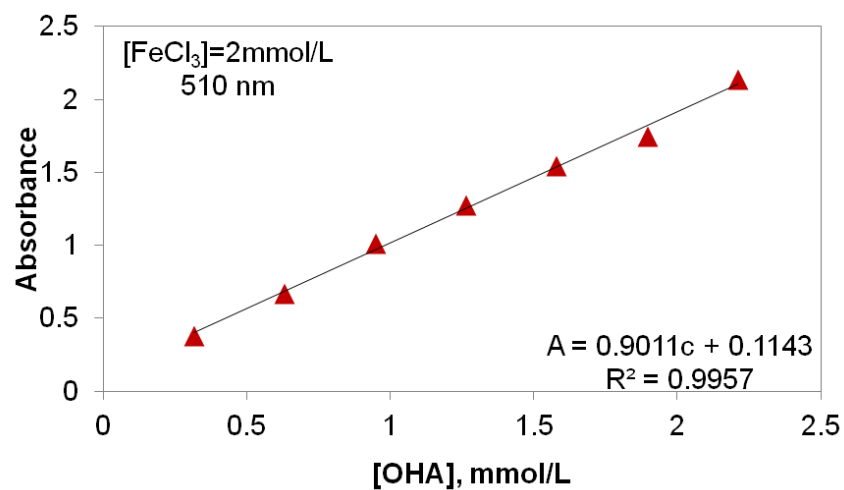
Appendix B. Determination of OHA concentration by UV-Vis spectrophotometry

OHA-ferric chelate has strong absorbance within wavelength range 500-520 nm (absorbance peak will shift slightly when concentration changes). In order to find a suitable wavelength with the best linear correlation in Beer-Lambert law, the absorbance of OHA-ferric solution with different concentrations was measured under three wavelengths. They are shown in following figure B.1.

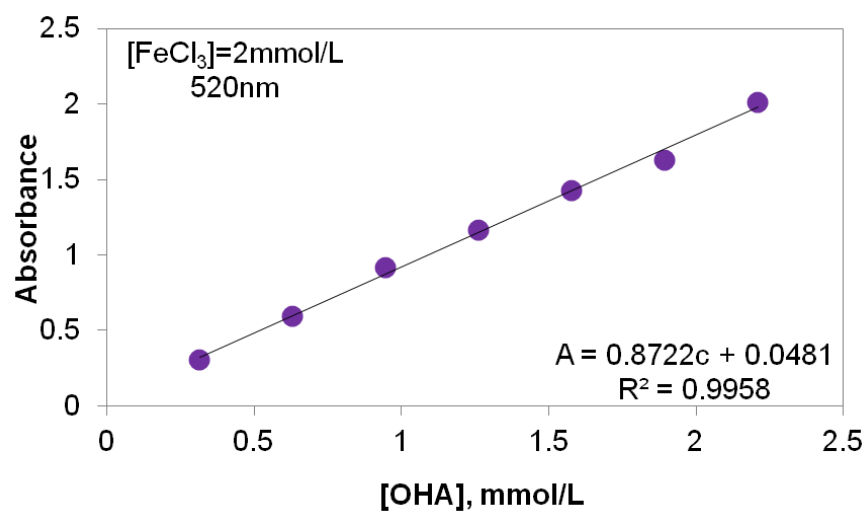
The absorbance of OHA-chelate solution was measured with 2 mmol/L FeCl_3 as reference. As can be seen, all calibration curves obey Beer-Lambert law within OHA concentration range of 0.5-2 mmol/L. So this OHA concentration range was used in our adsorption isotherm test. The absorbance obtained from test using 520 nm shows highest correlation coefficient, thus this wavelength was used for OHA concentration determination.



(a)



(b)



(c)

Figure B.1 The standard calibration curve and corresponding correlation coefficient of OHA-ferric solution obtained from tests using wavelength (a) 500 nm (b) 510 nm (c) 520 nm.

Appendix C. Raw data from XPS measurements

Table C.1 Raw data on normalized atomic concentration of selected elements on the mineral surfaces.

Peak	Raw Area (CPS)	RSF	Atomic Conc. %	Mass Conc. %
Untreated pyrochlore				
Fe 2p	857.6	2.957	1.57	4.23
O 1s	7017.3	0.780	48.32	37.40
N 1s	-	0.477	-	-
Ca 2p	1188.9	1.833	3.53	6.84
C 1s	1920.5	0.278	38.39	22.31
Nb 3d	2951.7	2.921	5.77	25.92
P 2p	197.5	0.486	2.39	3.59
OHA treated pyrochlore				
Fe 2p	715.4	2.957	1.25	3.65
O 1s	6585.0	0.780	43.42	36.24
N 1s	248.8	0.477	2.72	1.99
Ca 2p	1254.5	1.833	3.60	7.54
C 1s	2213.8	0.278	42.38	26.56
Nb 3d	2206.6	2.921	4.13	20.01
P 2p	213.9	0.486	2.48	4.01
NaHMP treated pyrochlore				
Fe 2p	776.8	2.957	2.06	4.33
O 1s	5840.1	0.780	59.44	35.73
N 1s	-	0.477	-	-
Ca 2p	1037	1.833	4.59	6.92
C 1s	311.64	0.278	9.16	4.13
Nb 3d	3385.1	2.921	9.56	33.36
P 2p	189.6	0.486	3.23	3.76
Untreated calcite				
O 1s	9054.7	0.780	48.38	44.50
N 1s	-	0.477	-	-
Ca 2p	3353.0	1.833	12.30	28.35
P 2p	-	0.486	-	-
C 1s	1678.6	0.278	39.32	27.15
OHA treated calcite				
O 1s	6499.9	0.780	27.22	28.54
N 1s	724.8	0.477	5.04	4.62
Ca 2p	4025.1	1.833	7.35	19.29
C 1s	4966.6	0.278	60.39	47.54
P 2p	-	0.486	-	-

Cont'd

Peak	Raw Area (CPS)	RSF	Atomic Conc. %	Mass Conc. %
NaHMP treated calcite				
O 1s	6747.1	0.780	47.36	43.35
N 1s	-	0.477	-	-
Ca 2p	3944.7	1.833	12.05	27.63
C 1s	1950.8	0.278	39.56	27.18
P 2p	88.1	0.486	1.04	1.83